ENHANCEMENT OF MICROGRID STABILITY BY USING ENERGY STORAGE

Thesis submitted for the award of the degree of

Doctor of Philosophy (Ph.D.)

in

Electrical Engineering

in the faculty of

Science and Technology

by

Khule Shridhar Shantaram

under the supervision of

Dr. Sharad W. Mohod

(Professor)

Prof. Ram Meghe Institute of Technology and Research, Badnera, Amravati - 444701 (MS)

to

Sant Gadge Baba Amravati University, Amravati

October, 2019

Vidarbh Youth Welfare Society's

Prof. Ram Meghe Institute of Technology and Research,

Badnera, Amravati - 444701 (MS)

Certificate

This is to certify that **Mr. Shridhar Shantaram Khule** is the registered scholar whose registration no. is **SGBAU/Ph.D./ELE.ENGG./7640/2015** has completed the research work entitled, "**Enhancement of Microgrid Stability by using Energy Storage**" in the subject **Electrical Engineering** in the faculty **Science and Technology** under the supervision of **Dr. Sharad W. Mohod**. He has successfully completed the pre-defence of the thesis and the thesis is hereby forwarded to the University for evaluation.

Prof. (Dr.) S. M. Deshmukh	**Prof. (Dr.) A. P. Bodkhe**
Head of Department	Principal

Date: **22/10/2019**

Place: **Amravati**

Declaration

I, the undersigned, hereby declare that the work presented in this thesis entitled, "**Enhancement of Microgrid Stability by using Energy Storage**" in the subject **Electrical Engineering** in the faculty **Science and Technology** is the original contribution carried out by me conforming to research norms under the supervision of **Prof. (Dr.) Sharad W. Mohod**. This work has not been submitted to any other university / institution for the award of any degree.

I further declare that, this work is free from any kind of plagiarism.

Name of Scholar: **Shridhar S. Khule**

Registration No.: **SGBAU/Ph.D./ELE.ENGG./7640/2015**

Date of Registration: **15/01/2015**

Date: **22/10/2019**

Place: **Amravati**

Certificate of the Supervisor

This is to certify that the work presented in this thesis entitled, "**Enhancement of Microgrid Stability by using Energy Storage**" is the own and original work of **Mr. Shridhar S. Khule** carried out under my supervision. The work embodied in this thesis has not been submitted earlier to any university/institution for any degree to the best of my knowledge.

I further certify that, this work is free from any kind of plagiarism.

Name of Supervisor: **Dr. Sharad W. Mohod**

Designation: **Professor**

Date: **22/10/2019**

Place: **Amravati**

Acknowledgements

I take this opportunity to express my profound gratitude to my guide **Prof. (Dr.) S. W. Mohod**, for his exemplary guidance, innovative ideas, monitoring and constant encouragement throughout the course of this thesis. I am deeply indebted to him for his valuable suggestions and critical evaluation of theoretical and simulated results. His scholarly inputs and research attitude shall carry me a long way in the journey of life on which I am about to embark. I also take this opportunity to express a deep sense of gratitude to **Prof. (Dr.) S. M. Deshmukh**, Head, Department of Electronics and Telecommunication Engineering. His research expertise and motivation helped me in completing this task through various stages.

It gives me immense pleasure to express my sincere thanks to **Dr. A. P. Bodkhe**, Principal, Prof. Ram Meghe Institute of Technology and Research, Badnera for his support and insightful guidance. Special thanks to **Prof. (Dr.) G. K. Kharate** for being a constant source of inspiration. I express my thanks to my colleagues and fellow research scholars for their support and encouragement. My acknowledgement would be incomplete without thanking the biggest source of my strength, my family.

Shridhar Shantaram Khule

Abstract

The non renewable nature of conventional sources and alarming global warming intensify the necessity of exploiting non conventional renewable energy sources. Moreover, the increasing energy demand may not be satisfied by the conventional sources due to the depleting fossil fuels. Pollution, the rising costs of fossil fuels and the finite nature of conventional fuels have forced the world to look for alternative energy sources. The renewable energy sources prove to be a better option because of their abundant availability, low cost, economical transportability and social compatibility.

In today's era of energy crisis, the solar energy is a promising alternative as it is perennial, non polluting and huge power house in the nature. The significance of solar Photovoltaic (PV) based solutions has gained importance with the rapidly growing renewable energy market. Especially the demand of Solar PV based Distributed Generations (DGs) for micro grid application is proliferated to cope with the consequent power crisis from the conventional power grids. However, the stochastic nature of solar PV and dynamic load profile pose problem in achieving reliable and quality power supply. Thus, the integration of solar PV DG is quite challenging with respect to grid stability and controllability, power management, reliability and protection aspects. Out of all these major issues, grid stability improvement especially in islanded mode is identified as one of the prior concerns for Solar PV based DG integration.

Conventionally, PI controller is used to maintain voltage and frequency stability. However, in the PI control method the control parameters are dependent upon the PV, battery and distribution system conditions and these control parameters must be re-tuned. Therefore, in this work a novel adaptive control strategy is proposed which incorporate a closed loop control system. The deviations in the control parameters are sensed and accordingly control action is taken in adaptive control technique. The proposed strategy senses the variations in irradiance, State of Charge (SOC) of battery and load variation; and adaptively retunes the control parameter to take the corrective action and thereby

improve the stability. This work therefore develops an adaptive control strategy for controlling voltage and frequency at Point of Common Coupling (PCC). The simulation results indicate that the response of proposed adaptive controller is faster than the PI controller. The systems regain its nominal voltage and frequency values within few seconds after disturbance. To extract maximum power from solar PV system, Maximum Power Point tracking (MPPT) algorithm is used in the proposed system.

To deal with the intermittent nature of solar PV system, storage devices can be used in a Microgrid. Therefore, in proposed system the energy buffer viz. battery is integrated with the Diesel Generator (DG) set for the coordinated load management and power flow within the system. Under varying conditions of generation and loads, battery charges during the daytime when the irradiance is large and the load is less. The battery supplies the load to compensate for any deficits. When there is imbalance between generation and demand, the DG set operates to maintain system frequency. The active and reactive power (P-Q) control with solar PV, MPPT and battery storage is proposed for the islanded mode. Furthermore in this work, an algorithm is developed to coordinate the micro sources in microgrid to ensure the battery state of charge constraints.

The proposed microgrid consists of a conventional synchronous generator, Solar PV system, Battery Energy Storage System (BESS), and loads in order to investigate the effective energy flow and stability. Incorporation of PV to local load is considered through Voltage Source Converter (VSC) and thus design of an independent local DG control for such VSC application is targeted in this thesis. Different case studies are carried out to show the effective transition from grid to islanded microgrid mode, effect of variation of irradiance and effect of load change. The performance analysis reveals that the proposed system provides a smooth transition from grid to islanded microgrid mode. Also the results show that the frequency stability of microgrid enhances by the use of battery storage. The microgrid with the proposed integrated and coordinated P-Q control strategy can be adequately used in supplying critical loads.

Contents

List of Figures

List of Tables

List of Abbreviation

PV	Photo-Voltaic
DG	Distributed Generator
BESS	Battery Energy Storage System
DERs	Distributed Energy Resources
RES	Renewable Energy Sources
PCC	Point of Common Coupling
CC	Centralized Control
CB	Circuit Breaker
UPS	Uninterruptable Power Supply
HEV	Hybrid Electric Vehicles
MPPT	Maximum Power Point Tracking
EPS	Electric Power System
IEA	International Energy Agency
PEI	Power Electronic Interface
EMS	Energy Management System
CHP	Combined Heat and Power
UPC	Unit Power Control
FFC	Feeder Flow Control

PEMFC	Proton Exchange Membrane Fuel Cell
VCVSI	Voltage Control Voltage Source Inverter
CCVSI	Current Control Voltage Source Inverter
MHPCS	Multi Hybrid Power Conversion System
FC	Fuel Cells
SC	Super Capacitor
SOC	State of Charge
IM	Induction Motor
CAES	Compressed Air Energy Storage
CESS	Composite Energy Storage System
STC	Standard Test Condition
EG	Energy Gap
KCL	Kirchhoff Current Law
MPP	Maximum Power Point
FF	Fill Factor
P & O	Perturb and Observe
HC	Hill Climbing
INC	Incremental Conductance
FL	Fuzzy Logic
NN	Neural Network
VSC	Voltage Source Converter

List of Symbols

E_{ph}	Energy available in a photon
h	Planck's constant
c	Speed of light
λ	Wavelength of photon
E_g	Energy gap
I_o	Reverse saturation current
V_{therm}	Thermal voltage
q	Charge of an electron
K	Boltzmann's constant
T	Temperature of the p-n junction
I_{sc}	Short circuit current
V_{oc}	Open circuit voltage
I_{pv}	Current generated by the incident light
R_s	Equivalent series resistance
R_{sh}	Equivalent shunt resistance
K_1	Short circuit current / temperature coefficient
T_n	Nominal temperature
G	Irradiation on the device surface
G_n	Nominal radiation
I_{mod}	Module output current
N_s	Number of series connected cells

N_p	Number of parallel connected cells
V_{array}	Array voltage
I_{array}	Array current
P_{max}	Maximum power
V_{mp}	Voltage at maximum power point
I_{mp}	Current at maximum power point
η	Conversion efficiency
V_{batt}	Battery voltage
V_o	Battery constant voltage
K	Polarization constant
Q	Battery capacity
i_t	Actual battery charge
i	Battery current
R	Internal resistance of battery
$v_t(t)$	Instantaneous PCC voltage
$v_c(t)$	Instantaneous inverter output voltage
α	Phase angle of inverter output voltage relative to the PCC voltage
$V_t(t)$	Average value of PCC voltage
$V_c(t)$	Average value of inverter output voltage
L_c	Coupling inductor
S(t)	Average apparent power from inverter
P(t)	Average active power from inverter
Q(t)	Average reactive power from inverter

ω	Angular frequency
δ	Duty cycle of DC-DC booster
P_{MPPref}	Reference maximum power
P_{pv}	PV active power output
${V_t}^*$	Reference voltage
f_{ref}	Reference microgrid frequency
f_{actual}	Measured microgrid frequency
P_{acmeas}	AC side average measured active power
P_{dc}	DC side average active power
Q_{ref}	Reference average reactive power
Q_{actual}	Actual generated reactive power
$Pi_{nverter}$	Inverter active power
$P_{Battref}$	Reference battery active power
P_{Batt}	Actual injected battery active power
P_{ref}	Reference average active power
P_{actual}	Actual measured active power
$\Delta\ V_{actual}$	Actual voltage deviation

Chapter 1

Introduction

This chapter describes the solar photovoltaic (PV) based Distributed Generator (DG) and its integration challenges in microgrid. The journey of passive distribution networks to active distribution network is discussed. The role of distributed generator and its integration in active distribution network is presented. The concept of microgrid, its types, modes of operation and standards applicable are adorned. Techno-economical benefits and challenges of microgrid development are explained. The overview of solar PV technology for microgrid operation is highlighted. The importance of Battery Energy Storage System (BESS) and comparative study of different types of batteries are mentioned. The problem statement of research work, aim of study, research objectives and contributions are reported. The thesis organization is given at the end of the chapter.

1.1 Distributed Generation and Active Distributed Network

Worldwide energy demand is increasing at a faster rate to meet fast growing economics of developing countries as well as developed countries. Presently the major energy requirements are catered by using conventional sources out of which coal based thermal generation is having major contribution. Considering the rate at which conventional sources are being consumed and their impact on environment, it is necessary to adopt alternative energy technologies for sustainable development. With the ever increasing concerns on energy issues, the development of renewable energy sources is becoming more and more attractive [1]-[6].

A new trend of generating power locally at distribution voltage level by using renewable energy sources like wind power, solar photovoltaic cells, fuel cells, micro-turbines, and their integration into the utility distribution network is gaining impetus. This type of power generation is termed as Distributed Generation (DG) and the energy sources are termed as Distributed Energy Resources (DERs).

The considerable issues related to the DG operation are elaborately inspected by the International Council on Large Electric Systems (CIGRE) in late '90s [7]. The detailed review reports are presented in International Conference and Exhibition on Electricity Distribution. There are different country specific definitions and standards for DG installation throughout the Globe. These speculations are according to plant rating, operational voltage rating, stability and protection standards, power quality maintenance issues etc. Thus some universal acceptances on DG implementation are presented from previous research studies:

- DGs are not planned or dispatched centrally by the Power Grids.
- The rated generation from DGs are normally below 50 MW.
- The rated voltage level for DGs is typically 230 Volts (single phase) / 415 Volts (three phase) and may vary up to 145 kV; as they are targeted for power system distribution networks.

The integration of DGs to the conventional unidirectional electrical distributed networks (i.e. generation $\rightarrow$ transmission $\rightarrow$ distribution) makes them new bidirectional networks (i.e. generation $\rightarrow$ transmission $\rightarrow$ distribution $\leftrightarrow$ distributed generations).

Thus the distribution system becomes active and hence they are termed as Active Distribution Networks [8]. The aim of such activeness is to meet the growing energy demand at utility side.

1.1.1 Integration of Distributed Generators

The integration of DGs to active distribution network leads to various technical, economical and environmental benefits. Thus, the integration of DGs has witnessed huge demand within last two decades [9][10]. New regulations to implement DG based power systems are adopted to deal with global pollution [11]. For example, the White Book on Renewable Energy Sources (RES) is accepted by the European Union in 1998, where target has been set to generate 12% of total generation capacity by renewable based DGs by 2010. As per the report by Directive of the European Parliament (2000), 22% of the total electricity production is achieved by DG implementations [12]. Presently the DG based active distribution network technology is spread worldwide in last decade and still emerging at faster rate. The main motivations behind the DG integration are as follows:

- Due to increasing load demand and depletion in fossil fuel reserves, solutions are in search for renewable energy based generation.

- Renewable based DGs are also potential solutions to reduce environmental pollution and global warming.

- The installation of DGs integration near to local load, improves the energy density and reduces utility grid dependency. Reduction in conduction losses and betterment in power quality are other desirable features of this approach. This increases the grid reliability, and operational flexibility.

- Standalone as well as utility grid synchronous operation for active distribution network is achievable by optimal DG operation. During standalone mode DG satisfies the local load requirements and during grid connected mode it takes care of utility grid voltage parametric (i.e. magnitude, phase) concerns.

1.1.2 Active Distributed Network and Microgrid

With incorporation of DGs, the classical distribution networks are going through an era of transition from unidirectional passiveness to bidirectional activeness. The electrical power supplied to the customers at distribution level is only supplied by the national grid system in a typical passive distribution grid [13]. The introduction of DGs to distribution networks causes bidirectional power flow in the conventional grid structure. The DG insertion to utility brings deregulation of power industry [14]. The local load centres become active participant to Electric markets, for providing power to consumers in a more reliable and flexible manner [15]. But, the operational complexity of active distribution network is increased significantly with the increased flexibility by the bidirectional power exchange. Thus, policies have been introduced to change the initial 'fit and forget' approach to 'integration' of DGs, where proper power system planning and operation through active management is required [16]. The microgrid ia an integrated energy system consisting of Distributed Energy Resources (DERs) and multiple electrical loads operating as an autonomous grid either in parallel or islanded from the existing utility power grid. A typical microgrid configuration is shown in Figure 1.1.

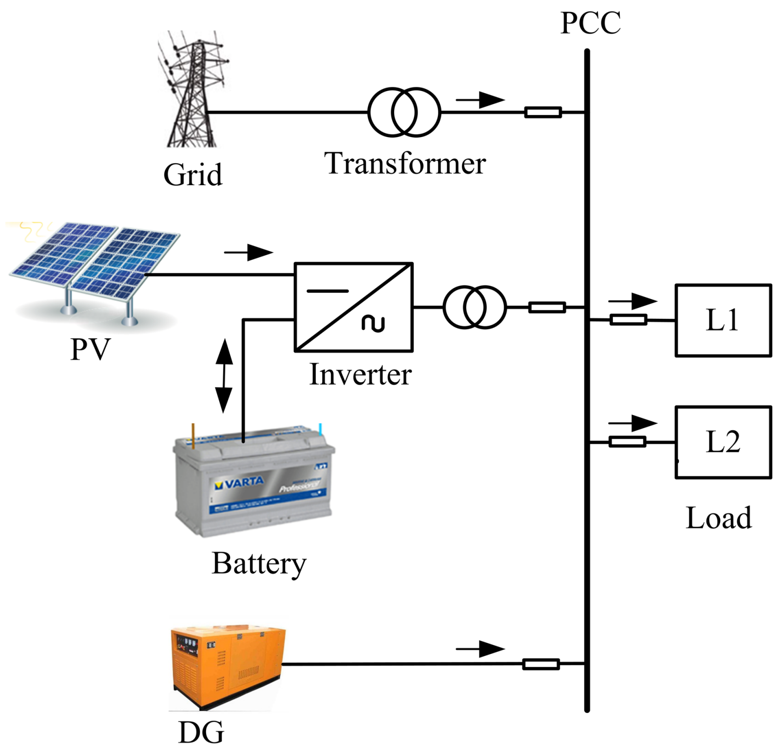

Figure 1.1: A typical microgrid configuration

1.1.3 Microgrid Types

There are different types of microgrid based on the applications [17].

- **A utility microgrid:** It is connected to the utility at one point (there could be also multiple connection points for grid connected reliability) of common coupling (PCC), can operate in island, spans over a large area (compared to a facility microgrid) and contains different types DERs and loads.

- **A remote microgrid:** It is never connected to the utility and operates mostly with decentralized control methods. The maximum power use is limited for the customers and the power quality requirements are much relaxed compared to a facility microgrid.

- **A facility microgrid:** It is normally connected with the host utility and commonly a single business-entity microgrid. A facility microgrid can continue to operate in an intentional or an unintentional island. Facility microgrid can be for an industrial or an institutional microgrid.

1.1.4 Modes of Microgrid Connection

Depending on interaction level between a microgrid and the main grid, a microgrid could be classified as autonomous or grid-connected. In an autonomous microgrid a connection to the main-grid is non existent, requiring the microgrid to be self sustaining [18]. In these types of microgrids the role of BESS is very important. On the other hand, grid-connected microgrids have the main grid as backup, but could also operate autonomously at certain times of the day, or when a scheduled maintenance is being performed at main-grid equipment.

1.1.4.1 Autonomous Mode

In this architecture, the microgrid operates in isolated mode, having to self-suffice energy demand, power quality and reliability needs of local customers. This mode of operation is envisioned for systems located in geographically remote areas where access to backbone grid is difficult or too expensive. The design and planning process of an autonomous microgrid is more complex than the grid-connected counterpart because of the sustainability dimensions of isolated operation. Sustainability is not limited to the energy equilibrium of the system, it extends to social and environmental balance of the communities where the microgrid is installed. It is to note that such type of microgrid is more likely to be constructed in rural and remote areas. The main drivers of autonomous operation are the availability of local energy resources, energy independence and reliability. Depending on the conditions of the location, the autonomous microgrids could use different type of DGs such as small-hydro, PV system, wind turbines and even diesel generator set could also be used.

1.1.4.2 Grid Connected Mode

The microgrid architectures could be used in utility systems to prevent outage and to maximize the integration of renewable energy sources. It has benefits of reducing system's losses, expand the supply mix, manage congestion and cut the greenhouse gases emissions. Also, the grid-connected architecture is suitable for industrial or commercial facilities (university campus, industrial zones, shopping centers, buildings). In these cases the main drivers are power quality and reliability enhancement and energy independence. Other advantages include demand response management, and the possibility to operate grid-independent in response to energy prices from the main grid. Viewed from the main-grid perspective, grid-connected microgrids represent a constant or controllable load with a controllable demand profile.

The comparison between grid connected and autonomous microgrid is highlighted in Table 1.1.

1.1.5 Standards of Microgrid

IEEE 1547 [19] describes Series of Interconnection Standards for Distributed Energy Resources (DERs). Standardization enhances the system integration of DER with grid

Table 1.1: Differences between grid-connected and autonomous microgrids.

Characteristic	**Autonomous**	**Grid Connected**
Mode of operation	Isolated	Grid connected
Main drivers	Sustainability of remote and rural areas, efficiency	Power quality / reliability enhancement, efficiency, costs
Use of demand response strategies	Required	Desirable
Use of Energy Storage	For self-reliance	For responding to price signals

to modernize electric infrastructure. Following are the international standards for DERs. Figure 1.2 shows IEEE 1547 part 1 to 4 for defining interconnection, operation, control and integration procedures for DERs.

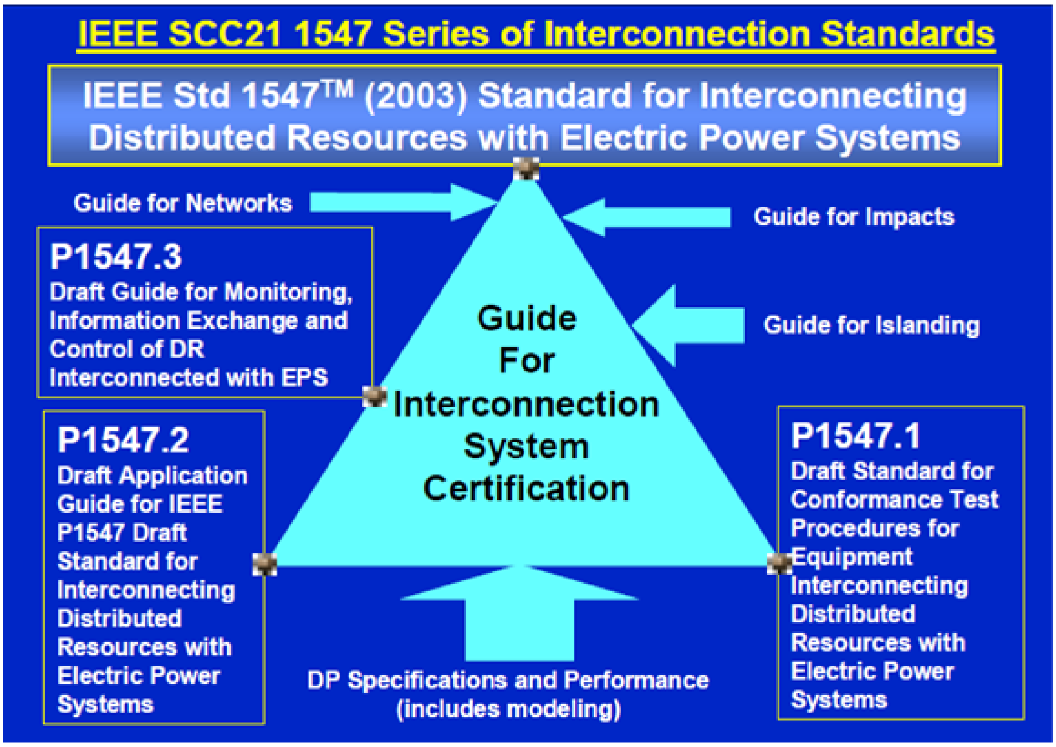

Figure 1.2: IEEE 1547 standard for interconnecting DERs with Electric Power System

1.1.6 Techno-Economical Benefits of Microgrid

(1) Autonomy: Microgrids allow generation, storage, and loads to seamlessly operate in an autonomous fashion, balancing out voltage and frequency issues with recent technology advances [20].

(2) Stability: Control approaches are based on frequency droops and voltage levels at the terminal of each device, allowing the entire network to operate in a stable manner, regardless of whether the larger grid is up or down.

(3) Compatibility: Microgrids are completely compatible with the existing centralized grid, serving as a functional unit that assists the existing system.

(4) Flexibility: Microgrids are technology neutral and able to tap a diverse mix of renewable and fossil fuels. The installation time required for expansion of such microgrid is very short and do not have to follow any precise forecast.

(5) Scalability: Microgrids facilitate the use of many small generations, storage, and load devices in a parallel and modular manner in order to scale up to higher power production and/or consumption levels.

(6) Efficiency: Energy management goals - including economic and environmental - can be optimized in a systematic fashion.

(7) Economics: Droop frequency control techniques allow for economic decision-making to be programmed into standard operating protocols.

(8) Accelerates improvement: The term microgrid reflects a new way of thinking about designing and building smart grids. The microgrid approach focuses on creating a design and plan for local energy delivery that meets the exact needs of the constituents being served, whether a city, university, neighbourhood, business park, or major mixed use development. At the local level, smart microgrids integrate consumers, buildings, distribution and generation most efficiently and economically.

(9) Increases reliability: Smart microgrids increase reliability locally through the establishment of a specific reliability improvement plan that integrates redundant distribution, smart switches, automation, power generation, power storage and other smart technologies. Local power generation and storage allow portions of the grid and critical facilities to operate independent of the larger grid when necessary and thus avoid blackouts.

(10) Helps consumers save money: Smart microgrids reliability significantly reduces the cost due to outages. Microgrids allow consumers to procure power in real-time at significantly lower costs while using local generation to hedge peak power costs.

(11) Generates revenue: Consumers and businesses can supply valuable services to the grid in return for payments from the serving utility or independent system operator. This includes demand response, real time price response, day-ahead price response, voltage support, capacity support.

(12) Encourages economic growth: More and more communities and nations are finding that microgrids can jump-start economies through new job creation at the local level and new business opportunities for stakeholders. Microgrids increase local investment through community on-bill financing of energy efficiency, local spending on grid improvements and integration of distributed energy and other smart technologies. By fostering the development of microgrids, some of these countries are establishing a new electricity business model that is more efficient, environmentally responsible, compatible with future technologies and likely to spur continuous innovation.

(13) Reduces carbon footprint: The most significant environmental benefit of a smart microgrid is its ability to use local generation and the resulting waste heat to displace coal fired generation. A local power generator can be renewable or natural gas-fueled. The smart microgrid can reuse the energy that is produced during electricity generation for heating buildings, hot water, sterilization, cooling and even refrigeration (through absorption chilling). Smart microgrids have flexibility to use wider range of clean, renewable energy sources such as wind and solar. This bottom-up consumer approach can reduce reliance on fossil fuels and lower greenhouse gas emissions.

1.1.7 Challenges of Microgrid Development

In spite of potential benefits, development of microgrid suffers from several challenges and potential drawbacks as discussed below-

(1) Distributed Generator's (DG's) Control: The objective of independent DG operation is to condition the power flow and maintain utility / load end voltage profile. The utility grid voltage, load voltage, frequency profile operations are targeted during grid connected and autonomous modes of operation, respectively [21]. These regulation aspects are to be achieved by individual DGs without communication channels, Centralized Control (C.C.), etc. Further optimal generation (parallel DGs), detection of mode of operation (i.e. grid connected and autonomous), load management for fault ride through operation etc. are achievable by the DG control schemes. Thus design of such independent controller for DG integration is an existing challenge for any effective microgrid operation. The independent DG controller is one of the major concerns for microgrid operation and is considered in present research work.

(2) Centralized Control: C.C. for optimal power dispatch to local loads, utility grid are required in a multiple DGs connected complex microgrid. Further protection coordination, active energy management and scheduling etc. also involves challenge in controlling grid [22].

(3) Active Energy Management: Energy management system is to provide active and reactive power references, voltage and frequency references to the individual DG controllers by means of artificial intelligence technologies, state of the art communication systems, etc. The load demands are dynamical in nature and thus energy management in an active manner is required [23].

(4) Protection Coordination: Microgrid operational modes are detectable by independent DG controllers and centralized control system architecture. Thus operation coordination according to load management schemes is obtained by protective Circuit Breakers (CBs). Fault ride through by CBs' coordination is another operational scenario in microgrid. The effective protection coordination with centralized / DG controller is one of the interesting research challenge [24].

(5) High Costs of Distributed Energy Resources: The high installation cost for microgrid is a great disadvantage. This can be reduced by arranging some form of subsidies from government bodies to encourage investments. This should be done at least for a transitory period for meeting up environmental and carbon capture goals. There is a global target set to enhance renewable green power generation to 20% by 2020 and to reduce carbon emission by 50% by 2050.

(6) Absence of Standards: Since microgrid is a comparatively new area; standards are not yet available for addressing operation and protection issues. Power quality data for different types of sources, standards and protocols for integration of micro sources and their participation in conventional and deregulated power markets, safety and protection guidelines, etc., could be laid down. Standards like G59/1 and IEEE 1547 could be reassessed and restructured for the successful implementation of microgrid and active distribution networks.

(7) Administrative and Legal Barriers: In most countries, no standard legislation and regulations are available to regulate the operation of microgrid. Governments of some countries are encouraging the establishment of green power microgrid, but standard regulations are yet to be framed for implementation in future.

(8) Market Monopoly: If the microgrids are allowed to supply energy autonomously to priority loads during any main grid contingency, then control on energy supply crises becomes very difficult during this period. Since the main grid will be disconnected and the current electricity market will lose its control on the energy price, microgrid might retail energy at a very high price exploiting market monopoly. Thus, suitable market infrastructure needs to be designed and implemented for sustaining development of microgrid.

1.1.8 Microgrid Stability

The stability issues in a microgrid can be divided as small signal, transient and voltage stability. The recurring reasons of each stability problem are shown in Figure 1.3 [17].

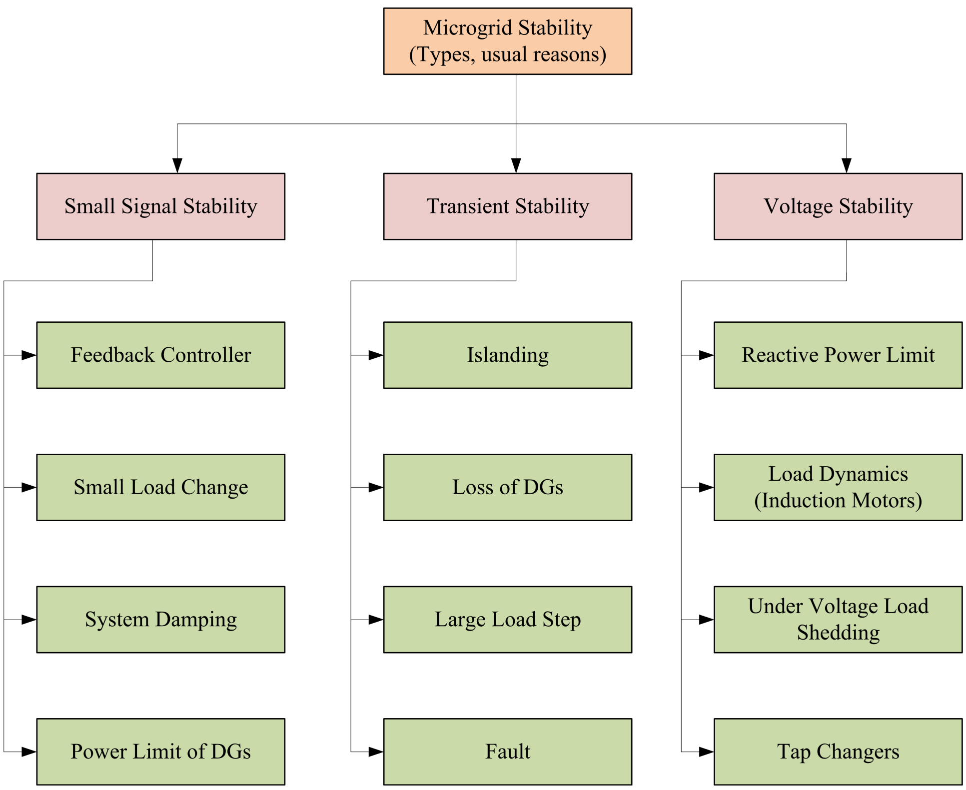

Figure 1.3: Different stability issues in microgrid and the usual reasons

Small signal stability in a microgrid is due to feedback controller, continuous load switching, and power limit of distributed generators. A fault with subsequent island, sudden change in load, disconnection of distributed generator causes transient stability. Reactive power limits, load dynamics, under voltage load shedding and tap changers create most of the voltage stability problem in a microgrid.

Different methods of microgrid stability improvement are given in Figure 1.4 [17]. The small signal stability can be improved by using supplementary control loops, coordinated control of DGs, stabilizers and energy management system. The transient stability improvement is achieved through use of storage, load shedding, adaptive protection devices and control of power electronics. The reactive power compensation methods, advance load controller and modified current limiters of distributed generators can ensure the voltage stability in a microgrid.

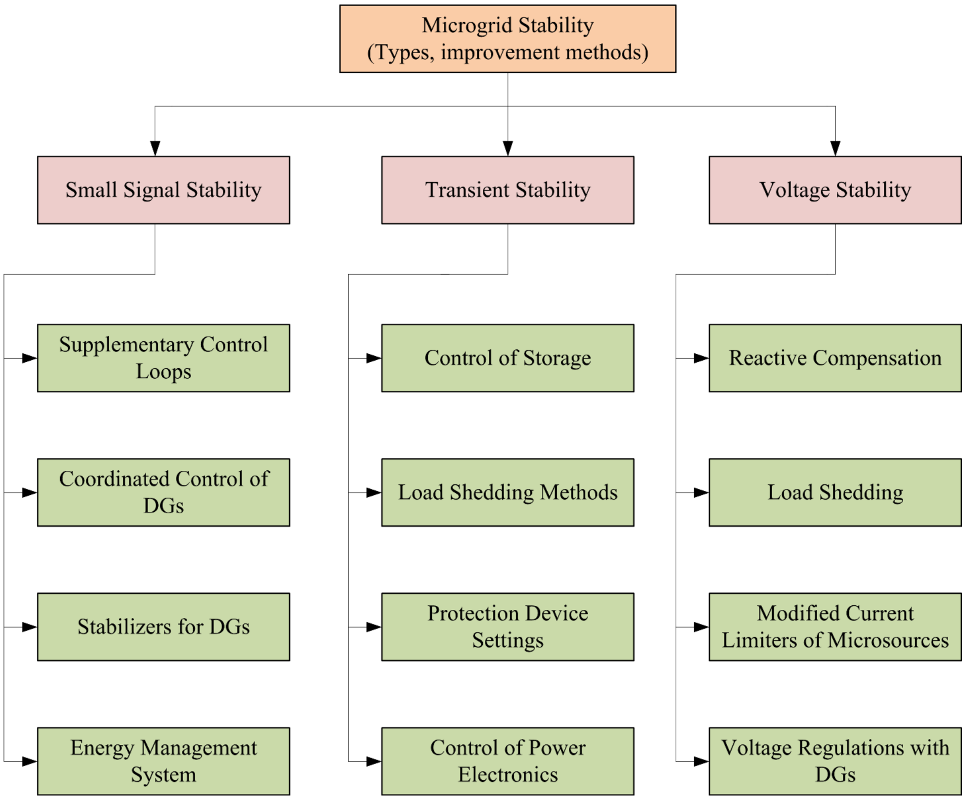

Figure 1.4: Different methods of stability improvement

1.2 Solar Photovoltaic (PV) Technology

1.2.1 Overview of Solar Energy

Electrical power (i.e. direct current or DC) generation from freely available Sun light is a feasible solution using solar PV generation system. Sun's irradiation is direct source of photon energy [25], which is converted to electrical energy by semiconductor technology based PV cells. The first installed large PV based grid interactive DG of 1 MWp was in Lugo, California, USA in 1982. The second large PV grid application of 6.5 MWp was in Carissa Plains, California, USA in 1985. After Kyoto Protocol (11 December 1997) adoption, the advancement in renewable based PV is evidenced throughout the globe. Countries like Italy, Switzerland, Germany, Austria, Spain, Japan have started to built PV based DG interfacing to active distribution networks with other renewable based generators. Several small capacity (25-500 kW) DGs are installed in Africa, Asia and Latin America [26]. A country like India is also equally participating in this venture. According to the International Energy Agency (IEA) report, India has targeted to contribute around one quarter of the total global energy demand by 2040, where 50% of it is targeted to be covered by renewable based DG integration and other than fossil fuel based generation. In 2016, India appears as the second largest solar market in globe, after China, USA and Japan. With successful completion (21 September 2016) of Kamuthi Solar Power Project (648 MWp), India is now having worlds' second largest PV plant after China's Longyangxia Dam Solar Park (850 MWp) [27]. In the last four years, India has shown a nine-times increase in the solar energy capacity, reaching 29.41 GW in June 2019 from 2.63 GW in 2014. By the end of June 2019, the total installed power generation capacity in India was 357.875 GW, 79.371 GW (22.22%) of which was generated from non-conventional renewable energy sources [28]. The power scenario in India as on 30^{th} June, 2019 is illustrated in Figure 1.5.

India is home for 18% of the world's population, still it uses only 6% of the world's primary energy [29]. Though India is abundant with solar irradiation throughout the year (more than 300 days), most of the rural and sub urban populations are still facing power crisis during peak demand in summer seasons. Thus, to cope with the growing energy crisis among urban customers and to supply electricity to suburban populations, PV based microgrid will be potential solution where independent PV based DG interface and control will be more appreciated [30]. Thus, PV based DG integration to microgrid in standalone mode is considered for present research work. DG based PV systems are targeted to feed local load demand. Surplus generation can be supplied to charge the battery. To compensate local load demand during insufficient PV generation (cloudy weather, night time etc.), Battery Energy Storage System (BESS) [28], Diesel generator [29] based auxiliary power sources are also incorporated in PV based microgrid [31][32]. For present research work, PV based microgrid interfacing and its independent controller design is considered.

Table 1.2 and Table 1.3 illustrate the total installed power generation capacity and installed capacity of non- conventional power in India respectively.

Table 1.2: Total installed power generation capacity in India as on 30^{th} June 2019

Type of Power Plant	**Capacity (in MW)**	**%**
Coal	200,749.50	56.1
Gas	24,937.22	7.0
Diesel	637.63	0.2
Nuclear	6,780.00	1.9
Large Hydro	45,399.22	12.7
Renewable	79,371.92	22.2
Total	**357,875.49**	**100.00**

Table 1.3: Installed capacity of non-conventional renewable power in India as on 30^{th} June 2019

Type of Power Plant	**Capacity (in MW)**	**%**
Solar	29,409.25	37.05
Wind	36,089.12	45.47
Small Hydro	4,603.75	5.8
Biomass	9,269.80	11.68
Total	**79,371.92**	**100**

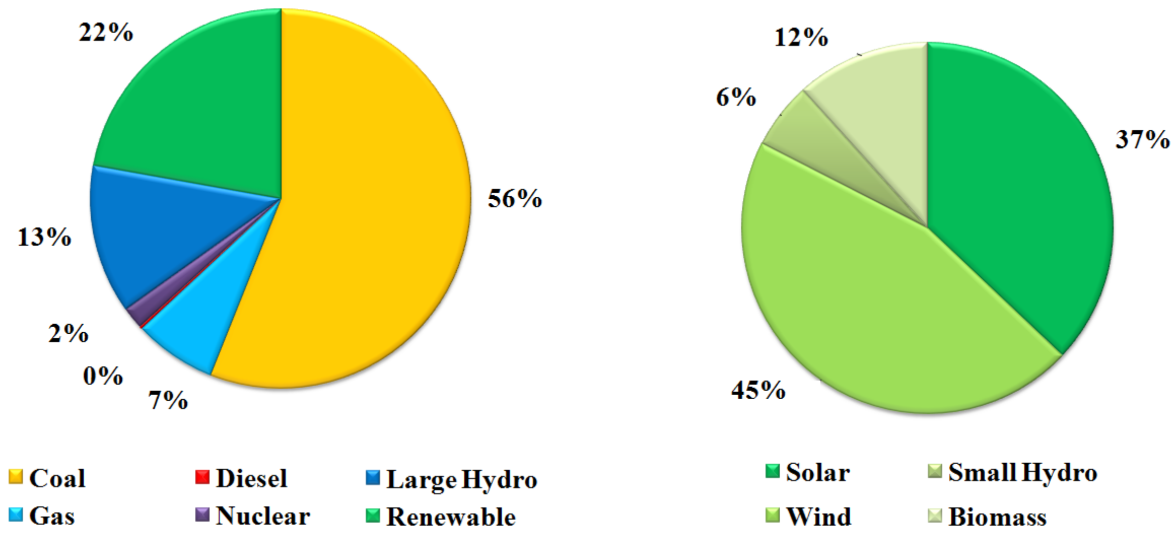

Figure 1.5: Illustrates power scenario in India (2019): (a) Total installed power capacity; (b) Installed non-conventional renewable based power capacity.

1.2.2 Solar PV Cell Working

A photovoltaic cell is basically a semiconductor diode whose p-n junction is exposed to light. Photovoltaic cells are made of several types of semiconductors using different manufacturing processes. The mono-crystalline and polycrystalline silicon cells are the only found at commercial scale at the present time. Silicon PV cells are made out of a thin layer of bulk Si or a thin Si film associated with electric terminals. Any one sides of the Si layer is doped to form the p-n junction. A thin metallic grid is placed on the Sun-facing surface of the semiconductor.

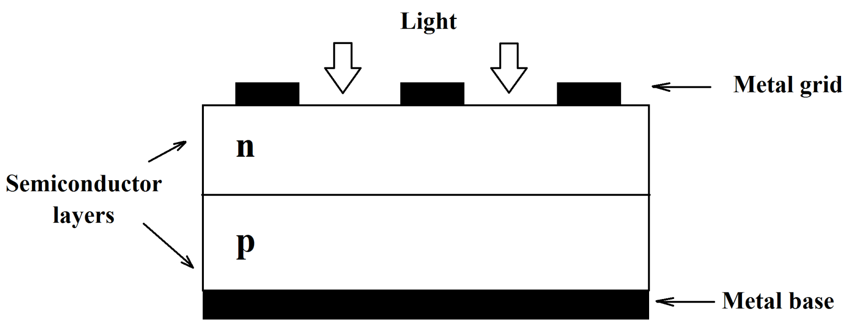

Figure 1.6: Physical structure of a PV cell

Figure 1.6 roughly illustrates the physical structure of a PV cell. If the cell is short circuited then the incidence of light on the cell generates charge carriers that causes an electric current. Charges are generated when the energy of the incident photon is sufficient to detach the covalent electrons of the semiconductor. This phenomenon depends on the semiconductor material and on the wavelength of the incident light. Fundamentally, the PV phenomenon might be portrayed as the absorption of solar radiation, the generation and transport of free carriers at the p-n junction, and the accumulation of these charges at the terminals of the PV device. Si is not the only best semiconductor material for PV cells, but its fabrication procedure is financially reasonable in large scale. Other materials can achieve better conversion efficiency, but they are not commercially reasonable.

1.2.3 Advantages of Solar PV system

The major advantages of a Solar PV system are:

- Sustainable nature of solar energy as fuel.
- Minimum environmental impact.
- Drastic reduction in customers' electricity bills due to free availability of sunlight.
- Long functional lifetime of over 30 years with minimum maintenance.
- Silent operation.

1.3 Battery Energy Storage System (BESS)

The backup energy storage devices must be included in microgrid to ensure uninterrupted power supply. These devices should be connected to the DC bus of the microgrid and provided with ride-through capabilities during system changes [33]. Batteries are devices that transform chemical energy directly into electrical energy through an Electro-chemical oxidation-reduction reaction and they are categorized as primary and secondary batteries. The former one cannot be charged electrically whereas the latter can. A BESS consists of a group of batteries linked together to produce a large enough voltage output and ampere hour reserve to provide power to an application that requires electrical energy. A battery bank can be made out of a large number of batteries connected together in series or in parallel. The way the batteries are connected together will depend upon whether it is intended to increase the voltage or ampere hour reserve. By connecting the batteries in series, the voltage output will double whilst the ampere hour reserve remains the same. Likewise, connecting the batteries in parallel will double the ampere hour reserve, whilst the voltage remains the same. A combination of both series and parallel batteries will be required to form a usable and powerful BESS. Secondary electro-chemical batteries are of great importance to electrical power systems due to their ability to capture and store energy and to immediately dispatch the energy to meet electrical demands of a grid. Some other main uses of batteries are:

- Uninterruptable Power Supplies (UPS), commonly found in banks, offices and hospitals where an alternative to undesired disruption to electricity supply is required.
- Battery Energy Storage Systems (BESS) that are connected to power grids with the sole purpose of compensating active and reactive powers.
- Hybrid Electric Vehicles (HEV) where batteries are used to capture and store electrical energy for transportation.

1.3.1 Necessity of BESS in Microgrid

The power grids of the future are fast integrating with distributed power generation systems. Due to the intermittent nature of renewable, the continuous variations of the load, energy storage is usually needed in a renewable powered microgrid. The renewable output power profile and the load profile are two important factors in deciding the capacity and type of the energy storage components. The variation in output power from a solar PV system is presented in [34], which is shown as curve (a) in Figure 1.7, whereas curve (b) of Figure 1.7 depicts a typical load profile.

The PV power output profile and the load profile shows low-frequency as well as high-frequency fluctuations, which are mutually independent in nature. Hourly average variations can be considered as low-frequency variation, whereas power transients, which sustain for minutes, seconds, or milliseconds come under the high-frequency segment.

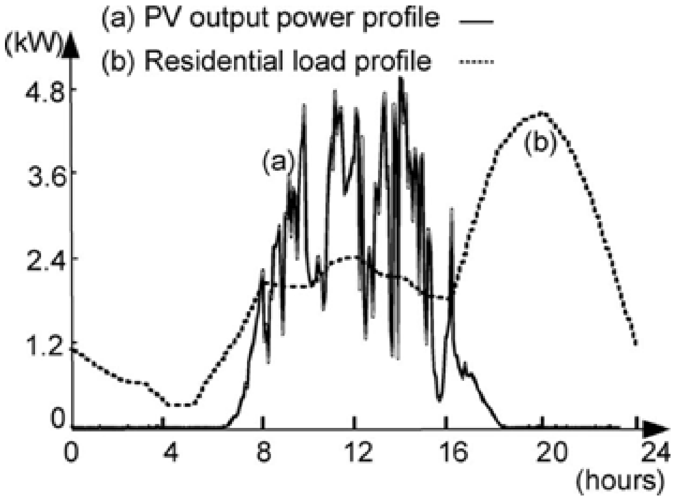

Figure 1.7: Typical 24-h (a) PV output power and (b) Residential load profile.

To buffer out the low-frequency oscillations and to compensate for the intermittency of the renewable energy sources, energy storage with high energy density is required. To provide high-frequency component of power and also to supply or absorb the high-power transients, energy storage with high power density is required. A properly designed BESS can provide an energy storage solution to renewable energy systems.

1.3.2 Comparison between Different Batteries

Table 1.4 shows the different type of batteries with their power density, energy density, efficiency, lifetime and cost, whereas Table 1.5 compares different type of battery energy storage technologies.

Table 1.4: Technical features of various batteries [35]-[37]

Battery Type	**Power Density kW/kg**	**Energy Density kWh/kg**	**Efficiency %**	**Life Time years**	**Cost Rs./kW**
Lead Acid	75-300	30-50	65-80	3-15	21000-42000
NiCd	150-300	50-75	75-85	5-20	35000-105000
NaS	150-230	150-240	75-90	10-15	70000-210000
Li-ion	150-315	75-200	90-97	5-100	84000-280000

Table 1.5: Comparison between different battery technologies

Type of Battery	**Advantages**	**Disadvantages**
Lead Acid	Inexpensive Lead is easily recyclable Low self-discharge (2-5% per month)	Shorty cycle-life (around 1500 cycles) Cycle life is affected by depth of charge Low energy density (about 30-50 kWh/kg)
Nickel Cadmium	High energy density (50-75 kWh/kg) High cycle count (1500-3000 cycles)	High degradation High cost Toxicity of cadmium metal
Sodium Sulphur	High energy density(150-240 kWh/kg) No self-discharge No degradation for deep charge High efficiency (75-90%)	Temperature of battery is kept between 300^0C to 350^0C
Lithium-ion	Very high efficiency (90-97%) Very low self-discharge (13% per month) Low maintenance	Very high cost Life cycle reduces by deep discharge Need special overcharge protection circuit

Lead Acid

Lead acid batteries are the most used batteries in the world since 1890s and are still extensively used in cost-sensitive applications where limited life cycle and less energy density are not of greater concern. Their application includes stand-alone system with photovoltaic (PV), emergency power supply system, mitigating output fluctuations from wind power systems, and as a starter batteries in transportation such as in vehicles. They have small daily self discharge rate, typically less than 0.3%, fast response time, low capital cost, and relatively high cycle efficiency. The cycle life is around 1500 cycles at 80% discharge depth and the efficiency ranges between 65 to 80%. Furthermore, lead-acid battery is a mature technology, available at lower cost, easy recyclability, and simpler charging technique. However, the drawbacks of this type of battery lies in lower energy density. Moreover, it is not suitable for discharges over 20% of its rated value as it further reduces the life cycle.

Nickel Cadmium

Nickel Cadmium (NiCd) batteries have been commercially in use since 1915s. The battery uses metallic cadmium at the negative electrode and nickel oxyhydroxide at the positive electrode. It has a greater number of cycles, higher power and energy density as compared to lead-acid batteries. The lifetime of NiCd batteries at deep discharge range from 1500 to 3000 cycles depends on the type of the used plate. The best performance is achieved when discharged between 20% to 50% of the rated value.

Sodium Sulphur

Sodum Sulphur (NaS) batteries consist of liquid sodium at the negative electrode and liquid sulphur at the positive electrode, in between these two materials there is beta aluminium tube acting as an electrolyte. The cycle life of NaS batteries is 4500 cycles which is a bit higher than lead-acid batteries and the efficiency is around 75%. It is being particularly used in Japan over 200 sites for peak shaving.

Lithium Ion

Lithium-ion batteries in recent times have been of greater importance since the start of 2000, particularly in the area of mobile and portable applications such as laptops, cell phones, and electric cars. It has been proved that these batteries have exceptional performance especially in medical devices and portable electronics. The nominal voltage level of each cell is around 3.7 volts as compared to 1.2 volts in the case of NiCd batteries. Another advantage is its higher energy and power density as compared to NiCd and lead-acid batteries. The main obstacle in using it, is the high cost due to the overcharge protection and its specific packaging. Moreover, the efficiency of these batteries are quite high usually in the range of 95-98%, and the cycle life is around 5000. Safety is another severe issue in Li-ion batteries as most of metal oxide electrodes are unstable and may decompose at elevated temperature. Hence, in order to cater to this situation, the batteries are equipped with a monetizing unit such that to avoid over-discharging and over-charging.

1.3.3 Advantages of BESS in Microgrid

- Battery storage is a reliable back-up power source to critical loads.
- Battery storage can be used to capture and store excess energy produced by power

generation systems.

- Battery storage require little to no maintenance, especially valve-regulated lead acid (VRLA) batteries.

- No fossil fuel is required to power the battery banks thus this can help to lower carbon dioxide emissions.

1.3.4 Disadvantages of BESS in Microgrid

- They are expensive to build from the ground up and require plenty of power electronic components, primarily DC to DC step-up voltage converter, bi-directional 3-phase inverters, charge controllers, and sophisticated power control.

- They have a limited life-span that is dependent upon the optimization processes to prolong the amount of years at a level that is beneficial to the power system.

- They are a potential fire and explosion hazard with harmful chemicals within the batteries may cause corrosion or poisoning if left to dissipate with the environment.

1.4 Motivation

Solar energy in India has an extremely bright future and there is no doubt that, in the renewable energy sector, solar power would play a predominant role in adding clean and non polluting energy to the country's grids. India has a huge potential of solar generation and every year lot of solar Photovoltaic systems are being added and interfaced to grid.

As compared to developed countries Indian grid system is very weak also having poor infrastructure. The significance of Photovoltaic (PV) based solutions has gained importance with the rapidly growing renewable energy market. Especially the demand of PV based Distributed Generations (DGs) for microgrid application is proliferated to cope with the consequent power crisis from the conventional power grids. The integration of DGs to achieve bidirectional active distribution networks is quite challenging with respect to grid stability and controllability, power management and reliability, protection aspects etc. Out of all these major issues microgrid stability improvement especially in islanded mode is identified as one of the prior concern for PV based DG integration. The various factors governing the stability issues are:

- Change in irradiation
- Partial shading
- Symmetrical / asymmetrical faults
- Load switching

There is need to study effect of these factors to identify the main issues which are responsible for stability of solar photovoltaic based microgrid. Hence, it is necessary to address stability issues for satisfactory operation of microgrid during normal as well as fault conditions.

1.5 Problem Statement

1.5.1 Problem Statement

The problems pointed out in the literature for microgrid are as follows-

1. When intentional or unintentional islanding of microgrid occurs, voltage and frequency stability is major concern during transition from grid connected to islanded microgrid mode.
2. The problem related to the power sharing and coordination among individual controller of Distributed Generators.
3. In solar PV base microgrid, the control parameters are dependent on the solar PV, battery, and load. This parameters must be retuned with the changing conditions.
4. Uninterrupted supply for critical load in case of grid failure or autonomous operation of microgrid.

1.5.2 Aim of Thesis

The aim of this thesis is to develop a control strategy for coordination among Distributed Generators (DGs) to improve the voltage and frequency stability of Microgrid.

1.5.3 Objectives of Thesis

Research objectives reported in the thesis are:

1. To understand the concept of microgrid and its stability issues.
2. To review the literature to understand different control techniques proposed by the researchers for control and operation of microgrid.
3. To develop an adaptive control strategy for voltage and frequency stability in microgrid.
4. To develop a scheme for extraction of maximum real power from solar PV system.
5. To propose a scheme for control of active and reactive power from the inverter in microgrid.
6. To develop the strategy for Battery Energy Storage to handle SoC constraint.
7. To analyze the performance of proposed microgrid in standalone mode with energy storage.
8. To validate the results of proposed work.

1.6 Outcome of Research

In compliance of the objectives for this research, the outcome of the research helps to improve the system performance as listed-

- The adaptive control strategy is developed and simulated in MATLAB / SIMULINK blockset which retuned the parameters of controller according to the PV power output generated, battery and load dynamics.

- The developed strategy for V-f control during transition from grid connected to autonomous microgrid mode helps to improve voltage and frequency of microgrid.
- The control strategy is developed to maintain the SoC constraint to improve the life cycle of battery.
- To maintain continuity of supply to critical load during autonomous mode of operation, the P-Q control strategy supports real and reactive power.
- The performance of microgrid is strengthened with battery storage.
- The Incremental Conductance MPPT algorithm extracts maximum power from solar PV system.

1.7 Thesis Organization

The targeted objectives of this PV based DG solution for microgrid applications are described in six major chapters in this thesis. The organization and contribution of individual chapters are discussed as:

Chapter I: Introduction

This chapter introduces the importance of solar photovoltaic (PV) based Distributed Generator (DG) and its integration challenges to microgrid applications. The journey of passive distribution networks to its active state of the art form is discussed with adequate literature survey. Different stability issues, usual reasons and improvement methods are discussed in brief. The necessity of BESS and different types of batteries in a renewable powered microgrid are presented. From exiting techno-economical benefits and challenges literature gap is drawn. The problem formulation, objectives of the thesis and research outcomes are mentioned.

Chapter II: Literature Review

The comprehensive literature review of existing control techniques is introduced in Chapter -II. The literature review is mainly divided into three sections. First section deals with introduction of microgrid and its requirement. Second section describes the existing techniques available to improve stability of microgrid. The necessity of Battery Energy Storage System (BESS) is accentuated in third section. Finally, the research gap is mentioned.

Chapter III: Solar PV Based Microgrid Modeling

This chapter deals with microgrid modeling and is divided in five sections. First section presents diode equivalent mathematical modeling of PV cells and their evolution to PV modules and array by series and parallel combination. The requirement of MPPT scheme for effective PV operation is detailed in section two. The battery modeling and power flow at VSC is presented in section three and four respectively. The section five discusses the results obtained by simulating the various case studies under consideration in MATLAB / SIMULINK environment.

Chapter IV: Controller Design for Proposed PV Based System

The section one provides block diagram of proposed solar PV based microgrid. An integrated control of solar PV system with Maximum Power Point Tracking (MPPT) algorithm is presented in section two. In section three, the control strategy is developed for battery energy storage to enhance the micro grid stability. A control algorithm is developed to handle State of Charge (SoC) constraint of battery in section four. A scheme to control active and reactive power from inverter to supply critical load in autonomous mode of microgrid is developed in section five. Section six, describes the proposed adaptive control strategy to retune control parameters with changing conditions.

Chapter V: Simulation Studies and Results

The various schematics of microgrid are simulated in MATLAB based simulation environment. This chapter reports and discusses the simulation results elaborately.

Chapter VI: Conclusions and Future Scope

In this chapter a final conclusion is drawn based on the findings of this thesis and suggests the direction for future work.

List of publications and references are given at the end.

Chapter 2

Literature Review

The concern for climate change is driving major changes in electricity generation and consumption patterns. Various countries have set a target of 20% greenhouse gas reduction by the year 2020. Large scale changes in both transmission and distribution levels are expected to occur in the near future. Transmission system will be bolstered to transmit power generated from large geothermal, solar PV and wind farm. At distribution level, many small generators like solar photovoltaic, fuel cells, micro hydro etc. will be connected to the network. However, their integration to distribution systems disturbs the radial nature of power flow through distribution feeders.

Therefore, the interconnection of DG to the grid through power electronic converters has raised concern about safety, stability and protection. Researchers have investigated the stability issues and proposed the strategies to mitigate these issues in order to enhance the performance of microgrid. This chapter deals with the review of various techniques proposed by the researchers.

2.1 Introduction

Microgrids have a long history. Thomas Edison's first power plant constructed in 1882 - the Manhattan Pearl Street Station - was essentially a microgrid since a centralized grid had not yet been established. By 1886, Edison's firm had installed fifty-eight direct current (DC) microgrids. However, shortly thereafter, the evolution of the electric services industry evolved to a state-regulated monopoly market, thus removing incentives for microgrid developments. It has been become increasingly clear that the fundamental architecture of today's electricity grid, which is based on the idea of a top-down system predicated on unidirectional energy flows, is obsolete [38]. The term Microgrid has been defined by many people in many ways. As recorded at University of Wisconsin, Madison, USA, the term microgrid has as many as twelve competiting definitions [39]. Different definitions of microgrid are as follows:

1. An integrated energy system consisting of distributed energy resources and multiple electrical loads operating as a single, autonomous grid either in parallel to or islanded from the existing utility power grid [38].

2. The term microgrid refers to the concept of single electrical power subsystems associated with a small number of Distributed Energy Resources (DERs), both renewable and/or conventional sources, including photovoltaic, wind power, hydro, internal combustion engine, gas turbine, and microturbine together with a cluster of loads [40].

3. One starting point for the idea of microgrid was a proposed concept with modular technology that can provide grid compatible PV power supply [41]. Reference [42] defined microgrid as interconnection of small, modular generation to low voltage distribution systems forms a new type of power system. Microgrids can be connected to the main power network or be operated autonomously, similar to power systems of physical islands.

4. European Commission defines microgrids as small electrical distribution systems that connect multiple customers to multiple distributed sources of generation and storage and commented that microgrids typically can provide power to communities up to 500 households in low voltage level.

5. Early definition by Lasseter [42] implied the concept of microgrid as a cluster of loads and microsources operating as a single controllable system that provides power to its local area. This concept provides a new paradigm for defining the operation of DG. It enables high penetration of DG without requiring re-design or re-engineering of the distribution system itself.

6. Arulampalam et al. [43] have described a microgrid as a combination of generation sources, loads and energy storage, interfaced through fast acting power electronics. This combination of units is connected to the distribution network through a single PCC and appears to the power network as a single unit.

7. As Pepermans et al. [44] describe, some countries define DG on the basis of voltage level while others follow a principle that DG is connected to circuits that feed consumer loads directly. Other countries define DG on the basis of some characteristics like using renewables, cogeneration, primarily, in the form of non-dispatched type.

8. The Institute of Electrical and Electronics Engineers (IEEE) has defined Distributed Resources (DRs) as sources of electric power that are not directly connected to a bulk power transmission system. DRs include both generators and energy storage technologies. While the definition of DG is given as electric generation facilities connected to an area Electric Power System (EPS) through a Point of Common Coupling (PCC) as a subset of DR [45], EPS is defined as facilities that deliver electric power to a load; local EPS is an EPS contained entirely within a single premises or group of premises and an area EPS is one that serves local EPSs. PCC is defined as the point where a local EPS is connected to an area EPS.

9. International Council on Large Electricity Systems (CIGRE) has a Working Group on DG. It defined DG as all generation units with a maximum capacity of 100 MW usually connected to the distribution network that are neither centrally planned nor dispatched.

10. International Energy Agency (IEA) views DG as units producing power on a customer's site or within local distribution utilities, and supplying power directly to the local distribution network.

11. Willis et al. stated that DG includes application of small generators, typically ranging in capacity from 15 to 10,000 KW, scattered throughout a power system, to provide the electric power needed by electrical consumers. As ordinarily applied, the term DG includes all uses of small electric power generators, whether located on the utility system, at the site of a utility customer, or at an isolated site not connected to the power grid [46].

12. However, most accepted definition by Dr. Robert H. Lasseter [47], is the Consortium for Electric Reliability Technology Solutions (CERTS). Microgrid concept assumes an aggregation of loads and micro sources operating as a single system providing both power and heat. The majority of the micro sources must be power electronic based to provide the required flexibility to ensure operation as a single aggregated system. This control flexibility allows the CERTS microgrid to present itself to the bulk power system as a single controlled unit that meets local needs for reliability and security.

2.1.1 Microgrid and its Requirements

The future electricity network must be flexible, accessible, reliable and economical according to the worldwide smart grid initiative. In order to facilitate these objectives and to reduce Green House Gas (GHG) emission, research on various configurations of microgrid system is gaining importance, particularly with high penetration of renewable energy sources. Depending on the resource availability, geographical locations, load demand, and existing electrical transmission and distribution system, microgrid can be either connected to the grid or can work in an autonomous mode. Storage can also be a part of the microgrid architecture. The benefits of grid-connected or isolated microgrid with storage have also been identified [48].

The application of individual distributed energy resources as micro generation can cause problems such as local voltage rise, the potential to exceed thermal limits of certain lines and transformers, islanding and have high capital cost [65]. Microgrid can be a better solution for these problems. In a microgrid system, the DERs must be equipped with proper Power Electronic Interfaces (PEIs) and control to ensure the flexibility to operate as a single aggregated system maintaining the power quality and energy output. Furthermore, microgrid can reduce environmental pollution and global warming by utilizing low-carbon technology [49]. The significant potential of smaller DER to meet customer's and utility's needs can be best captured by organizing resources into microgrids [47].

A microgrid may take the form of shopping centre, industrial park or college campus. To the utility, a microgrid is an electrical load that can be controlled in magnitude. The load could be constant, or the load could increase at night when electricity is cheaper, or the load could be held at zero during times of system stress. The purpose of the Energy Management System (EMS) is to make decisions regarding the best use of the generators for producing electric power and heat. These decisions will be based upon the heat requirements of the local equipment, the weather, the price of electric power, the cost of fuel and many other considerations. The EMS will dispatch the generators and provide an overview of the Combined Heat and Power (CHP) system [50].

2.2 Review of Microgrid Control Techniques

Researchers have analyzed the various issues pertaining to the microgrid and have suggested various strategies to mitigate these issues. Piagi and Lasseter [51] argued that the intentional islanding of generation and loads has the potential to provide a higher local reliability than that provided by the power system as a whole. Microgrids can operate either interconnected to the main distribution grid, or even in isolated mode. From the grid's point of view, a microgrid can be operated within a power system as a single aggregated load and as a small source of power. For a customer, it is a low voltage distribution service with additional features like increase in local reliability, improvement of voltage and power quality, reduction of emissions, decrease in cost of energy supply etc.

With the advent of renewable technology, researchers and designers have made remarkable progress in the development of different islanded hybrid system based algorithms. A control scheme is proposed for a three phase isolated photovoltaic (PV)-diesel microgrid without energy storage element. The scheme aims to: track maximum power from the sola PV system, regulate the load voltage, compensate the load unbalance viewed by the diesel generator, and to control the diesel-engine speed. The first three tasks are achieved by controlling the pulse width modulation inverter interfacing the PV array to the system. The fourth is realized by a modified fuzzy logic controller of the diesel engine. The system operation is investigated under a variety of conditions to prove the aptness of the proposed techniques [52]. The problem of voltage magnitude and frequency escalation under particular loading conditions is focused.

The disturbance defending ability of the isolated micro-grid is weak, and the randomness and the weak controllability of new energy generation are harmful to system stability. So a completed and accurate model of the isolated micro-grid is needed to do research on key technologies. C. Guanglin et. al. [53] have proposed an operating mode for the isolated micro-grid. A PSCAD simulation model of the isolated micro-grid with wind-solar-diesel-battery hybrid power generation is built based on the operating mode. The model parameters are obtained by parameter identification method. The feasibility and the effectiveness of the proposed approach are proved by simulation and model of an island planning microgrid. The isolated Wind-Solar- Diesel-Battery microgrid model, and the control system of the diesel generator control and energy storage master operation mode were designed and simulated respectively. To maintain the long-term safe and stable operation, the advanced application functions of the energy storing emergency frequency and voltage regulation control is presented.

Depending on the requirements of the consumer group and possibly some legal issues, one may choose either autonomous or non-autonomous operation of the microgrid that supports the energy use. Additionally, the micro grid concepts were discussed alongwith pros and cons of the concept [82]. C.L. Smallwood et. al. [54] discussed technical and non-technical challenges of microgrid. A microgrid was established utilizing PV and fuel cells operated in cogeneration modes.

D. Yamegueu et. al [55] presented the results of an experimental study of a PV/diesel hybrid system without storage. Experimental results showed that the sizing of a PV/diesel hybrid system by taking into account the solar radiation and the load/demand profile of a typical area may lead the diesel generator to operate near its optimal point (70 to 80% of its nominal power). The proposed method showed that for a reliability of a PV/diesel hybrid system, the rated power of the diesel generator should be equal to the peak load. The researchers concluded that the functioning of a PV/diesel hybrid system is efficient for higher load and higher solar radiation. Experimental results showed that the contribution of PV generator for a given load affects the performance of the diesel generator. The researchers proposed the use of dummy loads (for pumping or heating water) to absorb the excess output power and multiple diesel generators running in parallel could be a solution to enhance the system efficiency. However, the researchers did not explore the behavior of system under variable load.

The steady state and transient operation of a typical microgrid are studied. The models of two dispersed generation units (photovoltaic system, wind turbine) are presented [39]. Models of the power electronics interface and control strategies for fast control of frequency and voltage magnitude without communication are derived. The approach used by F. D. Kanellos et. al. [56] is the implementation of conventional f/U droops into the batteries inverters, thus down scaling the conventional grid control concept to the low voltage grid. The aforementioned models are combined together and the model of a typical microgrid is simulated. Loads sensitive to power quality include critical computing, data processing electronic equipment, and semiconductor fabrication machinery. Such sensitive loads demand a highly reliable power supply for a fail-safe operation. It is known that downtime of the sensitive load equipment caused by power quality events results in significant loss of revenue. Conventional approaches of solving these problems use UPS systems or backup generation systems driven by fossil fuel engines. The features are made possible by upgrading operational and control features to enable them to become solutions to the sensitive load problem. A case study is made for designing a microgrid for an office-cum-warehouse facility. The electrical design of this facility by the authors is made to determine the location and ratings of two DR [57].

J. A. Peas Lopes [58], suggested that a low voltage distribution network with large amounts of small sized dispersed generation can be operated as an isolated system in certain conditions. The control strategies to be used in such a system is to deal with islanded operation and to exploit the local generation resources as a way to help in power system restoration after a general blackout. From the results obtained, it was observed that storage devices play a key role for the success of system islanding and restoration. The identification of a set of rules and conditions to be checked during the restoration stage by the microgrid components was derived and evaluated through numerical simulation, proving the feasibility of such procedures. Such a successful verification constitutes a significant contribution and shows that micro generation resources should be exploited further.

For the active power control, a variant of the conventional droop control strategy, namely the voltage droop controller. However, because of the small size of the microgrid and the high share of renewables with an intermittent character, new means of flexibility in power balancing are required to ensure stable operation. Therefore, a novel active load control strategy is presented in [59]. The aim is to render a proof of concept for this control strategy in an islanded microgrid. The active load control is triggered by the microgrid voltage level. The latter is enabled by using the voltage-droop control strategy and its specific properties. It is concluded that the combination of the voltage-droop control strategy with the presented demand dispatch allows reliable power supply without inter unit communication for the primary control, leads to a more efficient usage of the renewable energy and can even lead to an increased share of renewables in the islanded microgrid. The loads can adjust their temporarily power consumption according to the voltage level to enable demand dispatch.

R.H. Lasseter [42] has discussed some of the key technical issues such as power flow balancing, voltage control and behaviour during disconnection from the PCC (islanding), protection and stability aspects. It is expected that microgrids will operate connected to the main grid under most conditions. When failures occur in the medium or high voltage systems, the microgrid is automatically transferred to islanded operation, supplied by it from the micro generators distributed with it, as nin the physical island power systems. One of the key benefits of grid-connected DG is the increase in service quality, reliability and security [39], the challenges faced by the autonomous micro grids are discussed in [54].

Renewable energy resources such as solar and wind energies are highly advantageous compared to the conventional sources of power in many ways. But the only drawback is that their outputs depend upon the climatic conditions. Wind-Photovoltaic Hybrid System [60] utilization is becoming popular due to increasing energy costs and decreasing prices of turbines and Photo-Voltaic (PV) panels. The work in [20] focused on optimal design of a hybrid wind-solar power system for either autonomous or grid-linked applications. The proposed analysis employed quadratic programming techniques to minimize the cost while meeting the load requirements in a reliable manner. The researchers proclaimed that by using this procedure, optimum number of PV Modules and wind turbines subject to minimum cost can be obtained with good accuracy. The proposed system re-

duces both the cost and the amount of CO2 emitted from the entire setup.
F.D. Kanellos and his colleagues [71] have focused the technology evolution, environmental concerns associated with central electric power plants and deregulation of the electric utility industry that are providing the opportunity for small distributed generators to become very important in order to satisfy the on - site customer expanding power demand. The steady state and transient operation of a typical microgrid were studied. Furthermore, the stability of the microgrid was ensured during connection and disconnection to the grid. Many older types of electrical generator technologies (Type A and B) could not interface successfully without the additional expense of external reactive power compensation. Newer turbine designs have largely solved this problem [61]. Type C and D generators now provide many of the same services as traditional power plants, and some studies have even indicated that these generators are faster to react and do a better job of maintaining voltage stability than traditional power plants.

The hybrid system consists of a Photovoltaic (PV) array and a Proton exchange membrane fuel cell (PEMFC) connected to the grid [62]. The researchers suggested that two operation modes, the unit-power control (UPC) mode and the feeder-flow control (FFC) mode, can be applied to the hybrid system. This work basically aimed to coordinate the two control modes and determine the reference values of the UPC mode and FFC mode so that all constraints are satisfied. The researchers claimed that this operating strategy will minimize the number of operating mode changes, improve performance of the system operation, and enhance system stability.The findings of the researchers showed that with the operating algorithm, PV always operates at maximum output power, PEMFC operates within the high-efficiency range, and feeder power flow is always less than its maximum value. In brief, the proposed operating algorithm is a simplified and flexible method to operate a hybrid source in a grid-connected microgrid. It can improve the performance of the systems operation; the system works more stably while maximizing the PV output power. R.H. Lasseter et. al. [63] have suggested that the small DER may best meet customer's needs and add benefit to the utility grid if these resources are organized into Microgrids operated as single, controllable systems that can connect to the utility grid or operate independently; is a new approach for integrating DER into the utility distribution system. Thus the microgrid provides an effective approach to integrating many small-scale distributed energy resources into the bulk electric grid.

Author Ali Bidram et al [64], proposed a distributed two-layer control structure for ac microgrids. The first layer dealt with the voltage and frequency control of VCVSIs. The second layer regulated the active and reactive powers of CCVSIs. These controllers were implemented through two communication networks with one-way communication links and were fully distributed; each DG only required its own information and the information of its neighbors on the communication network graph. In [65], a seamless control methodology for a photo voltaic (PV)-diesel generator (DG) microgrid to operate both in the grid connected and islanded mode was proposed. It did not require any islanding detection mechanism, to change the control philosophy from the grid connected mode to the islanded mode. A second order sliding mode control has been used to control the voltage source converter of the PV source whose set points was generated by PI controllers. The maximum power point tracking algorithm for the PV system was augmented with an auxiliary signal obtained using the electrical power output of the DG for economical operation of the DG unit. The DG unit is regulated with the frequency of the microgrid while the inverter used in the PV system regulated the voltage at the point of common coupling. Similarly, if the DG is uncontrollable due to any reason, the PV system was further added with an auxiliary signal based on the frequency deviation to maintain frequency stability.

The reference [66], proposed a hierarchical active power management strategy for a medium voltage islanded microgrid including a multi hybrid power conversion system (MHPCS). To guarantee excellent power management, a modular power conversion system was realized by parallel connection of small MHPCS units. The hybrid system included fuel cells (FC) as main and super capacitors (SC) as complementary power sources. The SC energy storage compensated the slow transient response of the FC stack and supported the FC to meet the grid power demand. The proposed control strategy of the MHPCS comprised of three control loops; dc-link voltage controller, power management controller, and load current sharing controller. Each distributed generation (DG) unit used an adaptive proportional resonance (PR) controller for regulating the load voltage, and a droop control strategy for average power sharing among the DG units.

The researchers in [67], proposed an enhanced control strategy that estimated the reactive power control error through injecting small real power disturbances, which was activated by the low-bandwidth synchronization signals from the central controller. Furthermore, complex microgrid configurations (looped or mesh networks) often make the reactive power sharing more challenging. A slow integration term for reactive power sharing error elimination was added to the conventional reactive power droop control. The proposed compensation method achieved accurate reactive power sharing at the steady state, just like the performance of real power sharing through frequency droop control.

Integrated modeling, analysis, and stabilization of MV droop-controlled microgrids with IM load was presented by the researchers in [68]. A detailed small-signal model of a typical MV droop-controlled microgrid system, based on the IEEE Standard 399, with both dynamic and static loads was developed. The proposed model accounted for the impact of supply frequency dynamics associated with the droop-control scheme to accurately link the microgrid frequency dynamics to the motor dynamics. To stabilize the microgrid system in the presence of IM loads, a 2-degree-of-freedom active damping controller was proposed to stabilize the newly introduced oscillatory dynamics.

A stationary-frame control method for voltage unbalance compensation in an islanded microgrid was proposed by the researchers [65]. This method was based on the proper control of DGs interface converters. The DGs were properly controlled to autonomously compensate for voltage unbalance while sharing the compensation effort and also active and reactive powers. The control system of the DGs mainly had active and reactive power droop controllers, a virtual impedance loop, voltage and current controllers, and an unbalance compensator.

The researchers in [70] described a control strategy that is used to implement grid-connected and intentional-islanding operations of distributed power generation. This work presented an intelligent load-shedding algorithm for intentional islanding and an algorithm of synchronization for grid reconnection.

An approach of coordinated and integrated control of solar PV generators with the maximum power point tracking (MPPT) control and battery storage control to provide voltage and frequency (V-f) support to an islanded microgrid was proposed by researchers in [71]. The proposed work illustrated an effective coordination among participating micro resources while considering the case of changing irradiance and battery state of charge (SOC) constraint.

An analytical approach is developed for determining the amount of storage required to meet a reliability target at a specific load point was developed by the researchers in [72] . Then the method was extended to a more complex island-capable microgrid system where initial reliability assessment and final verification of reliability guarantee were performed using sequential Monte Carlo simulation.

The researchers in [73] investigated the problem of appropriate load sharing in an autonomous microgrid. High gain angle droop control ensures proper load sharing, especially under weak system conditions. However, it has a negative impact on overall stability. A supplementary loop was proposed around a conventional droop control of each DG converter to stabilize the system while using high angle droop gains.

A dynamic voltage controller that coordinates all the reactive power sources in the system to provide the necessary reactive power during motor startup was presented by the researchers in [74]. The presented Model Predictive Control (MPC) based dynamic Volt/Var Control (VVC) scheme considered the dynamics of the microgrid in the VVC formulation to overcome the voltage dip caused by motor startup. This method used predictions of voltage behavior of the system based on a simplified system model and tried to eliminate the effect of motor startup by coordinating the reactive power sources in the system.

To ensure seamless transfer between grid-connected and stand-alone parallel modes of operation, power flow was controlled using the frequency and voltage drooping technique by the researchers in [75]. The drooping coefficients were chosen to limit the energy imported by the UPS when reconnecting to the grid and to give good transient response.

The researchers in [72] presented two solutions prevent sensitive equipment from disruptive operation. Both solutions made use of distributed generation systems to maintain the voltage across the equipment in the presence of voltage dips. The emphasis of this paper was on the transient response of both solutions to balanced as well as unbalanced voltage dips.

Some aspects of stability in microgrids were investigated by the researchers in [77]. This work briefly included the stability aspects of remote, utility connected and facility microgrids de-pending on the modes of operation, control topology, types of micro sources and network parameters. The small signal, transient and the voltage stability aspects in each type of the microgrid were discussed along with scope of improvements. The conventional stability study of microgrids presented in this work facilitated an organized way to plan the microsource operation, microgrid controller design, islanding procedure, frequency control and the load shedding criteria.

The researchers in [78] dealt with the stability analysis of a dc distribution network in a hybrid micro-grid. A micro-grid with ac and dc distribution networks based on multiport power electronic interfaces (MPEIs) was conceptualized. Furthermore, an extended averaging method for modeling systems with multiple switching converters is introduced. Using this method, the dc distribution network was modeled. Furthermore, the stability assessment of this network was performed using pole-zero analysis of the small-signal model.

A critical examination of the stability robustness measures of a microgrid at an industrial site was presented by the researchers in [79]. It is shown that the stability robustness of the plant can deteriorate as the number of onsite distributed energy resources (DERs) installations increases, making the industrial power system more vulnerable to instability. Finally, the researchers concluded that the system robustness can be improved by employing the framework of Flexible Distribution of Energy and Storage resources.

The researchers in [80] proposed three techniques for solving and reducing stability problem. In the first technique, a new fuzzy logic pitch angle controller was developed. In the second technique, an energy-storage ultra capacitor was designed which directly smoothed the output power of the wind turbine and enhances the performance of the MG during the islanding mode. In the third technique, storage batteries were used to support the MG in the islanding mode.

The standard IEEE 34 bus distribution feeder is adapted and managed as a microgrid by adding distributed generations and load profiles by the researchers in [81]. Supervisory power managements have been defined to manage the transitions and to minimize the transients on voltage and frequency. Detailed analyses for islanding, reconnection, and black start were presented for various conditions. The proposed control techniques accepted inputs from local measurements and supervisory controls in order to manage the system voltage and frequency.

Voltage and frequency control approaches, inverter control modes, and the need of storage devices are addressed by the researchers in [82]in order to ensure system stability, achieve robustness of operation, and not jeopardize power quality during service restoration in the low voltage area.

The researchers in [83] investigated the impacts of different control schemes of the inverter-based DG and microgrid load types, on the microgrid stability subsequent to fault-forced islanding are investigated. A microgrid model, simulated on Matlab / Simulink software, was analyzed including a mix of synchronous and inverter-based DG and a combination of passive RLC and induction motor (IM) loads. Simulation results showed that in the presence of IM loads, the microgrid may lose its stable operation even if the fault was isolated within a typical clearing time. The findings of the researchers showed that critical clearing time of a microgrid is highly dependent on the microgrid control strategy, DG interface control, and load type. The researchers further claimed that Induction motor loads can prove problematical to microgrid transient stability, particularly in situations in which the voltage dip can cause the induction motor to pull out.

2.3 Battery Energy Storage Systems

Connecting the storage and DG's to the grid have both technical and economic impacts. The researchers in [84] focused on aims at analyzing the technical and economic impacts of distributed generators along with energy storage devices on the distribution system. The technical analysis included the transient stability analysis of a system with DG's and energy storage devices, such as a battery and ultra capacitor.

Stabilizing future atmospheric carbon dioxide (CO2) levels at less than a doubling of pre-industrial levels will be a Herculean task, requiring a continuous flow of new carbon-free power 2-3 times greater than today's energy supply to sustain economic development for a global population approaching 10 billion by the mid 21st Century. The costs of solar and wind power are partially offset by their potential benefits as distributed electricity generation sources. However, even if future development reduces their cost substantially, widespread deployment of solar and wind power in the future will face the fundamental difficulty that they are intermittent, requiring demand flexibility, backup power sources, and very likely enough electricity storage for days to perhaps a week [85].

Energy storage technologies instead convert electricity to other energy forms (gravitational, pneumatic, kinetic, chemical), with a characteristic turn around efficiency usually driven by the simplicity or complexity of conversion and reconversion between electricity and the stored energy form. For example, it can be 90-95% efficient to convert electricity to kinetic energy and back again by speeding up or slowing down a spinning flywheel. Storing electricity by compressing and later re-expanding air is usually less efficient (75%), since rapid compression heats up a gas, increasing its pressure, making further compression difficult. The electric energy lost in energy storage drives up the overall cost of generating reliable electricity from 49 wind or solar power. Another cost of energy storage is the capital investment required for the energy storage system. These costs are driven by the weight of material or volume of containment vessels needed to store a given amount of energy, termed energy density (kWh/kg or kWh/liter), again characteristic of each energy storage form. Pumped hydroelectric and compressed air energy storage (CAES) are currently economic for energy storage.

Author Mohod S.W. et al in [86] presented the micro-wind energy conversion system with battery energy storage to exchange the controllable real and reactive power in the grid. The combination of battery storage with micro-wind energy generation system synthesized the output waveform by injecting or absorbing reactive power and enabled the real power flow required by the load. The system reduced the burden on the conventional source and utilized battery storage power under critical load constraints. The system provides rapid response to support the critical loads. The scheme can also be operated as a stand-alone system in case of grid failure like a uninterrupted power supply.

The author D. Wang et al [87], demonstrated a demand response (DR) and battery storage coordination algorithm for providing microgrid tie line smoothing services. A modified coordinating control strategy was implemented through two-way communication networks to manage distributed heat pumps in a microgrid for smoothing the tie-line power fluctuations. The impact of outdoor temperature changes and customer room temperature preferences is considered in the simulation. The results showed that coordinating with DR programs can significantly reduce the size of conventional energy storage systems for large-scale integration of renewable generation resources in microgrids and improve the power quality.

A composite energy storage system (CESS) that contains both high energy density storage battery and high power density storage ultra capacitor to meet the demand during islanding mode and during grid-connected mode is proposed. During islanding mode, the main responsibility of the storage was to perform energy balance by the researchers in [88].

During grid-connected mode, the goal is to prevent propagation of the renewable source intermittency and load fluctuations to the grid. Energy storage of a single type cannot perform all these jobs efficiently in a renewable powered microgrid. The intermittent nature of renewable energy sources like photovoltaic (PV) demands usage of storage with high energy density.

In cases where fixed power sources, slow reacting sources, and large load transients exist, supplementary fast-reacting power transmission and adsorption can effectively ensure or restore microgrid stability. A battery based energy storage unit is ideally suited to this requirement, because of the reasonable amount of energy storage that can be managed at a significantly slower rate than the natural time constants that exist in a power system as opposed to a solution implementing a flywheel or supercapacitors [89].

2.4 Research Gap

During intentional or unintentional transition from grid connected mode to islanded microgrid mode, voltage and frequency stability is major concern as reported by the researchers. There should be a proper coordination among individual controller of Distributed Generators for the power sharing. Moreover, in solar PV based microgrid, the control parameters are dependent on the solar PV, battery, and distribution system conditions and therefore these parameters must be retuned with the changing conditions. Furthermore, in case of grid failures or autonomous operation, microgrid should support the critical load which necessitates battery back-up. The previous work in the literature either lack the inclusion of energy storage devices or voltage control along with frequency control or incorporation of control transition in different scenarios. Therefore, to enhance the performance of PV based microgrid, there is need to develop a control strategy which takes into consideration the intermittent nature of solar PV DG and adaptively retune the parameters based on the changing conditions. The next chapter deals with the modeling of solar PV based microgrid system.

Chapter 3

Solar PV Based Microgrid Modeling

This chapter describes the design of a solar PV based microgrid system. The adequate model of PV system is important to understand the effect of PV side uncertainties for microgrid stability. The mathematical modeling of PV cells and their evolution to PV modules and array by series-parallel combination are presented. The requirement of incremental conductance algorithm for Maximum Power Point Tracking (MPPT) for effective PV operation is discussed. The effect of PV side uncertainties are verified in MATLAB based simulation environment with various case considerations. The simple battery model for charging and discharging of a battery is presented.

3.1 Solar Photovoltaic System Model

PV system is one of the clean renewable energy systems. The accelerated technological advancements has increased the conversion efficiency & decreased installation cost. This makes it a fast expanding technology, doubling its capacity in every two years worldwide. PV generates DC against the voltage induced from solar illumination on an exposed p-n junction and hence widely used for autonomous / grid tied DG based applications. Solar PV systems convert solar photon energy to DC electrical energy. The elemental conversion unit is known as PV cell / Solar cell. Commercial PV cell's efficiency varies in the range of 15-30% and is capable of producing power of 1-2 kWh/m^2/day at Standard Test Condition (STC). Commonly each PV cell is capable of producing voltage of about

0.5 V and current density of about 200 A/m^2 of cell at STC. The fundamentals and operation of solar PV cell is described in the next section.

3.1.1 Solar PV Cell Fundamentals

The elemental unit of PV system is PV cell. This PV cell is nothing but p-n junction semiconductor, exposed to source of photon energy [90]. Silicon (Si) is the typical choice for semiconductor due to its abundance availability. Si is a semiconductor material with four valance electrons, sharing in covalent bonding to yield crystal lattice. In an intrinsic semiconductor, Si doping process is adopted to increase the conductivity by increasing charge carriers (electrons and holes) density. Extrinsic (n-type or p-type) semiconductors are resultant of this doping process where donors (pentavalent impurities) and acceptors (trivalent impurities) are injected to yield n-type and p-type Si materials, respectively. If such n-type and p-type materials are joined together diffusion process occurs. Due to the recombination of charge carriers in the junction region a charge carrier density deficiency is evidenced. The ionized donor or acceptor impurities which are left in the junction due to opposite attraction force, creates depletion region. Mobile charge carriers and a barrier potential exist at both sides of this region, as shown in Figure 3.1 (a).

3.1.2 Concept of Photoconduction

In absolute zero temperature semiconductors act similar to a perfect insulator with no charge carriers. But there is enough charge carriers for conduction process in that same semiconductor at STC (i.e. 25^0 C). Because of this reason the performance of PV system varies with temperature. In a Si crystal to generate charge carriers, energy (thermal, optical etc) is required to overcome energy gap (Eg) between valance band and conduction band [91]. This energy gap (in eV) varies with different semiconductor materials. Energy available in a photon (E_{ph}) is expressed by Eq. (3.1).

$$E_{ph} = hv = \frac{hc}{\lambda} Joules \tag{3.1}$$

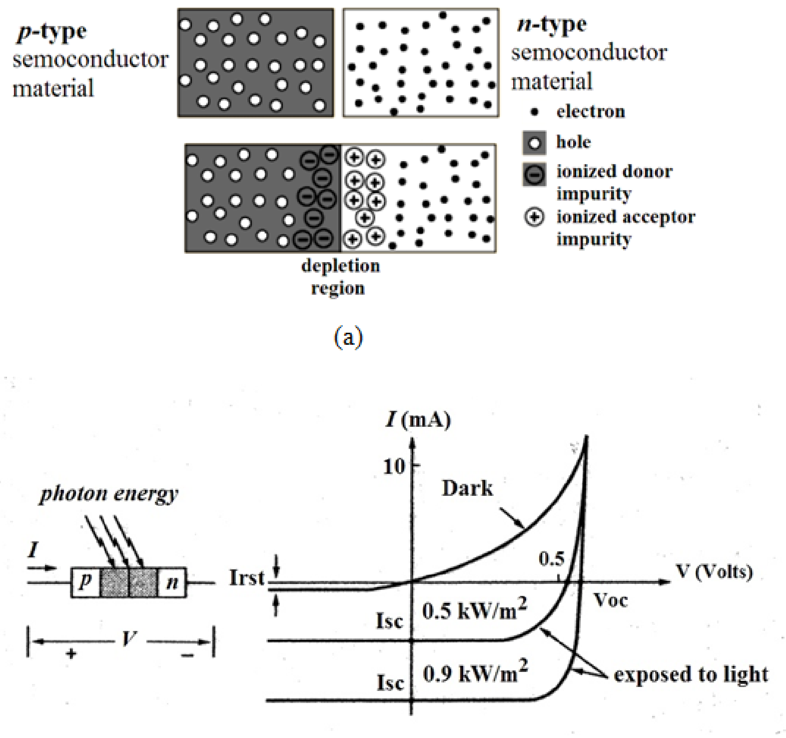

Figure 3.1: Fundamentals of solar PV cells: (a) typical p-n junction, (b) I-V characteristic of PV cell as compared with conventional p-n junction diode.

Where, h = Planck's constant (6.6310^{-34} Joules-sec.), v = frequency of photons (Hz), c = speed of light (2.9810^{8} m/sec), and λ = wavelength of photon (m). If the exposed p-n junction cell absorbs enough energy (i.e. Eph > Eg), electron-hole pair will generate from ionized impurities of depletion region. The energy will be lost in the form of heat if Eph < Eg. This loss is possible to be minimized by proper selection of PV cell's material and azimuth angle calculation [92]. These generated carriers are then swept away to their respective sides i.e. electrons to n-type side and holes to p-type side due to the barrier potential. This process increases the carrier density in both sides of p-n junction for a PV cell, and is the source of PV cell voltage.

3.1.3 Mathematical Modeling of PV System

To realize the real-time behavior of PV modules in simulation platform, a single diode equivalent model is considered [90]. Solar irradiation is highly inconsistent throughout the day, and the effect of the PV side uncertainties on the system stability is an important concern in the present study. Thus an adequate PV model is discussed from basic well known V-I characteristic of p-n junction diode. Only difference in between PV cells and p-n junction diode is that the former has exposed to sunlight where the later has considered in dark. The V-I characteristic of a conventional p-n junction diode is expressed as in Eq. (3.2).

$$I = I_0[exp(V/V_{therm}) - 1] \tag{3.2}$$

Where I_o = reverse saturation current, V_{therm} = thermal voltage = k T/ q. Here q = 1.60217646 x 10 $^{-19}$ C is the charge of an electron, k = 1.3806503 x10 $^{-23}$ J / K is Boltzmann's constant, T = temperature of the p-n junction in ^{o}K. When this p-n junction is illuminated by solar irradiation (W/m^2) the diode characteristic changes and is shifted downwards as the photon generated charge carriers are contributed with reverse leakage current, as shown in Figure 3.1 (b). Thus Eq. (3.2) can be rewritten by considering photocurrent (I_{ph}) expressed in Eq. (3.3) as

$$I = -I_{pv} + I_0[exp(V/V_{therm}) - 1] \tag{3.3}$$

If the p-n junction terminals are connected in a short circuit manner V will become zero eventually and a short circuit current (I_{sc}) will flow as I = - I_{sc}. The magnitude of I_{sc} is dependent on solar irradiation level as shown in Figure 3.1 (b). The current flow in a PV cell exposed to light is opposite in direction to the conventional p-n junction diode in darkness. If the junction terminals are not connected to any external path (i.e. isolated PV cell), then the current flow will become zero. During this scenario the induced voltage in between the p-n junction terminals is called open circuit voltage (V_{oc}) and it is expressed as in Eq. (3.4).

$$V_{oc} = V_{therm} \times ln\left(\frac{I_{sc}}{I_0} - 1\right) \tag{3.4}$$

PV cell is acting as an energy source when exposed to sunlight. The single diode equivalent circuit for ideal PV cell is shown in Figure 3.2.

Mathematical representation of I-V characteristic is given by Eq. (3.5).

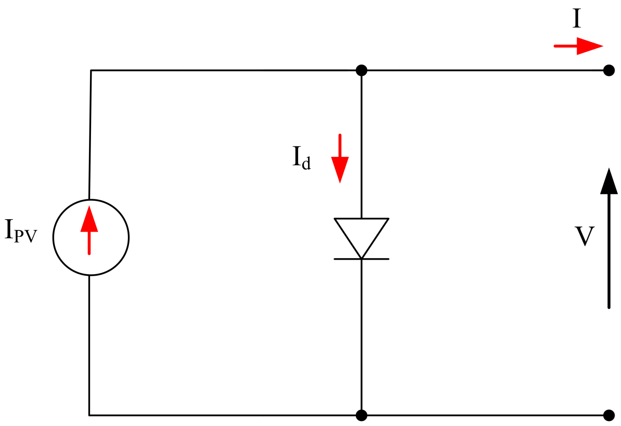

Figure 3.2: Single diode model of the ideal PV cell

Where I_{pv} is the current generated by the incident light, I_o is the reverse saturation current of the diode.

$$I = I_{pv} - I_0\Big[exp(V/V_{therm}) - 1\Big] \tag{3.5}$$

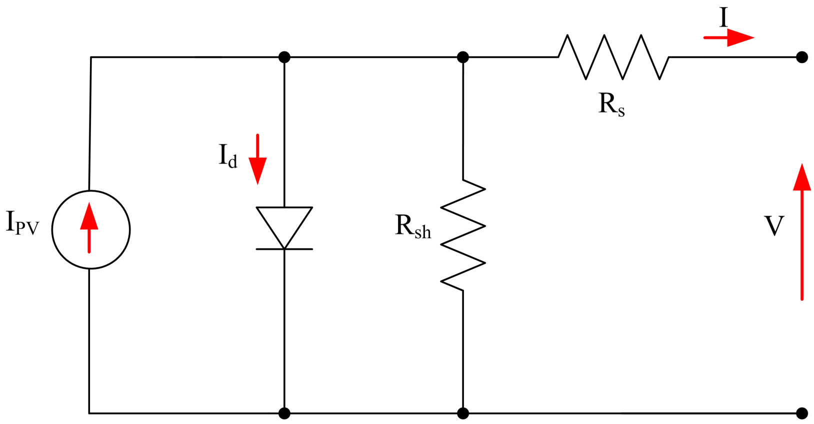

Figure 3.3: Equivalent circuit of a practical PV cell

The equivalent circuit of a practical PV cell is illustrated in Figure 3.3. By applying Kirchhoff current law (KCL), the PV cell output current can be derived as in Eq. (3.6).

$$I = I_{pv} - I_0\left[exp\left(\frac{V + IR_s}{aV_{therm}}\right) - 1\right] - \left(\frac{V + IR_s}{R_{sh}}\right) \tag{3.6}$$

where, R_s and R_{sh} are the equivalent series and shunt resistances of the cell, respectively. α is ideality factor of diode. The photocurrent of the PV cell depends linearly on the solar irradiance and the cell temperature as given in equation (3.7).

$$I_{pv} = (I_{PV}, n + K_1 \Delta T)\frac{G}{G_n} \tag{3.7}$$

Where, I_{PV},n = $\frac{R_{sh}+R_s}{R_{sh}}$ I_{sc} is the photocurrent at 25^0C and 1000W/ m^2, is the short circuit current / temperature coefficient. These coefficient values are achievable from the PV. Δ T = T - T_n (T and T_n being the actual and nominal temperature [in Kelvin], respectively), G is the irradiation on the device surface in W/m^2, and G_n is the nominal radiation in W/m^2.

The reverse saturation current (I_o) of the diode is dependent on the temperature and can be determined as in Eq. (3.8).

$$I_o = I_{o,n}\left(\frac{T_n}{T}\right)^3 \times exp\left[\frac{q \times E_g}{k \times a}\left(\frac{1}{T_n} - \frac{1}{T}\right)\right] \tag{3.8}$$

Where, E_g is the band gap energy of the semiconductor, E_g = 1.12 eV for the poly-crystal line Si at 25^0C. These PV cells are connected in series and parallel manner to obtain PV module. The PV module output current (I_{mod}) is expressed in Eq. (3.9). The PV module characteristic can be obtained in simulation platform by iterative solution of this equation.

$$I_{mod}^k = N_p I_{ph}^k - N_p I_o^k\left[exp\left(\frac{1}{V_{therm}a} \times \left(\frac{V_{mod}^k + I_{mod}^{k-1}R_s}{N_s}\right)\right) - 1\right] - \left(\frac{(N_s/N_p)V_{mod}^k + I_{mod}^{k-1}R_s}{R_{sh}}\right) \tag{3.9}$$

Where, N_s is number of series connected cells and Np is number of parallel connected cells, k is the iterative instance to obtain PV module characteristic. To configure a PV array these modules are again configured in series and parallel for higher rated power (P_{array} = V_{array} I_{array}) applications. Here V_{array} = array voltage and V_{array} = array current output as shown in Figure 3.4.

A 100 kW solar PV system is configured in simulation platform. PV array composed of 20 parallel strings and each string having 25 series connected modules. In this work Kyocera Solar KC200GT model is used. The Maximum Power Point (MPP) for a single module at 1000 W/m^2 and 25^{0}C (STC) is 200.143 W. Hence the maximum power of solar PV array at STC is 20 $\times$ 25 $\times$ 200.143 = 100.071 kW. Electrical characteristics data of Kyocera KC200GT solar module at STC is given in Table 3.1.

Table 3.1: Electrical characteristics data of Kyocera KC200GT solar module

Parameters	**Values**
Maximum Power (P_{max})	200.143 W
Voltage at Maximum Power Point (V_{mp})	26.3 V
Current at Maximum Power Point (I_{mp})	7.61 A
Open circuit voltage (V_{oc})	32.9 V
Short circuit current (I_{sc})	8.21 A
Cells per module (Ncell)	54
Temperature coefficient of V_{oc} (%/deg.C)	-0.35502
Temperature coefficient of I_{sc} (%/deg.C)	0.06

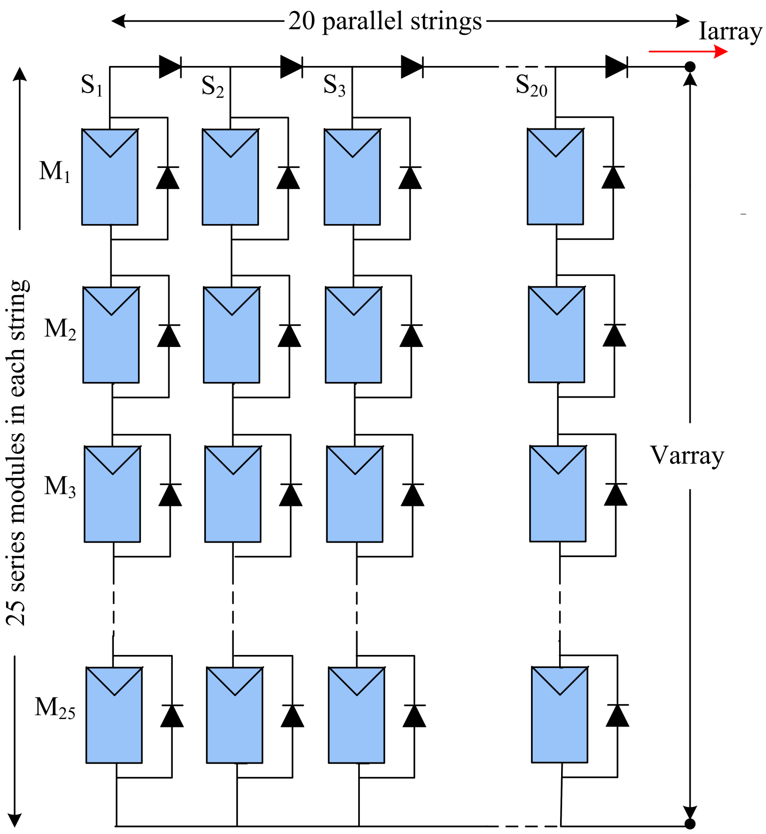

Figure 3.4: PV array schematic from series parallel combination of PV modules

3.2 Maximum Power Point Tracking

Irrespective of its application, PV is expected to be operated in a manner that maximum power can be obtained from the installed PV system. To extract maximum possible energy from PV array it is desirable to operate the PV application to the maximum power point (MPP). The PV array characteristic (i.e. Voltage vs. Current and Voltage vs. Power) is nonlinear in nature as shown in Figure 3.7 and Figure 3.8. The characteristic nonlinearity is directly dependent on quality of the PV cell, which is determined in terms of Fill factor (FF). FF is calculated to the measure quality of PV cell which is a ratio of MPP and product of V_{oc} and I_{sc} as shown in Eq. (3.10).

$$FillFactor = \frac{V_{mp} \times I_{mp}}{V_{oc} \times I_{sc}} \tag{3.10}$$

The FF of an ideal PV cell is unity where for commercial polycrystal line Si based PV cells it varies in the range between 0.5 to 0.85. The conversion efficiency (η) as in Eq. (3.11) is another parameter to understand cell performance.

$$Conversioneff. = \frac{P_{output}}{P_{input}} = \frac{V_{mp} \times I_{mp}}{P_{input}}$$

$$\eta = \frac{FF \times V_{oc} \times I_{sc}}{Insolation(\frac{KW}{m^2}) \times Areaofpanel(m^2)} \tag{3.11}$$

The nonlinear PV characteristics are variable in nature with respect to solar irradiation and PV array temperature variation. The irradiation varies throughout the day, and so does the panel temperature. The I_{sc} current depends linearly while the V_{oc} depends logarithmically on irradiation variation, while considering the array temperature constant (Figure 3.7 (a) and (b)). The conversion efficiency is less for commercial PV cells and it varies between 20% to 35%. This less efficiency of PV cells are due to deficient exposure of depletion region to solar irradiation and hence less absorption of photon energy. The photon wavelength is not sufficient for photo-generation if the cell is not properly exposed to STC (air mass, A.M 1.5). The remaining photon energy gets converted to heat.

The increased heat of PV cell reduces the band gap between conduction and valance band.

Due to this photo generated charge carriers are increased and hence current profile increased minimal. But with raise in temperature cell voltage drops 2.2 mV/^{o}C, which is a direct on contribution to overall power loss of the PV array (Figure 3.8 (a) and (b)). Now to track maximum power from such nonlinear characteristic, computation of PV array voltage (V_{arr}) and current (I_{arr}) is required, where theoretical consideration is obtained by drawing a hyperbola, representing $V_{arr} \times I_{arr}$ = constant on V-P characteristic. The computation of solar irradiation, array temperature, voltage, current etc. to extract MPP is called MPPT scheme.

In recent years different types of MPPT algorithm have been proposed and among them Perturb and Observe (P & O) [93], Hill Climbing (HC) [94] and Incremental Conductance (INC) [95, 96] methods are generally used in the MPPT controller due to their simplicity and easy applications. Oscillations around MPP value is a common problem in both P & O and HC techniques due to the fixed step perturbation and it causes power loss. In case of partial shading condition these two methods are confused and incapable to differentiate the actual global peak. INC method uses the incremental consistency (-dI/dV $\approx$ 0) or the change in power with respect to voltage (dP/dV $\approx$ 0) of the photovoltaic array to compute the MPP. Due to the fixed iteration step size, the speed of tracking is reduced and while reaching nearer MPP, it produces oscillations. The Fuzzy Logic (FL) [97] and Neural Network (NN) [98] are effective methods but under varying environmental conditions they require lots of computation (i.e. due to bulky architecture and iterative based solution). FL involves lengthy calculation to process to track MPP and large amount of data is required for the training process in NN. As the focus of the study is to evaluate VSC based microgrid system stability, an Incremental Conductance based MPPT scheme [99] is used.

3.2.1 MPP Tracking by Incremental Conductance Algorithm

From the above mentioned model equations, the PV array output characteristics are nonlinear and dependency on solar irradiation and operational temperature are clearly noticeable (Figure 3.7 and Figure 3.8). MPPT algorithms are necessary in PV applications in order to obtain the maximum power from a solar array because the maximum power point of a solar panel varies with the irradiation and temperature. The incremental conductance algorithm uses two voltages and current sensors to sense the output voltage and current of the array. In this method the array terminal voltage is always adjusted according to the MPP voltage; it is based on the incremental and instantaneous conductance of the PV module.

Figure 3.5 shows that the slope of the PV array power curve is zero at the MPP, increases on the left of the MPP and decreases on the right hand side of the MPP. The fundamental equations of this method are as follows,

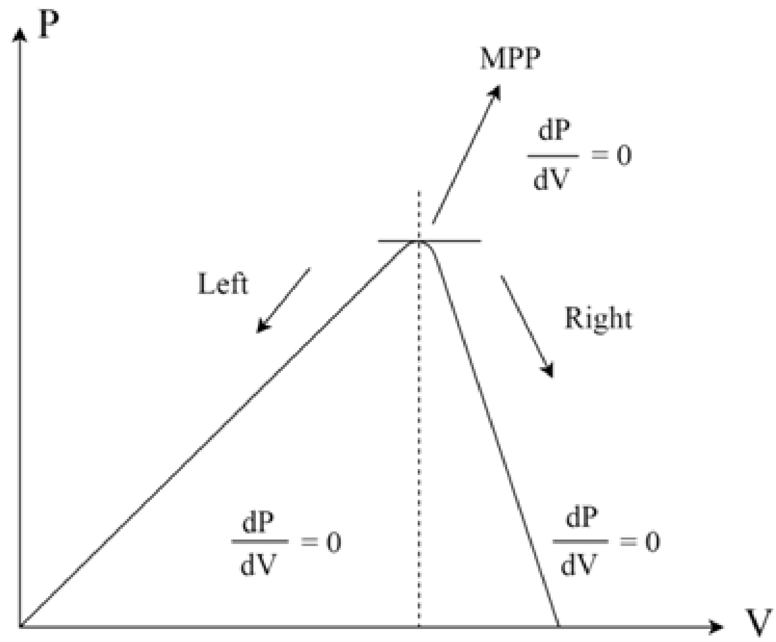

Figure 3.5: Basic of Incremental Conductance Method on a PV curve of solar module

$$dI/dV = -I/V \text{ At MPP}$$

dI/dV >- I/V Left of MPP

dI/dV <- I/V Right of MPP

where I and V are PV array output current and voltage respectively. The left side of equations represents incremental conductance of PV module and the right hand side represents the instantaneous conductance. When the ratio of change in output conductance is equal to the negative output conductance, the solar array will operate at the maximum power point. This method exploits the assumption of the ratio of change in output conductance is equal to the negative output instantaneous conductance.

We have, P=VI

Applying the chain rule for the derivative of product yields to

$$\partial P/\partial V = [\partial(VI)]/\partial V \tag{3.12}$$

At MPP, as ∂ P/∂ V = 0

The above equation could be written in terms of array voltage V and array current I as

$$\partial P/\partial V = -I/V \tag{3.13}$$

The MPPT regulates the PWM control signal of the DC-DC boost converter until the condition (∂I/∂V) + (I/V) = 0 is satisfies. In this method the peak power of the module lies at above 98% of its incremental conductance. The flow chart of incremental conductance MPPT is shown in Figure 3.6.

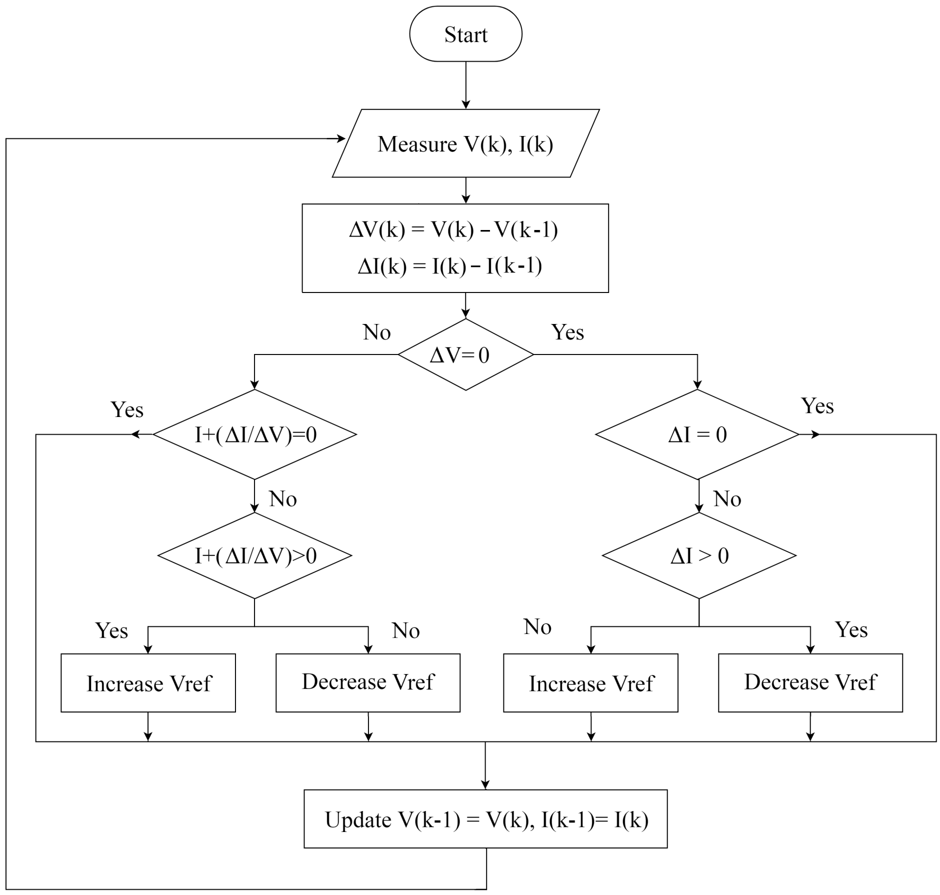

Figure 3.6: Flow chart of Incremental Conductance Method

3.2.2 Performance Verification of Solar PV Array

The PV array output validations is carried out for change in irradiation and temperature. The performance of proposed MPPT tracking is also verified for both the uncertainties.

3.2.2.1 Change in Irradiation

The solar irradiation varies throughout the day and hence the PV power generation is inconsistent in nature. This inconsistency in PV power is having direct influence on VSC dynamic stability. In Figures 3.7 (a) and (b), the I-V and P-V characteristic of PV array for different irradiation conditions are exhibited, respectively.

3.2.2.2 Change in Temperature

Photo current is directly proportional to insolation. With the increase in temperature, photo current will increase, the band gap energy reduces, this will allow more valence

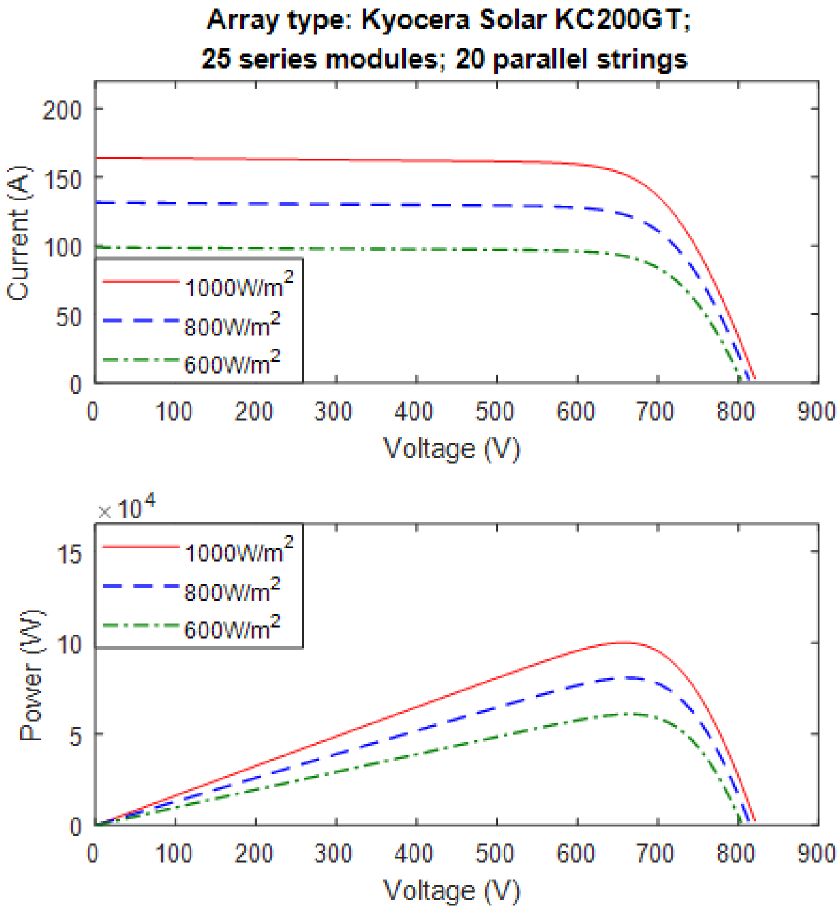

Figure 3.7: PV array (a) I-V and; (b) P-V characteristic with varying irradiance at a cell temperature of 25^0C

electrons jump into the conduction band, therefore photo current increases. On the other hand the open circuit voltage decreases as temperature increases. This results in output power of PV array decreases as temperature increases. Figures 3.8 (a) and (b), shows the I-V and P-V characteristic of PV array for different temperatures respectively.

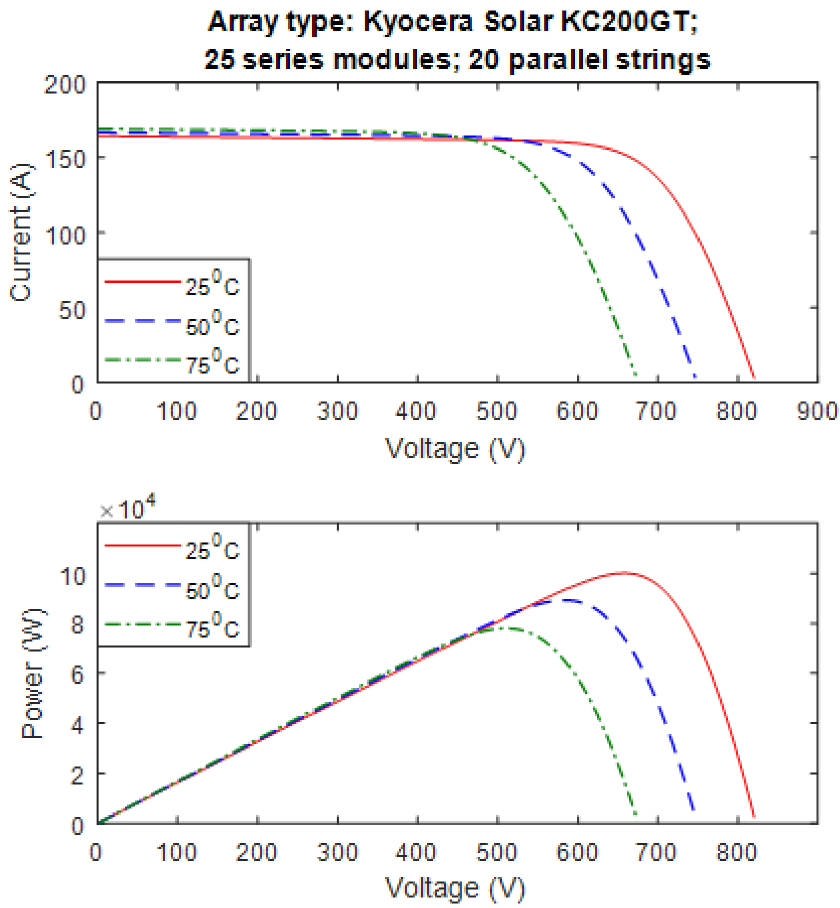

Figure 3.8: PV array (a) I-V and; (b) P-V characteristic with varying cell temperature at 1000 W/m^2 irradiance.

3.3 Battery Modeling

In this work, simple battery model is consider from the MATLAB SimPower System library with appropriate parameters which will be used for the integration in microgrid. The intermittent and unpredictable solar power output and varying load demands necessitates the need of energy buffer in microgrid. The deep cycle lead acid batteries are more feasible because the maximum capacity of the battery can be utilized. Therefore lead acid batteries are incorporated in the proposed system. It is consider that the lead acid battery can be charged up to 80% and discharged up to 20% of SoC. The simple battery model is shown in Figure 3.9. The battery discharge model for a lead acid battery is given by equation (3.14),

$$V_{batt} = V_0 - R_i - K\frac{Q}{Q - it}(it + t^*) + Exp(t) \tag{3.14}$$

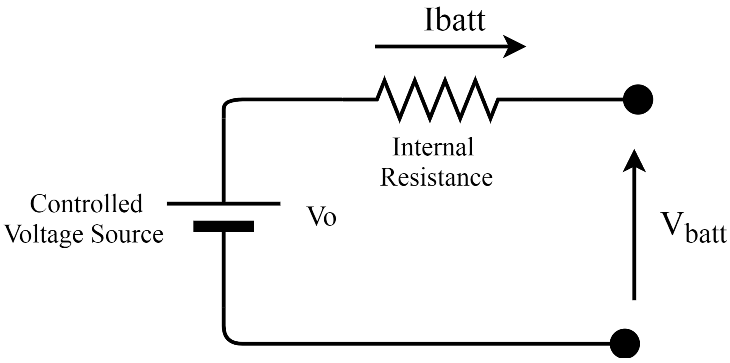

Figure 3.9: Simple battery model

The battery charge model for a lead acid battery is given by equation (3.15),

$$V_{batt} = V_0 - R_i - \left[K\frac{Q}{it - 0.1Q}\right]t^* - \left[K\frac{Q}{Q - it}\right]it + Exp(t) \tag{3.15}$$

Where V_{batt} is the battery voltage (V), V_0 is the battery constant voltage (V), is polarisation constant (V/Ah), Q is battery capacity (Ah), it = $\int$ idt actual battery charge (Ah), is the internal resistance (Ω), i is the battery current (A), i^* is filtered current (A). The size of battery is selected in such a way that it will provide a maximum backup power in case of very small or no irradiance level. Here, MPP of PV source at STC is considered as 100kW. Hence, the battery is chosen to provide this amount of power for a maximum of 1.5 hours with an energy content of 100 kWh. The battery discharge characteristic for various battery discharge current is shown in Figure 3.10.

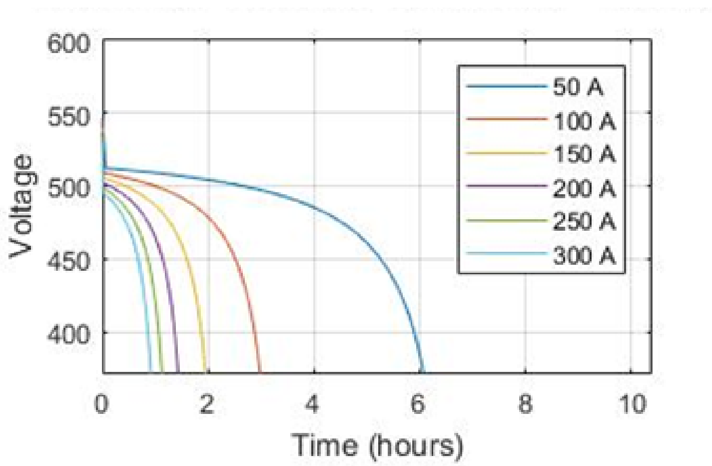

Figure 3.10: Battery discharge characteristics

3.4 Voltage Source Converter (VSC) in Microgrid

To integrate a solar PV array to AC microgrid, VSC is the usual choice where photo-generated DC power of PV gets converted to required AC power. The integration is possible to obtain in a single stage (i.e. PV array and VSC) or two stage (i.e. PV array, DC-DC converter and VSC) manner.

In a single stage conversion the extracted optimal PV power by MPPT scheme is directly considered as input to VSC, where the MPP voltage (V_{pv}) and / or current (I_{pv}) is obtained as reference to the VSC dynamic grid synchronized operation. For a two stage conversion the MPPT extracted power is contributed to the intermediate DC-DC converter where V_{pv} is used for duty cycle calculation of this unit. The DC-DC converted power is then applied as input to the VSC where DC output voltage and current are considered for grid synchronization. As the present focus of study is on improvement of microgrid stability through a nonlinear control for VSC dynamic model, two stage conversion is considered here as shown in Figure 3.11.

For the PV base microgrid, integration to utility grid requires three phase AC power and thus a 6-pulse IGBT based VSC is considered for the proposed study. Microgrids are short distance active distribution networks connected to different DGs, local load centers and / or utility grid, and hence are resistive (R) in nature as compared to inductive (X) property. To obtain mentioned stability analysis, a simple microgrid structure is considered as in Figure 3.11, where a double stage PV system is incorporated to a single local load center and utility grid. The proposed low voltage microgrid is considered as weak grid, and hence the active power regulation is according to voltage magnitude difference and reactive power regulation is on power angle between VSC output and PCC voltage [100].

An instantaneous active power and reactive power theory is adopted. Consistent with the standard steady state power definitions, this theory is an extension of the standard definitions and other instantaneous power theories. It defines the instantaneous active

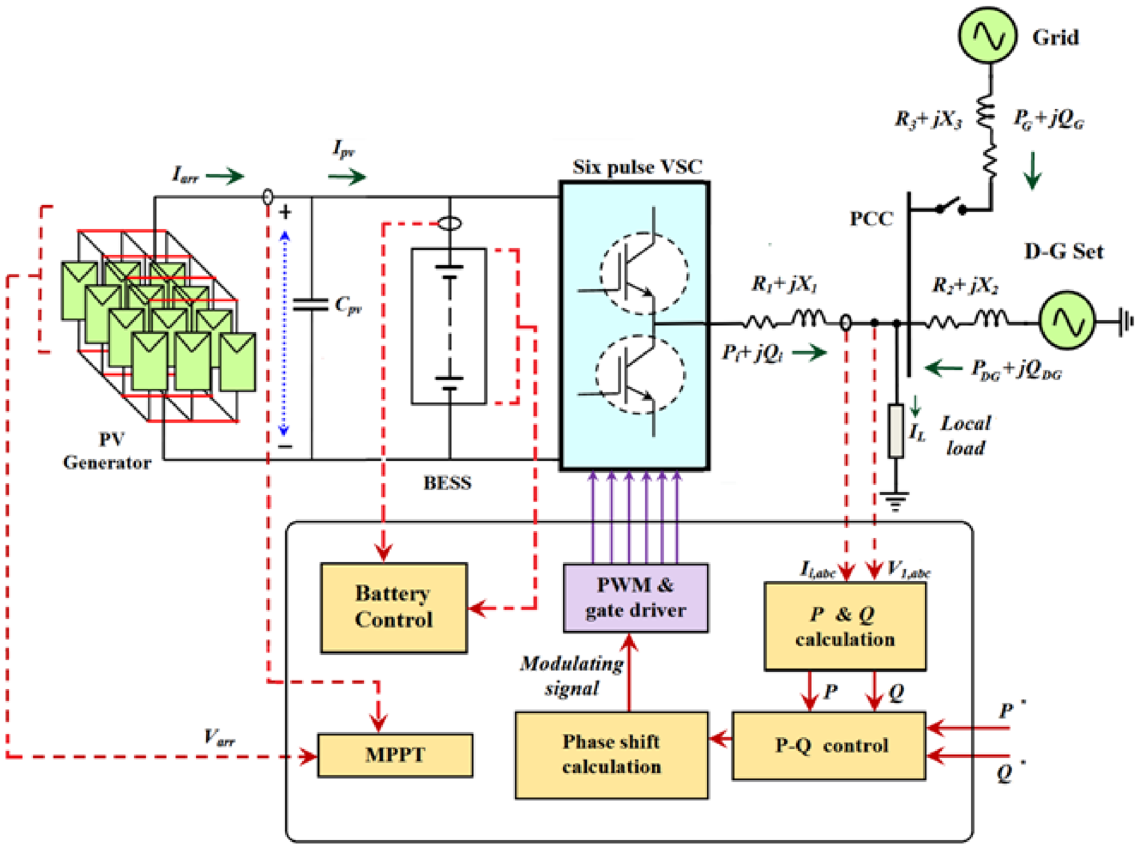

Figure 3.11: PV based VSC integration to microgrid

current, instantaneous reactive current, instantaneous active power and instantaneous reactive power. It also defines the average power, average active power, average reactive power, apparent power, apparent active power and apparent reactive power. These power definitions are instantaneous values, and functions of time. Similarly, the rms values of voltages and currents are also defined as instantaneous values. The instantaneous active power and reactive power theory is valid in various power systems, whether single-phase or three-phase, sinusoidal or non-sinusoidal, balanced or unbalanced.

The DER system shown in Figure 3.11 can also be simplified as the single-phase equivalent circuit in Figure 3.12.

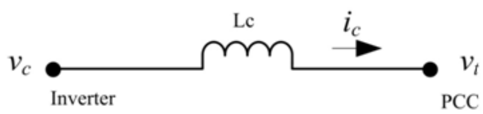

Figure 3.12: Simplified equivalent circuit

Let $v_t(t)$ and $v_c(t)$ denote the instantaneous PCC voltage and the inverter output voltage respectively, α is the phase angle of $v_c(t)$ relative to the PCC voltage.

$$v_t(t) = \sqrt{2}V_t cos(\omega t) \tag{3.16}$$

$$v_c(t) = \sqrt{2}V_c cos(\omega t + \alpha) \tag{3.17}$$

The rms values of $v_t(t)$ and $v_c(t)$ are given in (3.18) and (3.19), respectively.

$$V_t(t) = \sqrt{\frac{2}{T}\int_{t-\frac{T}{2}}^{t} V_t^2(t)dt} \tag{3.18}$$

$$V_c(t) = \sqrt{\frac{2}{T}\int_{t-\frac{T}{2}}^{t} V_c^2(t)dt} \tag{3.19}$$

where T/2 is one half of the period of the voltage. In the instantaneous reactive power theory, the averaging interval can be different values depending on the system characteristics. In a sinusoidal system with period T, the averaging interval is usually chosen as T/2. $V_t(t)$ and $V_c(t)$ are instantaneous variables, function of time t.

The current from the inverter to the PCC is denoted as i_c (t):

$$i_c(t) = \frac{\sqrt{2}}{\omega L_c}\Big[V_c sin(\omega t + \alpha) - V_t sin(\omega t)\Big] \tag{3.20}$$

where α is the phase angle between the PCC voltage $V_t(t)$ and the inverter current $i_c(t)$. The average power of the DER is denoted as P(t):

$$P_t(t) = \frac{2}{T}\int_{t-\frac{T}{2}}^{t} v_t(t)i_c(t)dt = \frac{V_t V_c}{\omega L_c} sin\alpha \tag{3.21}$$

The instantaneous active current component of the inverter current $i_c(t)$ is defined as,

$$i_{ca}(t) = \frac{P(t)}{V_t^2(t)} i_c(t) \tag{3.22}$$

The instantaneous reactive current of the inverter current is defined as,

$$i_{cn}(t) = i_c(t) - i_{ca}(t) \tag{3.23}$$

The i_{ca}(t) and i_{cn}(t) are the active component and the reactive component of the inverter current i_c(t). By controlling these two current components, the active power and the reactive power of the DER can be controlled independently. The rms values of i_{ca}(t) and i_{cn}(t) are defined as I_{ca}(t) and I_{cn}(t), respectively.

$$I_{ca}(t) = \sqrt{\frac{2}{T}\int_{t-\frac{T}{2}}^{t} i_{ca}^2(t)dt} \tag{3.24}$$

$$I_{cn}(t) = \sqrt{\frac{2}{T}\int_{t-\frac{T}{2}}^{t} i_{cn}^2(t)dt} \tag{3.25}$$

The apparent power S(t) and the average reactive power Q(t) of the DER are:

$$S(t) = V_t(t)I_c(t) = \frac{V_t}{\omega L_c}\sqrt{V_t^2 + V_c^2 - 2V_tV_c cos\alpha} \tag{3.26}$$

$$Q(t) = V_t(t)I_{cn}(t) = \sqrt{S^2(t) + P^2(t)} = \frac{V_t}{\omega L_c}(V_c cos\alpha - V_t) \tag{3.27}$$

where Q(t) is defined as positive if the inverter injects reactive power to the PCC, and negative if the inverter absorbs reactive power from the PCC. P(t) and Q(t) in (3.21) and (3.27) can be approximated by the first terms of the Taylor series if the angle α is small, as shown in (3.28) and (3.29),

$$P(t) \approx \frac{V_tV_c}{\omega L_c} \tag{3.28}$$

$$Q(t) \approx \frac{V_t}{\omega L_c}(V_t - V_c) \tag{3.29}$$

3.5 Conclusion

In this chapter solar PV integration through Voltage Source Converter (VSC) to operate as DG for microgrid operation is discussed. Basically microgrid is a weak distribution network and hence, effect of PV side uncertainties is of primary concern in this chapter. After a brief theory, modeling of PV array with MPPT scheme is presented here. Battery charge and discharge model is discussed. An instantaneous active and reactive power theory is used to develop control algorithm for this system. A MATLAB based simulation study is presented to evidence the effectiveness of MPPT scheme for various PV side uncertainties. In next chapter, controller design for proposed PV based microgrid will be discussed in detail.

Chapter 4

Controller Design for Proposed PV Based System

In this chapter the proposed solar PV based microgrid is designed with MPPT integrated V-f control and P-Q control strategy. To enhance the microgrid stability when disturbance occurs due to load change or fluctuations in renewable generation, the control strategy is developed for battery energy storage and highlighted. This control strategy also handles State of Charge (SOC) constraint of battery. The adaptive control strategy for proposed system is developed to retune control parameters of controller with changing system conditions.

4.1 Proposed Solar PV Based Microgrid

The block diagram of proposed solar PV based microgrid is shown in Figure 4.1. The solar PV system is operating at Maximum Power Point (MPP) and battery energy storage is considered as back up to supply critical load.

The Microgrid is connected to the distribution voltage level utility grid at the Point of Common Coupling (PCC) through the circuit breakers. The PV array is integrated through a power electronic converter and controlled using a Maximum Power Point Tracking (MPPT) algorithm to obtain the maximum power under varying operating conditions. The energy buffer viz. battery is integrated with the Diesel Generator (DG) set for the

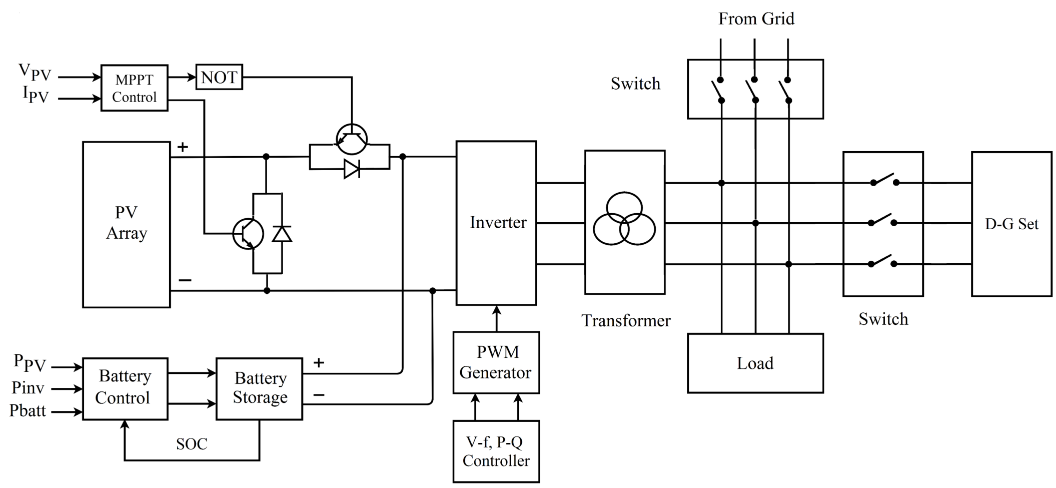

Figure 4.1: Block diagram of proposed solar PV based microgrid

coordinated load management and power flow within the system. When there is imbalance between generation and demand, the DG set operates to maintain system frequency [101]-[102].

4.2 MPPT Integrated Voltage-Frequency (V-f) Controller

The proposed MPPT integrated V-f controller is designed to help the voltage and frequency control in solar PV based microgrid. The control system consist of one loop for MPPT control at DC-DC converter, second loop for voltage control and third loop for frequency control at DC-AC inverter. The individual controller are explained in next section.

4.2.1 Maximum Power Point Tracking (MPPT) Controller

The MPPT controller is used to track Maximum Power Point (MPP) of PV array is shown in Figure 4.2(a). Reference Maximum Power Point (P_{MPPref}) is obtained from look table of irradiance verses MPP. After which it compares measured solar PV output power ($P_{pvactual}$) with this reference MPP power. The error obtained is given to a PI_1

controller. This controller gives the duty cycle output (δ) for the DC-DC boost converter so that PV array will always operates at the reference MPP point. The duty cycle is given by Eq.(4.1).

$$\delta = K_{p1} * (P_{MPPref} - P_{PV}) + K_{i1} \int_0^1 (P_{MPPref} - P_{PV}) dt \tag{4.1}$$

Where, K_{p1} is controller proportional gain and K_{i1} controller integral gains respectively.

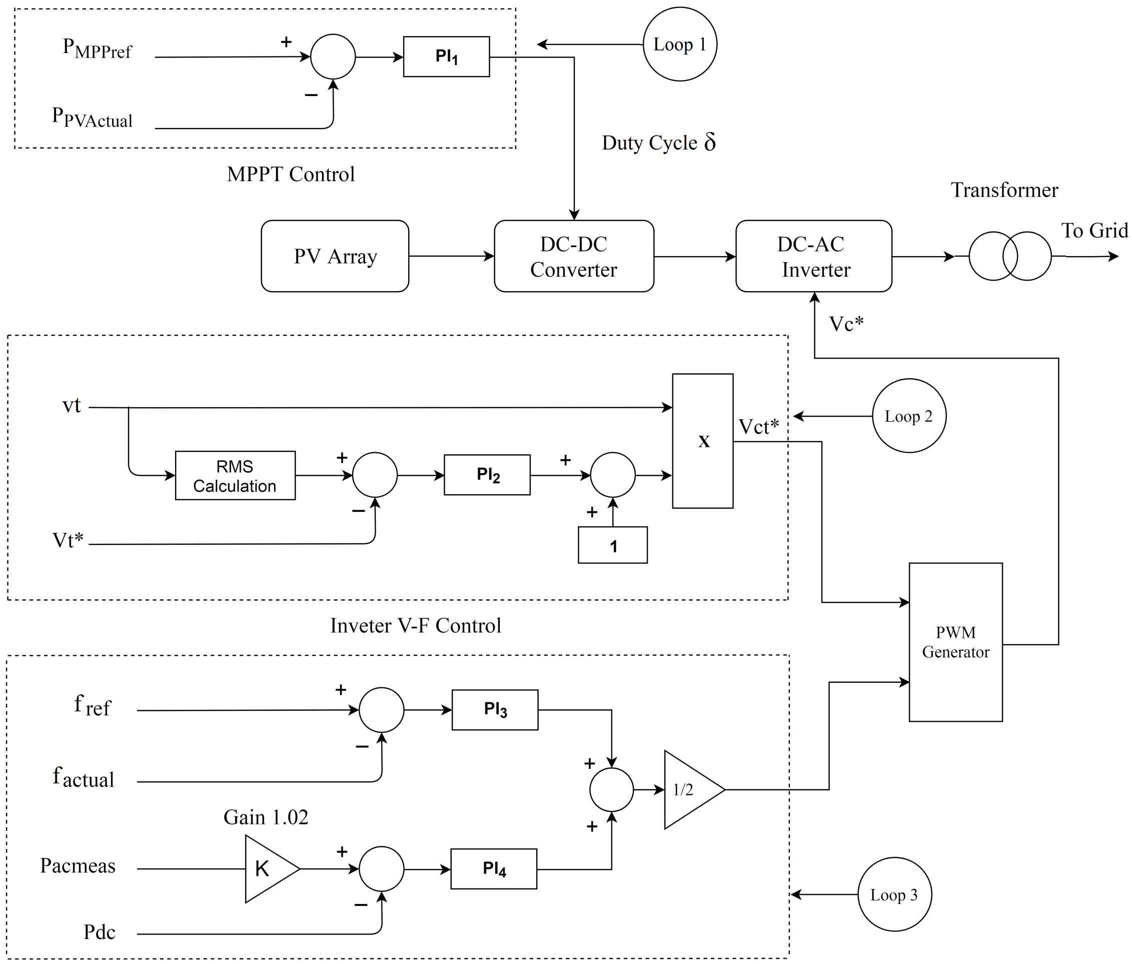

Figure 4.2: The scheme of MPPT integrated V-f control method for solar PV system (a)Loop 1: MPPT controller, (b)Loop 2: Voltage controller, (c)Loop 3: Frequency controller

4.2.2 Voltage Controller

Voltage at AC side can be controlled by using PI_2 controller. The PCC voltage is measured (v_t) and then its rms value (V_t) is calculated. This rms value of PCC voltage (V_t) is compared with reference $V_t{}^*$ and then error is given to a PI_2 controller. The inverter output voltage $V_c{}^*$ is controlled in such a way that it remains in phase with PCC voltage, and the magnitude of inverter output voltage is controlled so that PCC voltage is maintained at a reference $V_t{}^*$. The inverter output voltage is given by Eq.(4.2). The proposed voltage controller is shown in Figure 4.2(b).

$$v_{ct}^*(t) = v_t(t)[1 + K_{p2}(V_t^*(t) - V_t(t)) + K_{i2}\int_0^t (V_t^*(t) - V_t(t))dt] \tag{4.2}$$

where, K_{p2} is controller proportional gain and K_{i2} is controller integral gain.

4.2.3 Frequency Controller

The frequency can be controlled by controlling the inverter side real output power. The measured frequency is compared with reference frequency and then error is given to P_{i3} controller which will give the phase shift α_1. The phase shift α_1 shifts the voltage waveform in timescale such that the active power injected is sufficient to maintain 50Hz frequency. This phase shift is given by Eq.(4.3).

$$\alpha_1 = K_{p3}(f_{ref} - f_{measured}) + K_{i3}\int_0^t (f_{ref} - f_{measured})dt \tag{4.3}$$

To keep the real power balance at DC and AC side of inverter, PI_4 controller is used. The AC side calculated real power is multiplied by a multiplying factor of 1.02 considering efficiency of inverter as 98%. The DC real power is compared with this value of AC power and then error is given to PI_4 controller which will give the phase shift α_2. This phase shift is given by Eq.(4.4).

$$\alpha_2 = K_{p4}(1.02 * P_{AC} - P_{DC}) + K_{i4}\int_0^t (1.02 * P_{AC} - P_{DC})dt \tag{4.4}$$

The phase shift contributions from both sides of inverter are averaged which will obtain the final phase shift given by Eq.(4.5) and then it will generates the reference signal of voltage v_c^* for the inverter PWM.

$$\alpha = \frac{\alpha_1 + \alpha_2}{2} \tag{4.5}$$

Here, the reason for considering phase shift contributions from both DC and AC side active power is to control the DC side voltage and achieve the desired value. By making α_1 and α_2 close in range through the controller gains, it can be assured that the active power at the DC and AC sides is balanced. This, coupled with the voltage control loop, assures that the DC side voltage is maintained at the value desired by the AC side voltage. The proposed frequency controller is shown in Figure 4.2(c).

4.3 Battery Storage Controller

The solar PV system is supported by Battery Energy Storage (BES) to supply or absorb active power and support frequency control. When there is abundant solar power, solar PV output power at MPP is more than the active power required for controlling the microgrid frequency, then battery gets charged. If there is reduced solar irradiance, the active power required to control the microgrid frequency is more than the solar PV output power, then battery gets discharged and supplies deficit power to maintain 50Hz frequency. To fulfill such requirement of energy balance, battery charge controller is developed as shown in Figure 4.3. This controller also handles State of Charge (SOC) constraint of battery.

For the battery control required reference active power ($P_{Battref}$) is calculated dynamically. The active power injected by inverter ($P_{inverter}$) is subtracted from solar PV power (P_{pv}) to give reference active power to battery. The actual battery power (P_{Batt}) is subtracted from reference active power ($P_{Battref}$); this error signal is given to PI_5 controller. The output signal from PI_5 is then compared with a triangular waveform to generate signal S*. The mathematical modeling for S* is illustrated in Eq.(4.6).

$$S^{*} = K_{p5}(P_{Battref} - P_{Batt}) + K_{i5}\int_{0}^{t}(P_{Battref} - P_{Batt})dt. \tag{4.6}$$

K_{p5} is proportional gain and K_{i5} is integral gain. To differentiate the charging and discharging mode of the battery, P_{pv} is compared with $P_{inverter}$. When there is abundant solar power and solar PV output power at MPP (P_{pv}) is more than or equal to the active power required for controlling the frequency ($P_{inverter}$) i.e. $P_{pv} >= P_{inverter}$, then the battery is in charging mode. The result of this comparison is passed through a logical AND to generate a switching signal which activates the Buck mode of the DC-DC converter. If there is reduced solar irradiance and the active power required to control the frequency ($P_{inverter}$) is more than the solar PV output power (P_{pv}) i.e. $P_{inverter} > P_{pv}$, then the battery is in discharging mode. The opposite of this comparison is passed through a logical AND to generate a switching signal which activates the Boost mode of the DC-DC converter. Hence, with this control logic, the converter is capable of operating in both directions and therefore, effectively charging and discharging the battery whenever required.

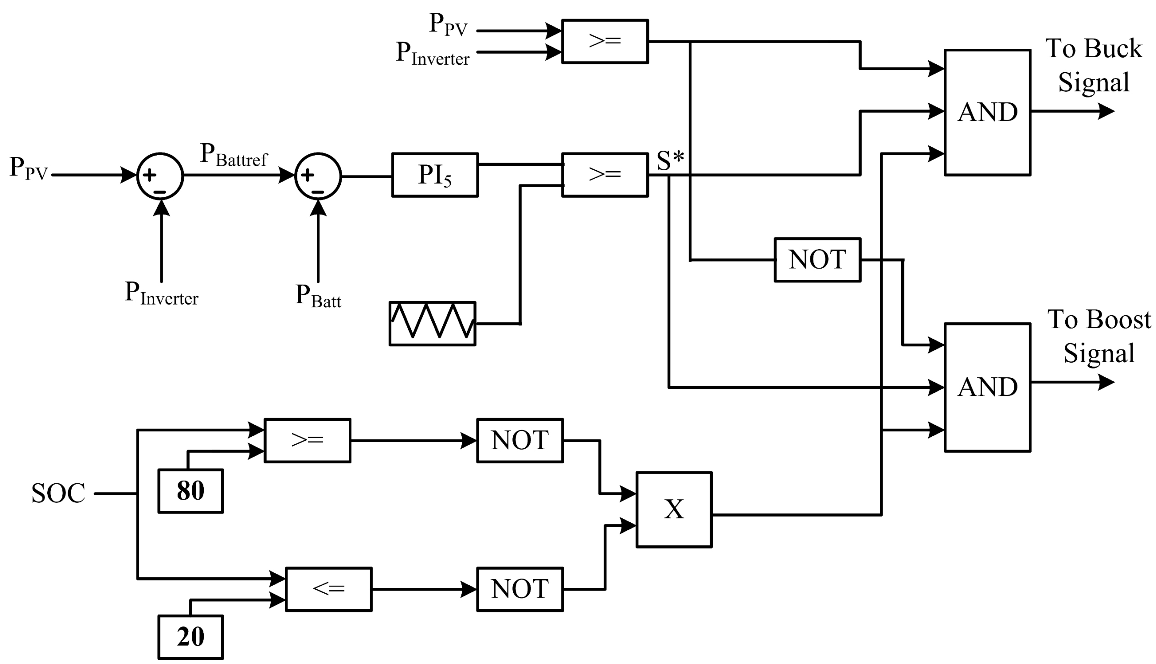

Figure 4.3: Battery charge controller

4.4 Modification of V-f Control With Battery SOC Constraint

When there is abundant solar irradiance available and the active power required for the microgrid frequency control is less than active power produced by the PV generator at MPP i.e., $P_{inverter}$ < Ppvmpp and at the same time the battery SOC is 80%, then, the battery cannot be charged beyond this upper limit of SOC. In such case, decreasing the output power of PV generator would lead to under utilization of the solar resource. Hence, a global control mechanism is required in a microgrid which can transition the PV control from frequency control mode to constant power mode with power to be generated at Ppvmpp. Meanwhile, there should be a mechanism to allow any other generator of the microgrid to handle the frequency control problem. In the microgrid system under consideration, there is a diesel generator which can decrease its generation in order to match the PV generation increase. Hence, the power balance of the system will be maintained in order to control the microgrid frequency.

Similarly, when the irradiance is low such that the maximum power from PV generator is not enough to maintain the microgrid frequency i.e., Pinverter > Ppvmpp and at the same time, the battery SOC is 20%, then the battery will not be able to back up the PV generator. In such case, the frequency control function needs to be transferred to other available generator if possible, in this case, a diesel generator. Again, a global control mechanism becomes an absolute necessity for allowing the transition of PV generator control from frequency control mode to constant MPP mode and the diesel generator control from constant active power mode to frequency control mode such that the frequency stability of the microgrid can be achieved. Figure 4.4 shows modification in frequency control loop of the inverter which includes the transition from frequency control to constant active power control.

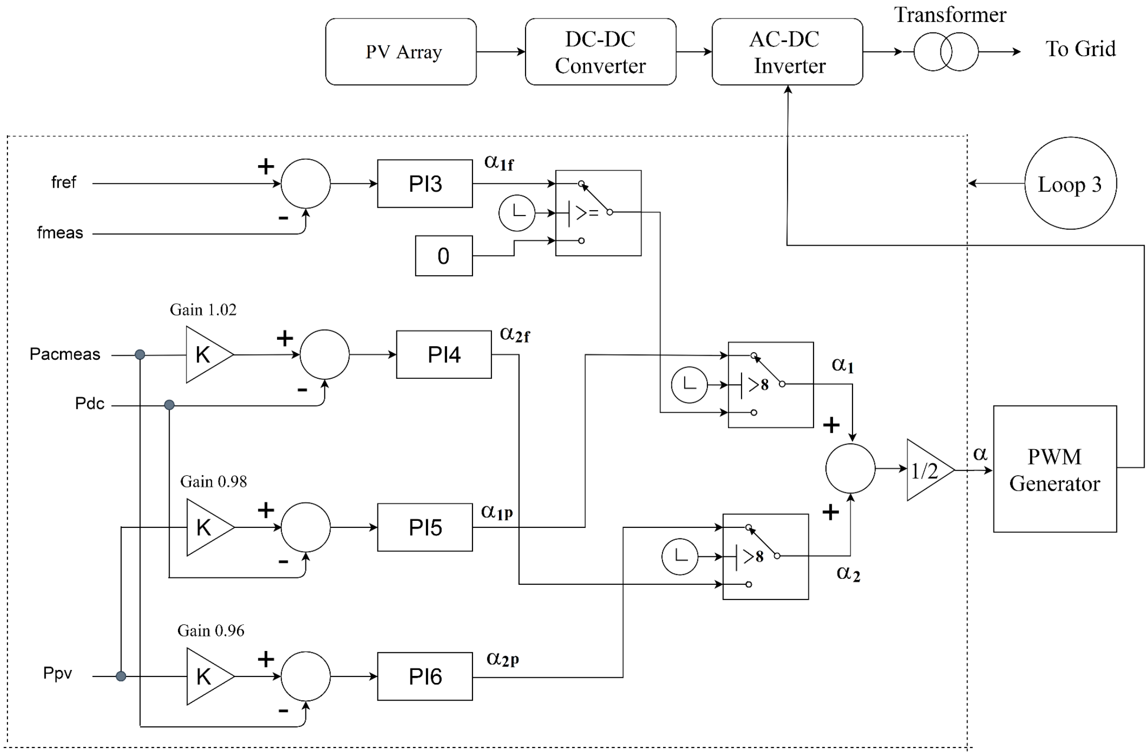

Figure 4.4: Modified V-f controller to handle Battery SOC constraint

4.5 MPPT Integrated P-Q Controller

The proposed MPPT integrated P-Q controller is designed to control active and reactive power. There are some consumers like Hospitals, Process industry requires an uninterrupted power supply. This control strategy is suitable to supply critical load of such consumers. The integrated P-Q controller for critical load application is shown in Figure 4.5. The control strategy consist of one loop for MPPT control at DC-DC converter, second loop for reactive power control and third loop for active power control at DC-AC converter. The MPPT control part is discussed in section 4.2.1.

4.5.1 Active Power Controller

In active power controller, the actual measured active power (P_{actual}) is compared with reference active power (P_{ref}) and then error is given to PI_3 controller which will give the phase shift α_1.This phase shift is given by Eq.(4.7).

$$\alpha_1 = K_{p3}(P_{ref} - P_{actual}) + K_{i3}\int_0^t (P_{ref} - P_{actual})dt \tag{4.7}$$

To keep the real power balance at DC and AC side of inverter PI_4 controller is used. The AC side measured real power ($P_{ACmeasured}$) is multiplied by a factor of 1.02 considering efficiency of inverter as 98%. The DC real power (P_{dc}) is compared with this value of AC power and then error is given to PI_4 controller which will give the phase shift α_2. This phase shift is given by Eq.(4.8).

$$\alpha_2 = K_{p4}(1.02 * P_{ACmeasured} - P_{DC}) + K_{i4}\int_0^t (1.02 * P_{ACmeasured} - P_{DC})dt \tag{4.8}$$

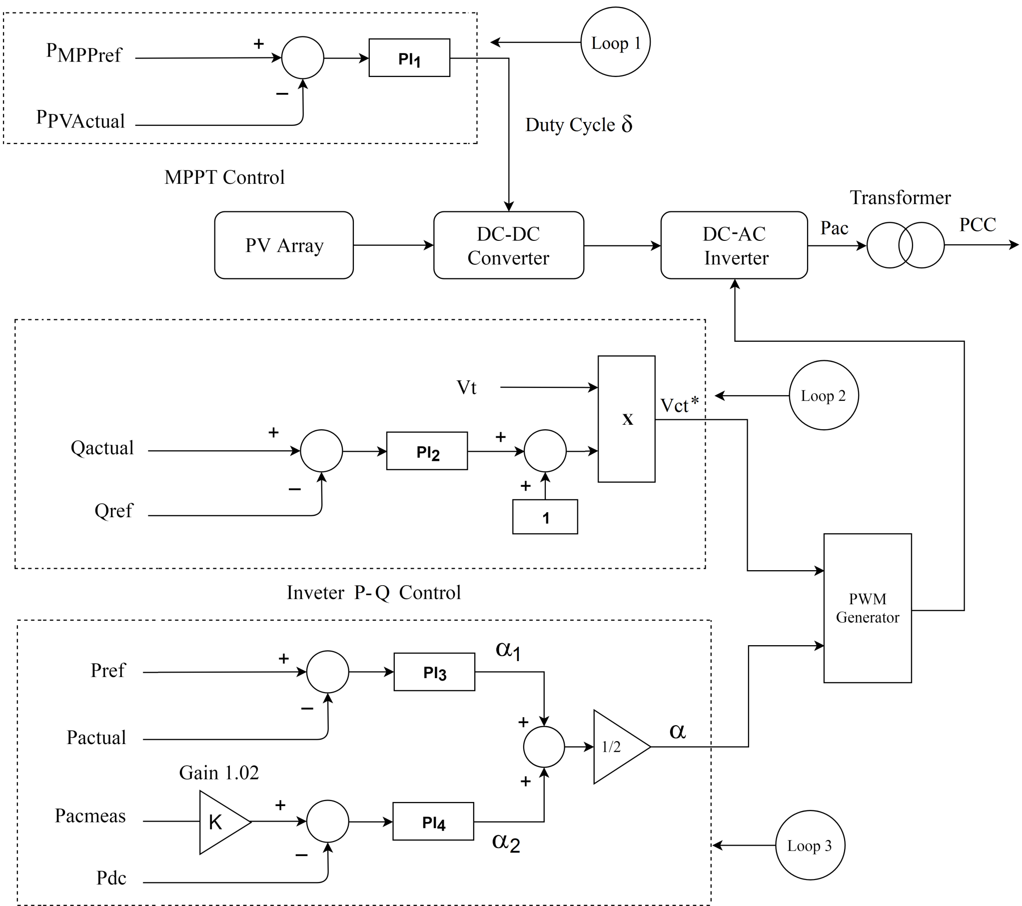

Figure 4.5: The MPPT integrated P-Q controller for critical load applications

The active power can be controlled by controlling the inverter side real output power. The phase shift contributions from both sides of inverter are averaged which will obtain the final phase shift given by equation 4.9 and then it will generates the reference signal of voltage v_c^* for the inverter PWM.

$$\alpha = \frac{\alpha_1 + \alpha_2}{2} \tag{4.9}$$

4.5.2 Reactive Power Controller

Reactive power controller compares the measured reactive power (Q_{actual}) injection at PCC with the reference reactive power (Q_{ref}) and this error signal is passed to the PI controller, PI_2. Then, the term obtained is multiplied by the terminal voltage v_t to obtain the reference voltage $v_c{}^*$ which is in phase with v_t. The inverter output voltage is given by equation 4.10

$$v_{ct}^* = (K_{p2}(Q_{ref} - Q_{actual})) + K_{i2}\int_0^t (Q_{ref} - Q_{actual})dt + 1)v_t \tag{4.10}$$

The battery charge controller for P-Q control is the same as one discussed in section 4.3.

4.6 Adaptive Control Strategy

An adaptive controller has a mechanism for re-tuning the gain parameters. The controller becomes nonlinear because of parameter adjustment mechanism. An adaptive control system has two loops. One loop is a normal feedback with the process and the controller. The other loop is the parameter adjustment loop [103-104]. A block diagram of an adaptive system is shown in Figure 4 6.

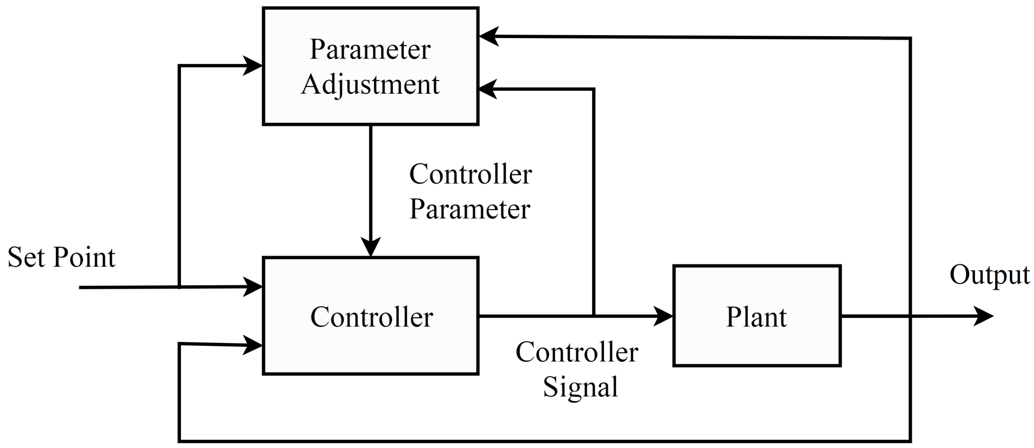

Figure 4.6: Block diagram of an adaptive system

If the controller gains K_p and K_I are not altered appropriately as per the fluctuations, the system response may be poor and even cause instability. So it is important to retune the control gain as per the alterations in environment and system condition. Figure 4.7 shows proposed adaptive voltage regulation with a PI feedback controller. In the proposed system, the control system is designed in such a way that it dynamically adjust the PI controller gain based on real time abrupt parameter variation caused by PV, battery and/or external grid conditions.

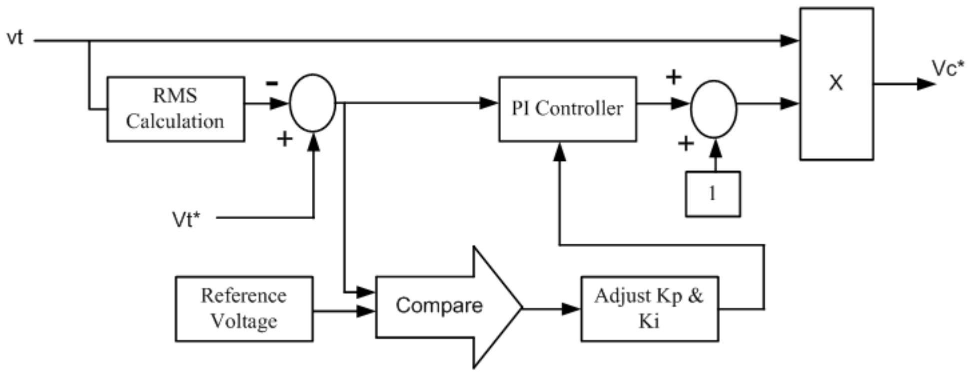

Figure 4.7: Proposed Adaptive control for the voltage regulation

The PCC voltage (v_t) is measured and its RMS value V_t is calculated. The error between the RMS value of measured voltage V_t and reference voltage $V_t{}^*$ is fed back to adjust the reference compensator output voltage $V_c{}^*$, which is the reference for generating pulse-width modulation (PWM) signals to drive the inverter. The compensator output voltage $V_c{}^*$ is changed until Vt becomes equal to the reference voltage $V_t{}^*$. By the adaptive control, the actual voltage is compared with the desired voltage deviation and the PI control gains are adjusted based on the scaling factor γ v given by equation (4.11),

$$\gamma V = \frac{\Delta V_{actual}}{\Delta V_{ideal}} \tag{4.11}$$

Where Δ V_{actual} =actual voltage deviation and Δ V_{ideal} is ideal voltage deviation. This work proposes a control method that can ensure a quick and consistent desired response when the system operation condition varies. In other words, the change of the external condition will not have a negative impact, such as slower response, overshoot, or instability on the performance.

Figure 4.8 shows flowchart of the proposed adaptive PI control.

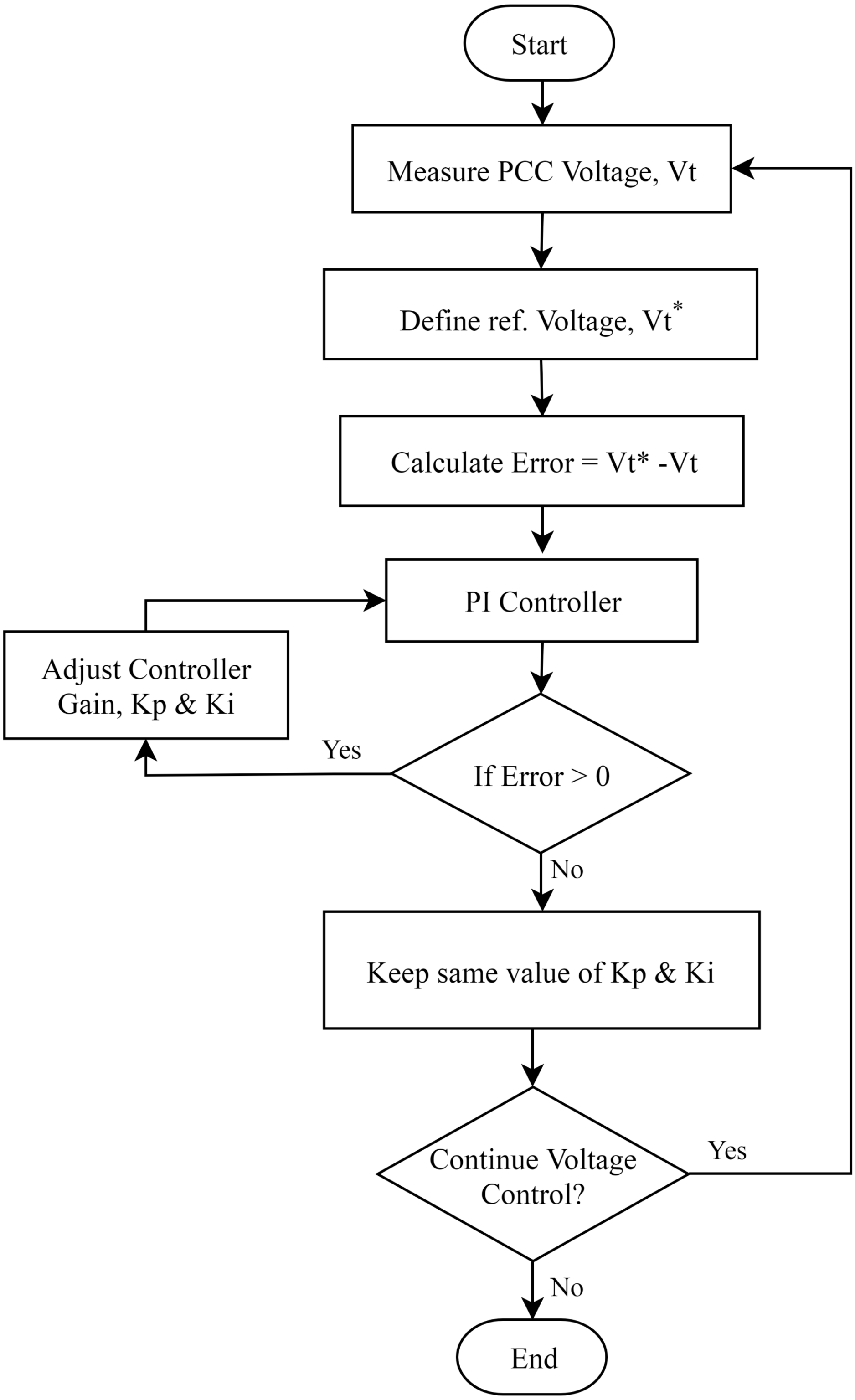

Figure 4.8: Flow chart of Adaptive PI control algorithm

Adaptive PI control algorithm is developed to retune the control parameters K_p and

K_i, which help to improve the performance of proposed system.

4.7 Conclusion

In this chapter various controllers are proposed for enhancing the microgrid performance. MPPT integrated V-f controller is designed to track maximum power from solar PV system, to control magnitude and phase angle of injected voltage at PCC. Battery energy storage controller is developed to enhance the life cycle of battery by maintaining SOC constraint. Battery energy storage also helps to strengthen the microgrid performance. In the V-f controller modification are suggested in frequency control loop for an effective seamless transition of controls from V-f to constant active power at the PV side and from constant active power to frequency control at the diesel generator. The adaptive controller is developed for retuning the controller gain parameters.

Chapter 5

Simulation Studies and Results

This chapter provides the various simulation studies of proposed system. The system configuration shown in Figure 5.1 is simulated in MATLAB / SIMULINK block for V-f and P-Q control. The solar PV system is connected to the grid through a coupling inductor (Lc). The coupling inductor filters out the ripples from the PV output current. The solar PV is the active power source and capacitor act as the reactive power source.

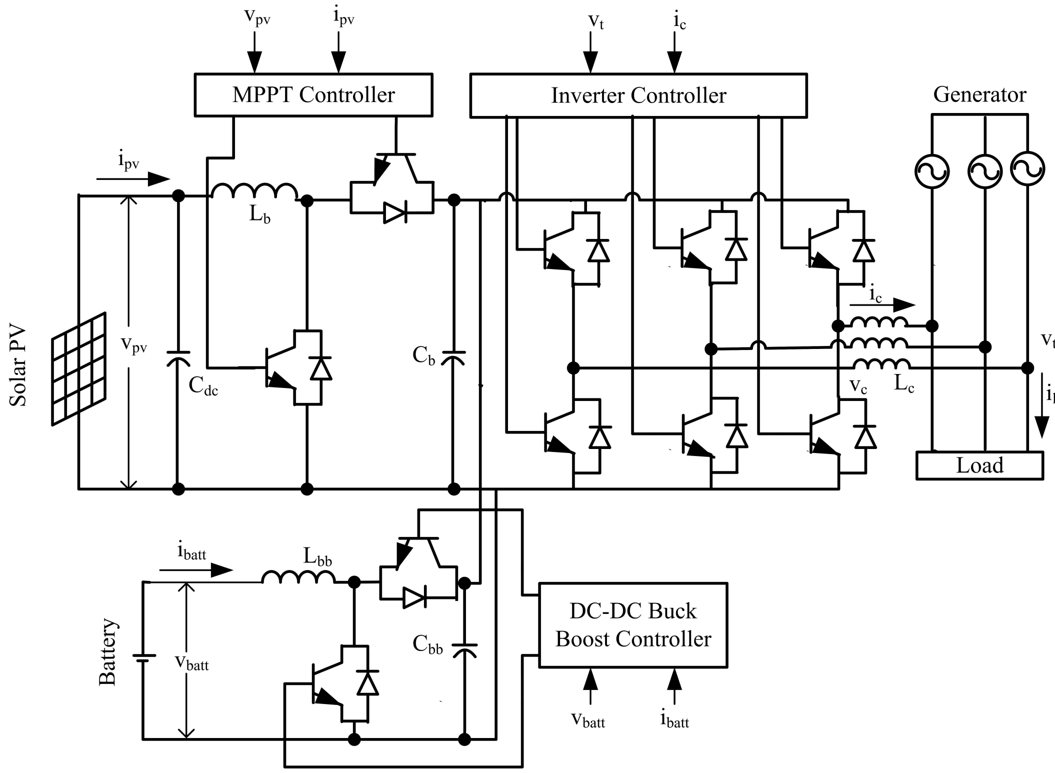

Figure 5.1: The system configuration for V-f and P-Q control

5.1 Case Study I: Experimental Simulation of V-f Control Method for PV Based Microgrid

A case study is carried out to show dynamic characteristics of the proposed voltage-frequency algorithm for stability improvement using battery storage during transition from grid connected to islanded microgrid mode. The system is built in MATLAB / SIMULINK blockset shown in figure 5.2. Table 5.1 illustrates the simulation parameters used in the study.

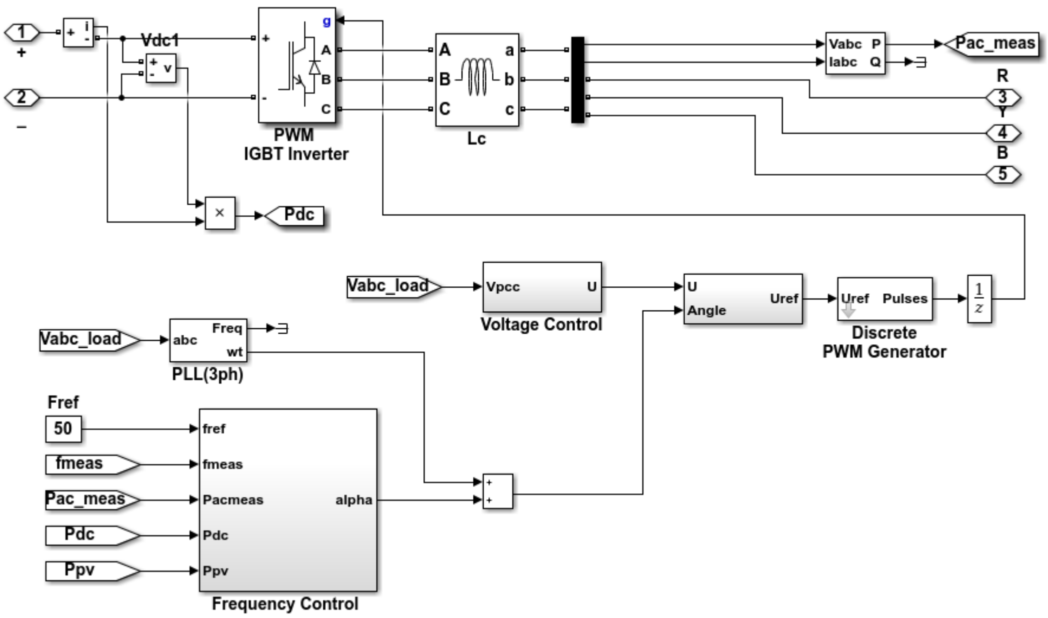

Figure 5.2: SIMULINK model for voltage-frequency control

Table 5.1: Microgrid system parameters for case I

Description	Values
Point of Common Coupling	3-phase, 440 V, 50 Hz
Solar PV System	100 kW
Battery	42 Batteries each of 300Ah capacity
Interfacing Transformer	200kVA, 440/480 V, Y-Δ, 50 Hz
Diesel Generator Set	150 kVA, 440 V, 50 Hz
Load	3-phase, 120 kW

5.1.1 Case A: Stability Analysis without Battery Storage

Initially microgrid is connected to the utility grid. The switch is opened at t = 4 sec microgrid starts operating in islanded mode. During islanded mode, the microgrid is fed by solar PV Generator, D-G set only.

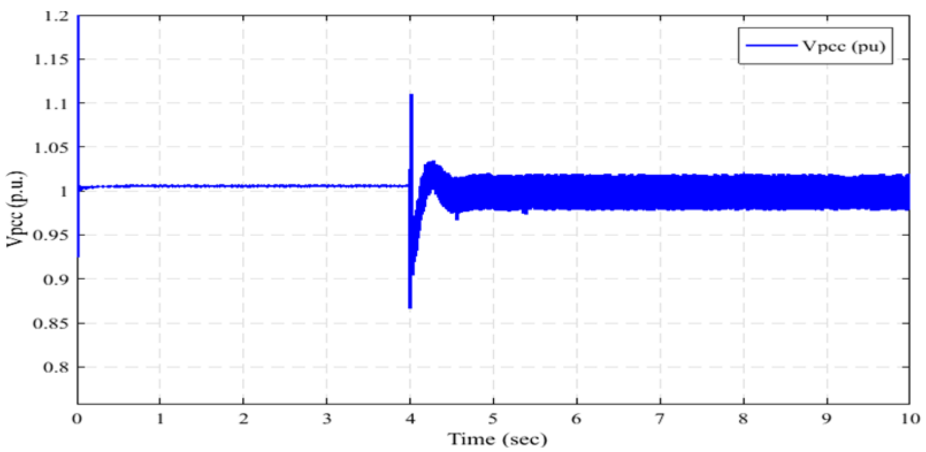

Figure 5.3: PCC voltage versus time

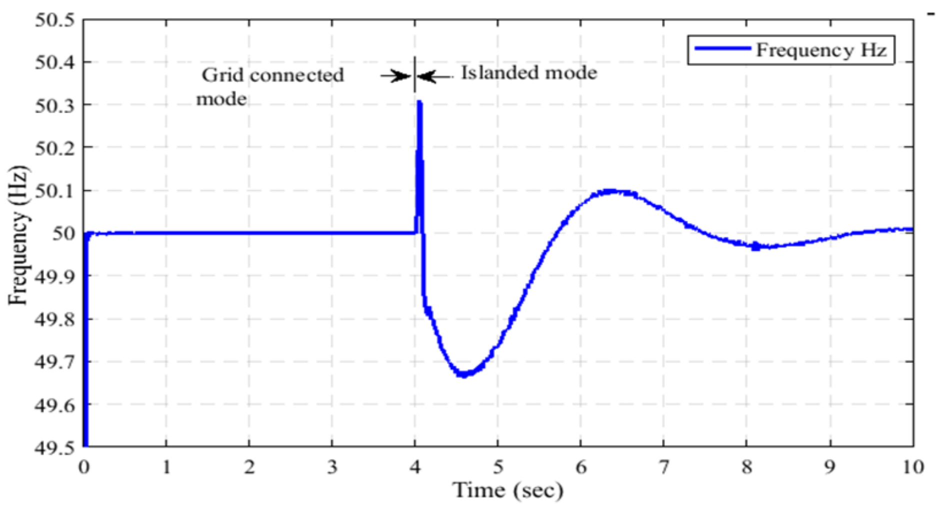

Figure 5.4: Frequency versus time

Figure 5.3 shows the voltage at PCC in p.u. At the time of disconnection, voltage drops suddenly to 0.87 p.u. and recovers within 1 sec. Figure 5.4 shows the frequency of the system in grid connected and islanded mode. During islanding frequency drops to 49.66 Hz and takes approximately 6 sec to settle down to the nominal value. The active and reactive power supplied by the D-G set is shown in Figure 5.5. As islanding occurs at 4 sec, D-G set starts supplying power after 4 sec. It supplies 22 kW active and 50 kVAR reactive power to the load.

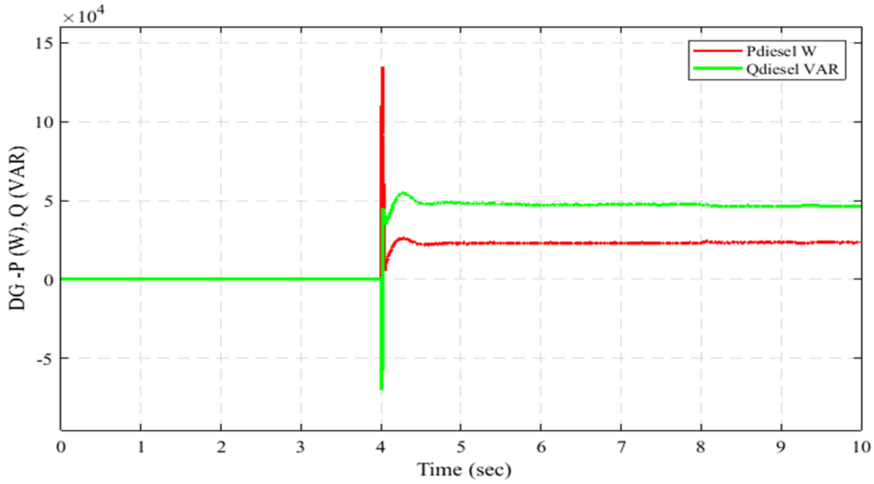

Figure 5.5: D-G set active and reactive power

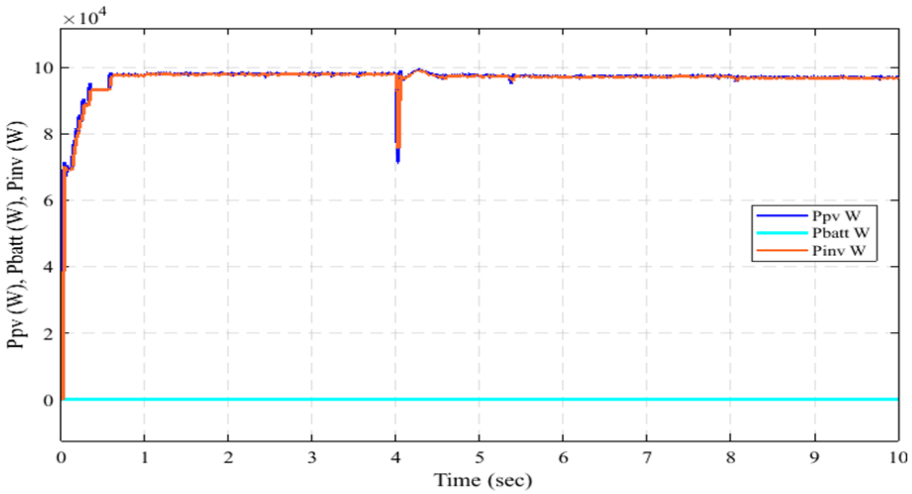

Figure 5.6: PV, battery, inverter active power

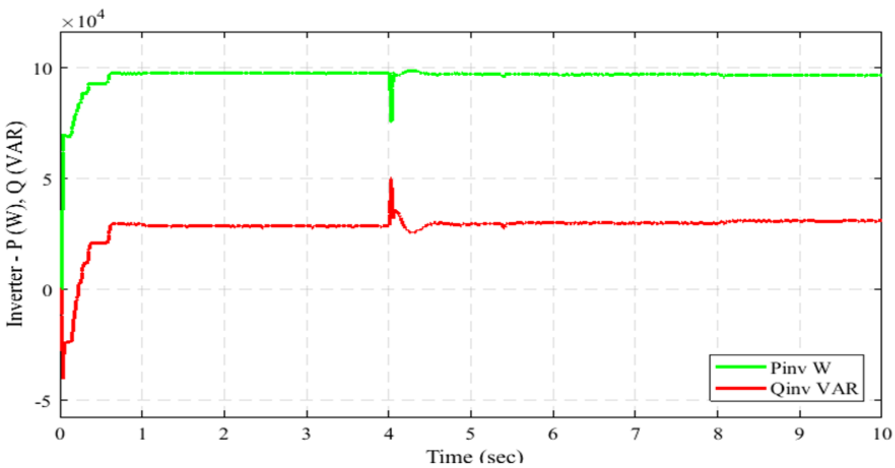

Figure 5.7: Inverter active and reactive power

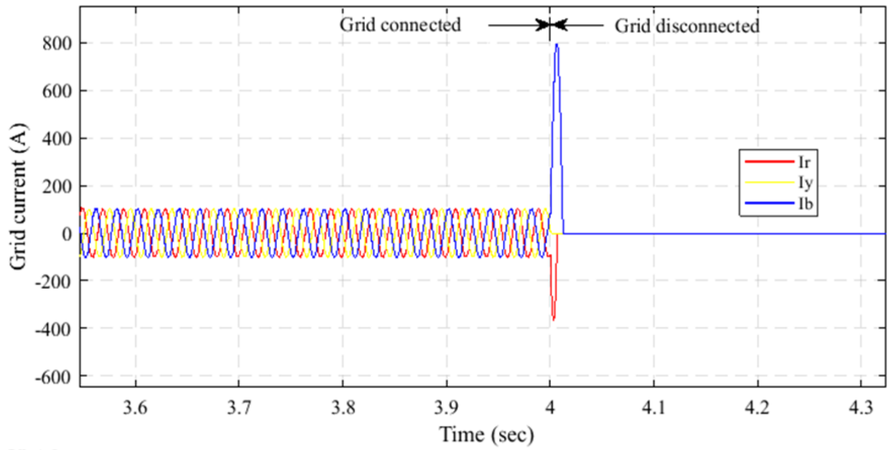

Figure 5.8: Grid current

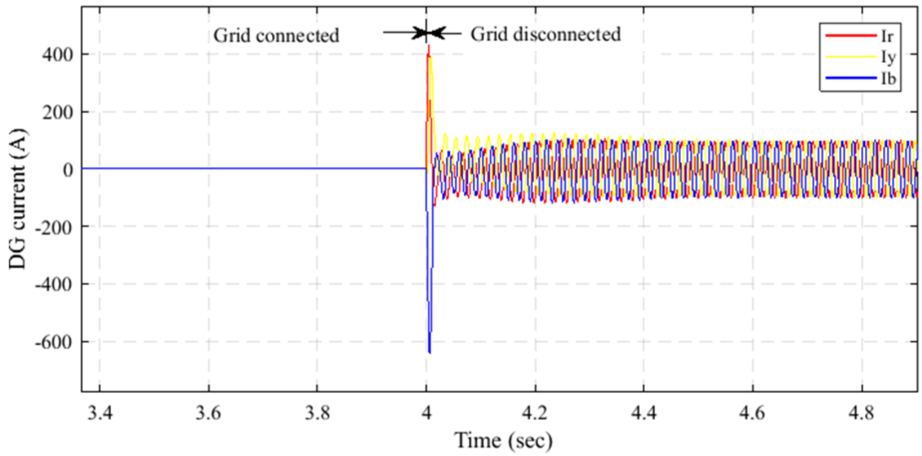

Figure 5.9: D-G set current

Figure 5.6 shows the power supplied by the solar PV Generator and inverter. Here in this case 1000 W/m^2 irradiance is considered. Hence solar PV generates 98 kW power. The inverter output power is also 98 kW, since battery storage system is not considered. Figure 5.7 shows active and reactive power from inverter. Since microgrid is connected to the grid upto 4 sec., grid supplies current to the load upto 4 sec only which is shown in Figure 5.8. Figure 5.9 shows the current supplied by the D-G set.

5.1.2 Case B: Stability Analysis with Battery Storage

Here battery storage is considered as a backup power supply. The switch is opened at t = 4 sec microgrid starts operating in islanded mode. During islanded mode, the microgrid is fed by solar PV Generator, battery and D-G set. Figure 5.10 shows the voltage at

PCC in p.u.

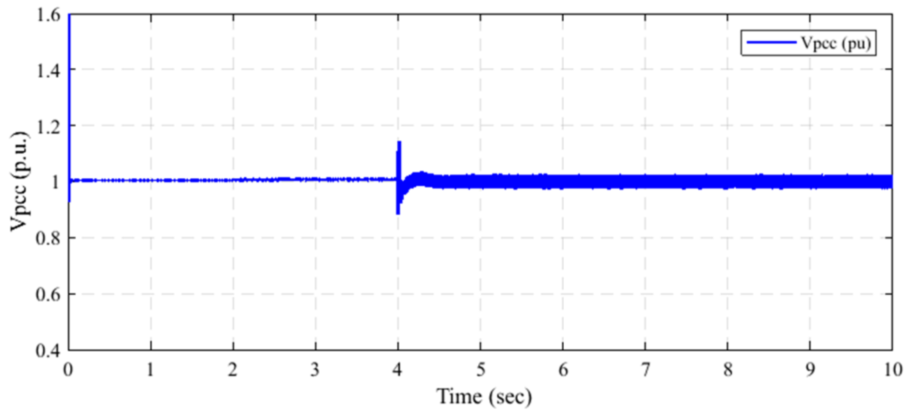

Figure 5.10: PCC voltage Vs time

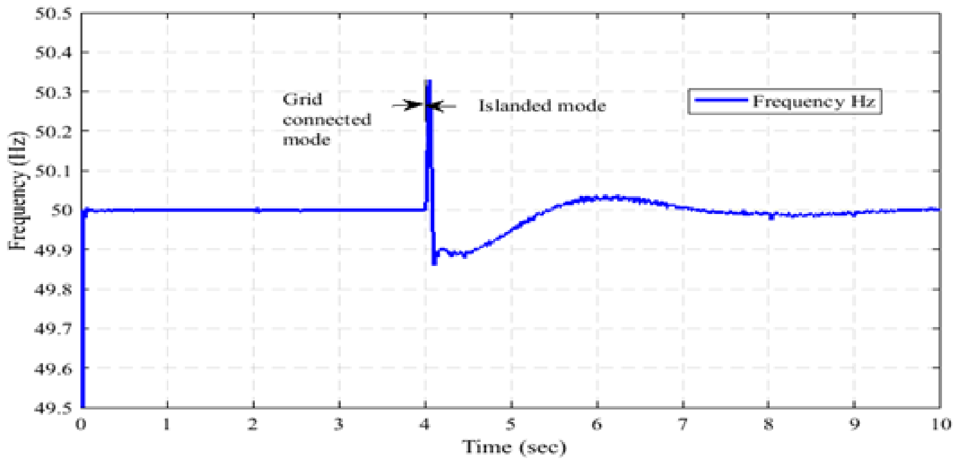

Figure 5.11: Frequency Vs time

At the time of disconnection, voltage drops to 0.9 p.u. and recovers within 0.4 sec only. It is observed that by using battery storage voltage drop at PCC reduces and PCC voltage stables quickly to the nominal value. Figure 5.11 shows the frequency of the system in grid connected and islanded mode. During islanding frequency drops to 49.88 Hz and takes 4 sec to settle down to the nominal value. The active and reactive power supplied by the D-G set is shown in Figure 5.12. As islanding occurs at 4 sec, D-G set starts supplying power after 4 sec. It supplies 4 kW active and 15 kVAR reactive power to the load.

Figure 5.13 shows the power supplied by the solar PV Generator, battery and inverter. Here in this case 1000 W/m^2 irradiance is considered. Hence solar PV generates 98 kW power. Here battery supplies 18 kW power to the load. Hence inverter output power is also 116 kW

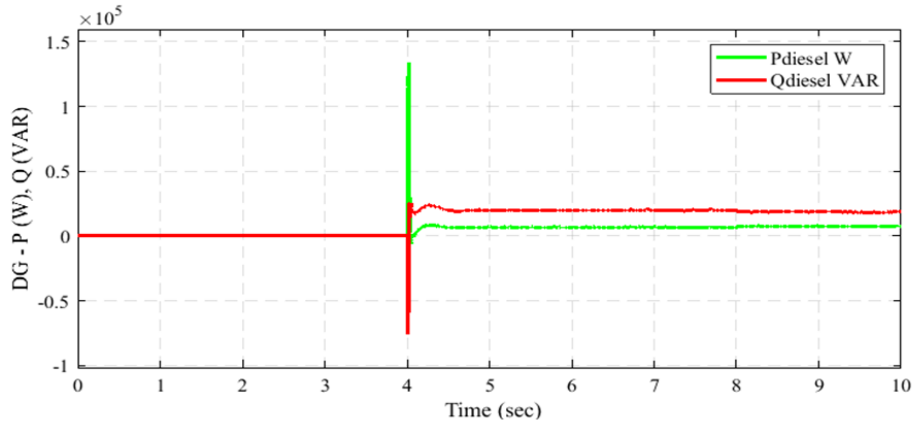

Figure 5.12: D-G set active and reactive power

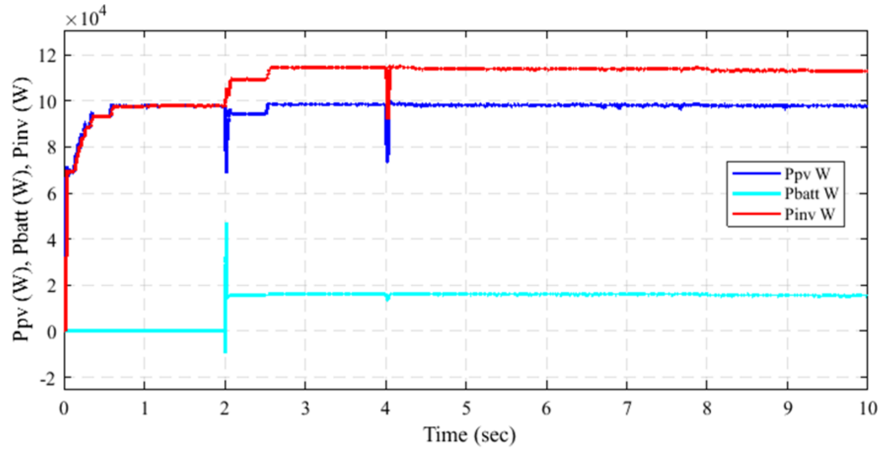

Figure 5.13: PV, battery, inverter active power

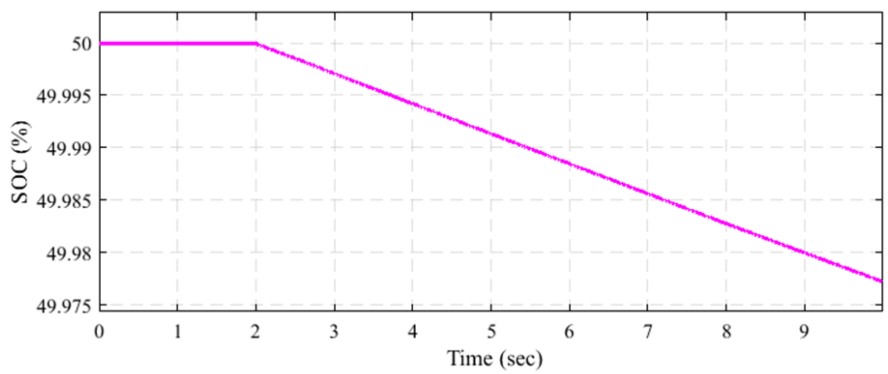

Figure 5.14: State of Charge (SOC) of battery

As load requirement is more than solar PV power and battery SOC is more than 20%, battery supplies deficit power to the load. Hence SOC of battery decreases which

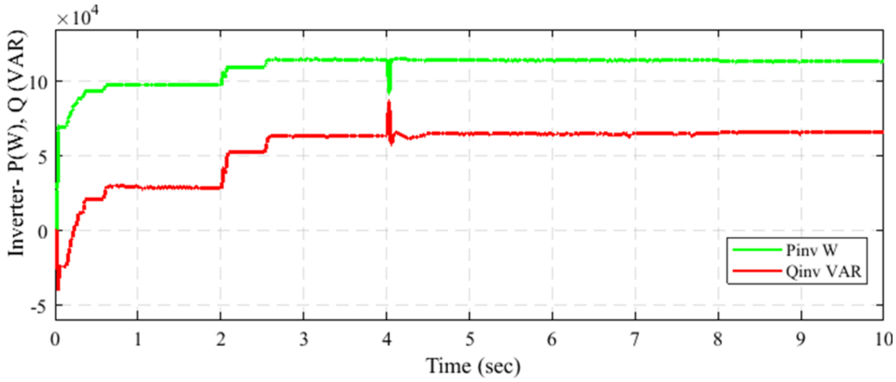

Figure 5.15: Inverter active and reactive power

is shown if Figure 5.14. Figure 5.15 shows active and reactive power from inverter. Since microgrid is connected to the grid upto 4 sec., grid supplies current to the load upto 4 sec only which is shown in Figure 5.16. Figure 5.17 shows the current supplied by the D-G set.

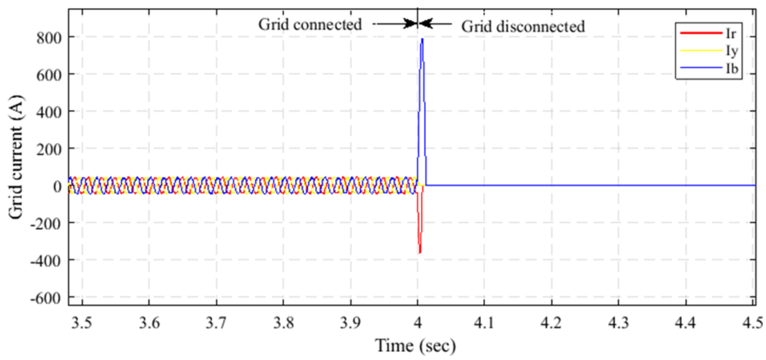

Figure 5.16: Grid current

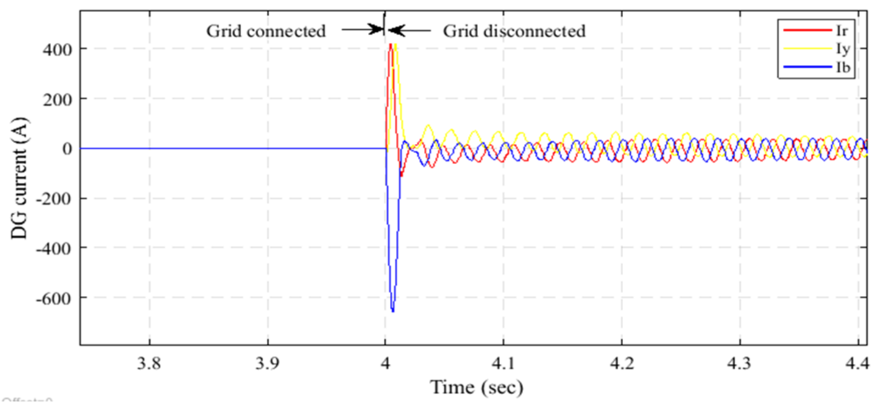

Figure 5.17: D-G set current

5.2 Case Study II: Autonomous Microgrid Operation

This case study is carried out to demonstrate V-F control technique to verify irradiance veriation effect on voltage and frequency. The scheme of MPPT integrated voltage - frequency control method for solar PV system is shown in Figure 4.2. The results which are discussed in this section clearly show that voltage and frequency stability improves by the proposed method. Table 5.2 illustrates the corresponding microgrid system parameters. To verify irradiance veriation effect on voltage and frequency, two different irradiance cases are considered, namely Case A with irradiance = 1000W/m^2 and Case B with irradiance = 750W/m^2

Table 5.2: Microgrid system parameters for case II

Description	**Values**
Point of Common Coupling	3-phase, 440 V, 50 Hz
Solar PV System	100 kW
Battery	42 Batteries each of 300Ah capacity, Type- Lead acid
Interfacing Transformer	200kVA, 440/480 V, Y-Δ, 50 Hz
Diesel Generator	100 kVA, 440 V, 50 Hz
Load	3-phase, 120 kW

5.2.1 Case A: Irradiance = 1000W/m^2

When microgrid operates in islanded mode, the active power generated by the D-G set is not sufficient to cater the power demand of the microgrid. Figure 5.18(a) shows the plot of PCC voltage in p.u. The solar PV voltage control starts at 1 sec which regulates the voltage of PCC at 1 p.u. Figure 5.18(b) shows the microgrid frequency which initially drops to a value 47Hz due supply-demand imbalance. The invereter frequency control

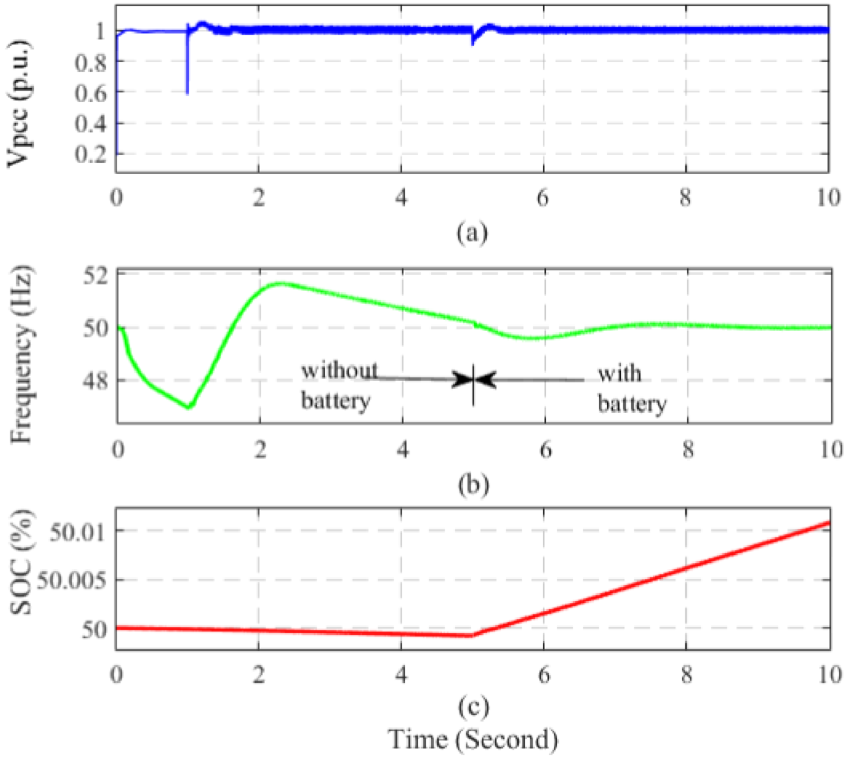

Figure 5.18: (a) Voltage at PCC, (b) Frequency and (c) SOC

starts at 1sec which responds to regulate frequency to 50Hz in 4 sec. The battery control begins at t=5sec which quickly regulates 50Hz frequency in 2 sec. Figure 5.18(c) shows the state of charge of lead acid battery. In this case solar PV output power is sufficient to fulfill load demand; excess power is fed to charge the battery. The Figure 5.19(a) shows D-G set active and reactive power. D-G set produces fixed amount of power upto 1 sec. At t = 1sec, solar PV system and at t = 5 sec, battery control starts. Inverter active and reactive power is shown in Figure 5.19(b). As solar PV starts at 1 sec, upto 1sec inverter output power is zero and after 1sec inverter output power is 100 kW. At 5 sec battery control starts functioning and battery SOC is less than 80%, PV supplies 80kW to the load and 20 kW to the battery.

Figure 5.19(d) which shows the active power from solar PV, battery and inverter, respectively. In this case solar irradiance is 1000W/m^2; hence the solar PV system generates the maximum power of 100 kW.

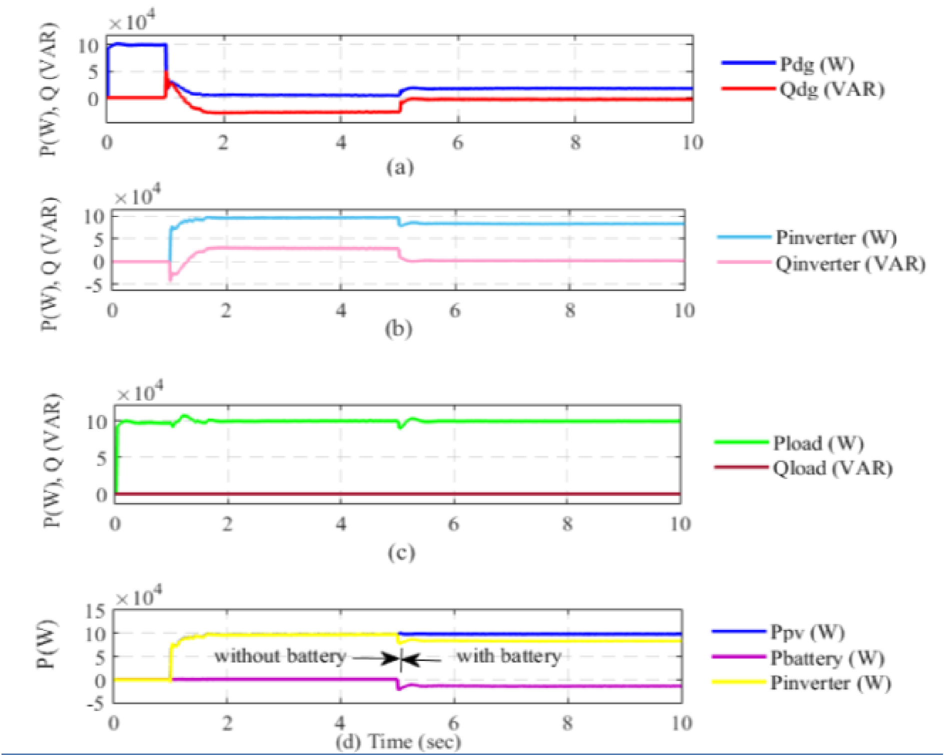

Figure 5.19: : (a) D-G set active and reactive power, (b) Inverter active and reactive power, (c) Load active and reactive power and (d) PV, battery, inverter active power

5.2.2 Case B: Irradiance = 750W/m^2

When microgrid operates in islanded mode, the active power generated by the D-G set is not sufficient to cater the power demand of the microgrid. Figure 5.20(a) shows the plot of PCC voltage in p.u. The solar PV voltage control starts at 1 sec which regulates the voltage of PCC at 1 p.u.

Figure 5.20(b) shows the microgrid frequency which initially drops to a value 47Hz due supply-demand imbalance. The solar PV frequency control starts at 1sec which responds to regulate frequency to 50Hz in 4 sec. The battery control begins at t=5sec which quickly regulates 50Hz frequency in 2 sec. Figure 5.20(c) shows the state of charge of lead acid battery. In this case solar PV output power is not sufficient to fulfill load demand; deficit power of around 5kW is supplied by the battery.

The Figure 5.21(a) shows D-G set active and reactive power. D-G set produces fixed amount of power upto 1 sec. At t = 1sec, solar PV system and at t = 5 sec, battery con-

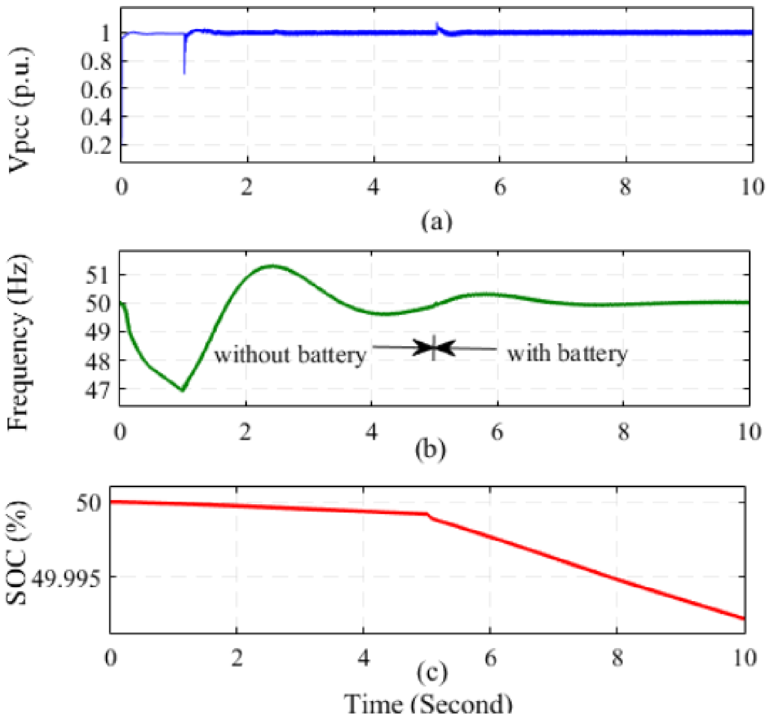

Figure 5.20: (a) Voltage at PCC, (b) Frequency and (c) SOC

trol starts. Inverter active and reactive power is shown in Figure 5.21(b). Figure 5.21(d) which shows the active power from solar PV, battery and inverter, respectively. In this case solar irradiance is 750W/m^2; hence the solar PV system generates the maximum power of 75 kW. As solar PV starts at 1 sec, upto 1sec inverter output power is zero and after 1sec inverter output power is 75 kW. At 5 sec battery control starts functioning and battery SOC is more than 20%, battery supplies 5 kW to the load.

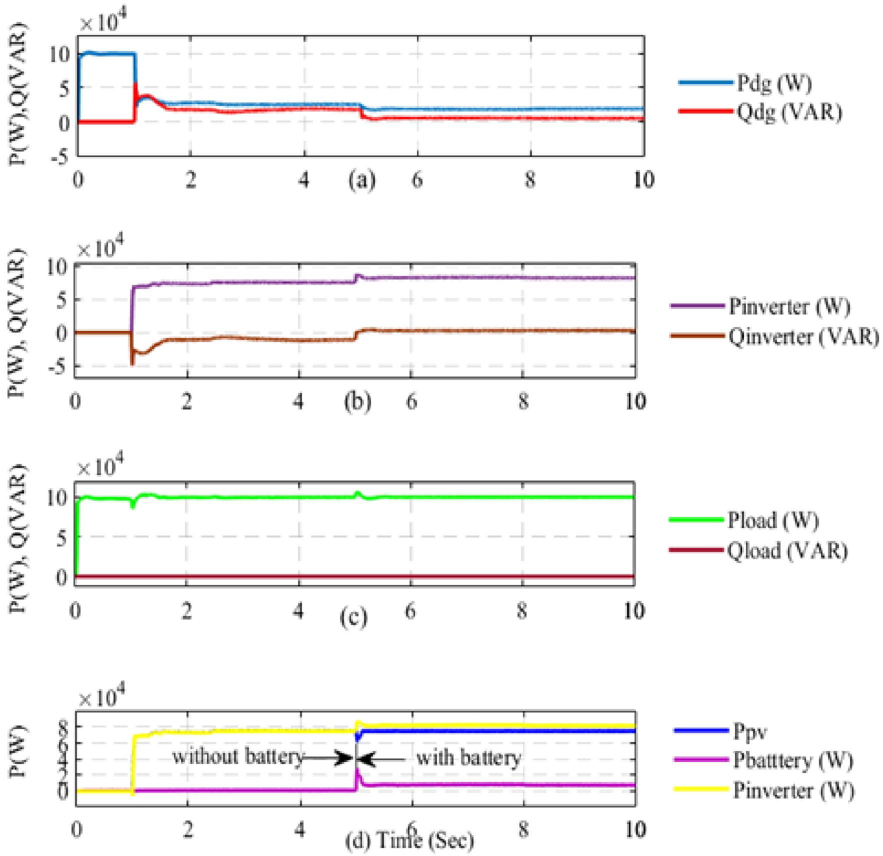

Figure 5.21: (a) D-G set active and reactive power, (b) Inverter active and reactive power, (c) Load active and reactive power and (d) PV, battery, inverter active power

5.3 Case Study III: Experimental Simulation of Proposed System with Adaptive Controller

The proposed adaptive control scheme for the voltage regulation as illustrated in Figure 4.7 is developed and simulated in MATLAB SIMULINK. The comparison of simulation results obtained by using conventional PI and Adaptive controller for voltage and frequency control is discussed in this section.

This section presents the comparison of simulation results obtained by using PI controller and Adaptive controller for voltage and frequency control.

Figure 5.22 shows the control of Microgrid frequency which initially drops to 47 Hz due to the demand-supply imbalance. The frequency control with adaptive controller starts at 1 second regulates the frequency to 50 Hz in 1.01 seconds while PI controller takes 5.26 seconds. The active power from solar PV system is shown in Figure 5.23. Solar irradiance considered in this work is 1000 W/m^2 and hence the PV generates maximum power of 100 kW. Adaptive controller regulates active power to 100 kW within 2.02 seconds whereas PI controller takes 7.07 seconds.

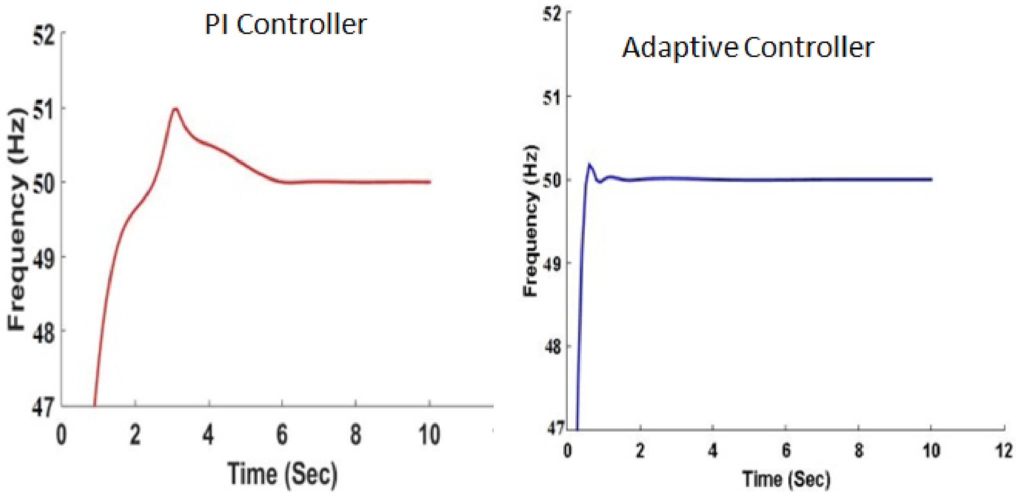

Figure 5.22: Results of frequency control by using PI and Adaptive Controller

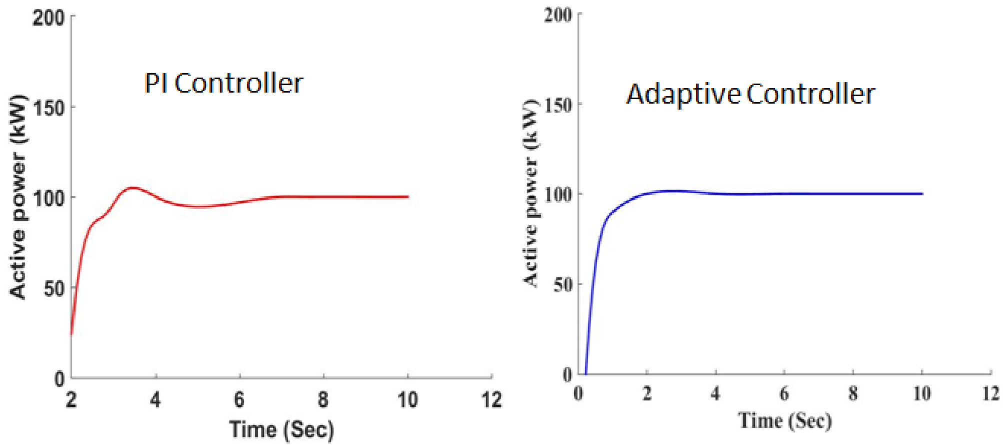

Figure 5.23: Results for control of active power from the PV by using PI and Adaptive Controller

Figure 5.24 shows the plot of PCC voltage in p. u. It can be observed that adaptive controller regulates PCC voltage to 1 p. u. within 2.22 seconds while PI controller takes 3.63 seconds. In Microgrid, while transition from grid connected to islanded mode,

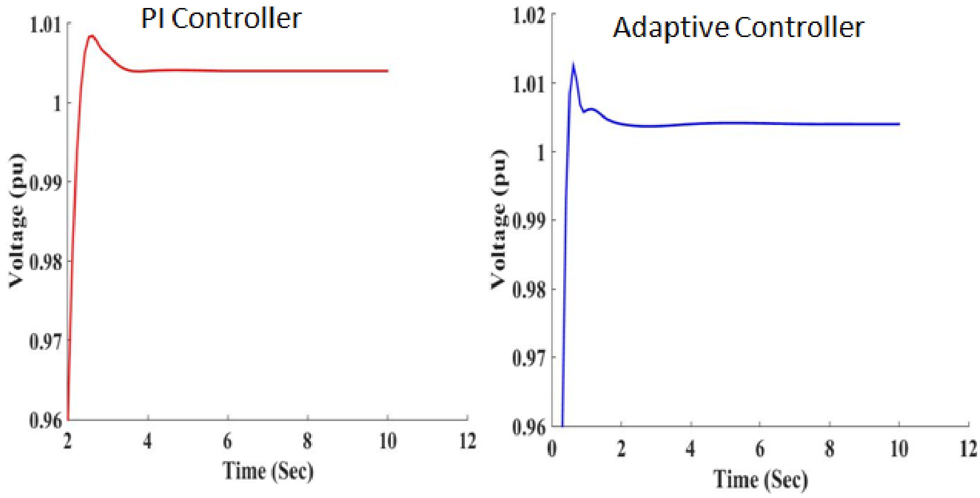

Figure 5.24: shows the plot of PCC voltage in p. u.

the diesel generator is controlled to generate fixed amount of active power. The proposed adaptive controller stabilizes the diesel generator output of 1.25MW at faster rate compared to the PI controller as illustrated in Figure 5.25.

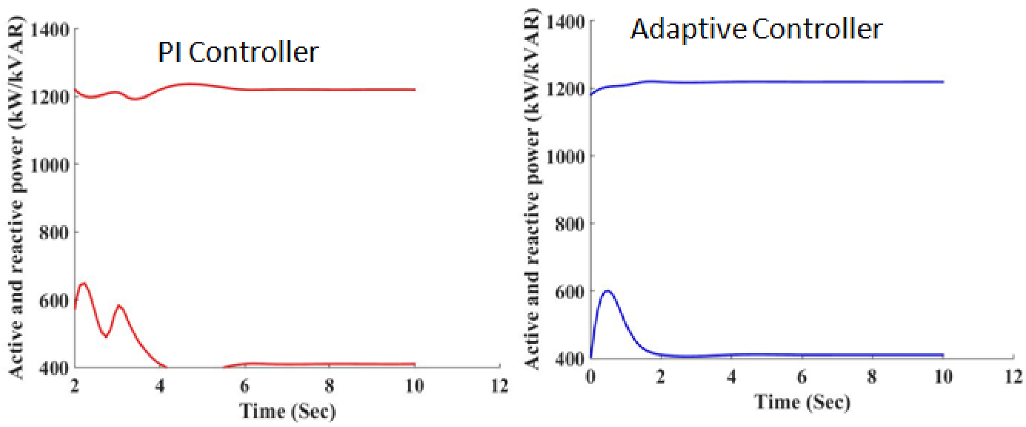

Figure 5.25: Results of active and reactive power generation by using diesel generator

Figure 5.26 shows the active power from battery. At 1000 W/m2, active power of 100 kW is generated by PV array. But to maintain 50 Hz frequency only 80 kW is required. The surplus 20 kW is used to charge the battery. The battery charging mode is indicated by negative sign. The required active power from inverter is 80 KW to maintain the frequency at 50 Hz. This required 80 KW is achieved within very less time period as compared with PI controller as shown in Figure 5.27.

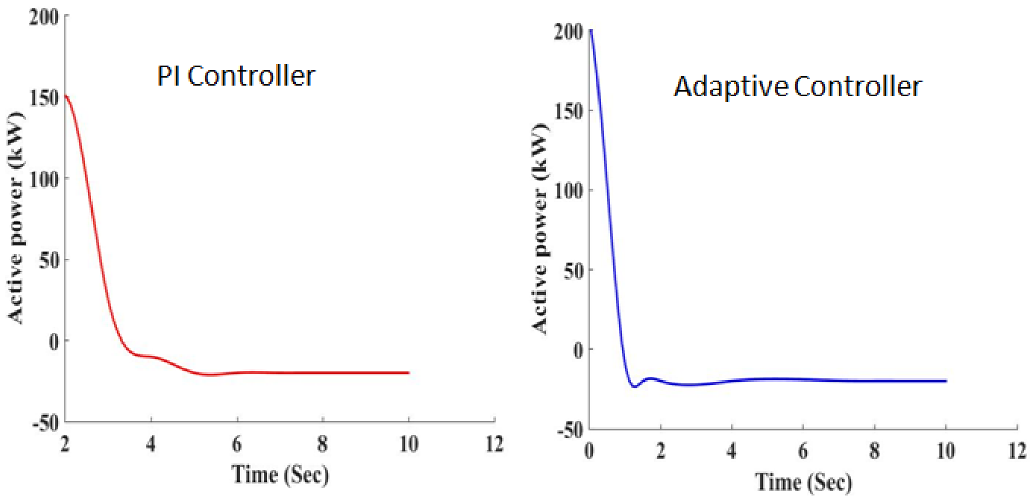

Figure 5.26: Results for battery active power control by using PI and Adaptive Controller

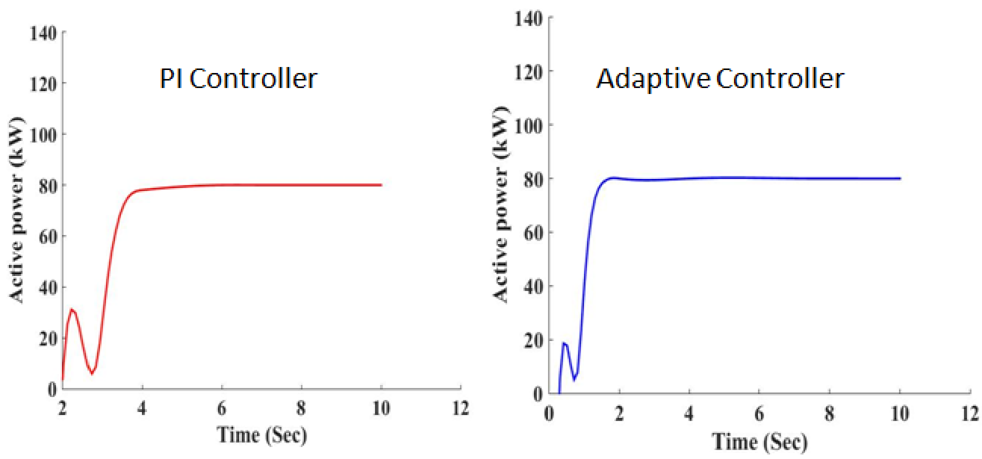

Figure 5.27: Results of inverter active power control by using PI and Adaptive Controller

5.3.1 Comparison of Conventional PI and Adaptive Controller

Table 5.3 shows the performance comparison of conventional PI controller and proposed adaptive controller. Thus, the proposed adaptive controller exhibits faster response, since the parameter variations are sensed in real time and correspondingly the gain values of PI controller are adjusted. The study shows that the significant improvement in the performance of the system by using adaptive controller.

Table 5.3: Performance comparison of PI controller and Adaptive controller

Parameter	*Values*	PI Controller	Adaptive Controller
		Time (Sec)	Time (Sec)
Frequency	49.99 Hz	6.23	1.01
PPV	100.1 kW	7.07	2.02
PCC voltage	1.004 p.u	3.63	2.22
PDiesel generator	1220 kW	5.96	1.51
QDiesel generator	408.1 kVAR	5.86	3.63
Pbatt	-19.9 kW	6.06	4.04
Pinverter	79.96 kW	5.85	2.02

5.4 Case Study IV: P-Q Controller to Support the Critical Load in Autonomous Operation of Microgrid

A case study is carried out to show the effectiveness of the proposed active-reactive power algorithm to supply critical load in autonomous microgrid. The proposed system is simulated in MATLAB / SIMULINK environment shown in Figure 5.28. Table 5.4 illustrates the corresponding microgrid system parameters.

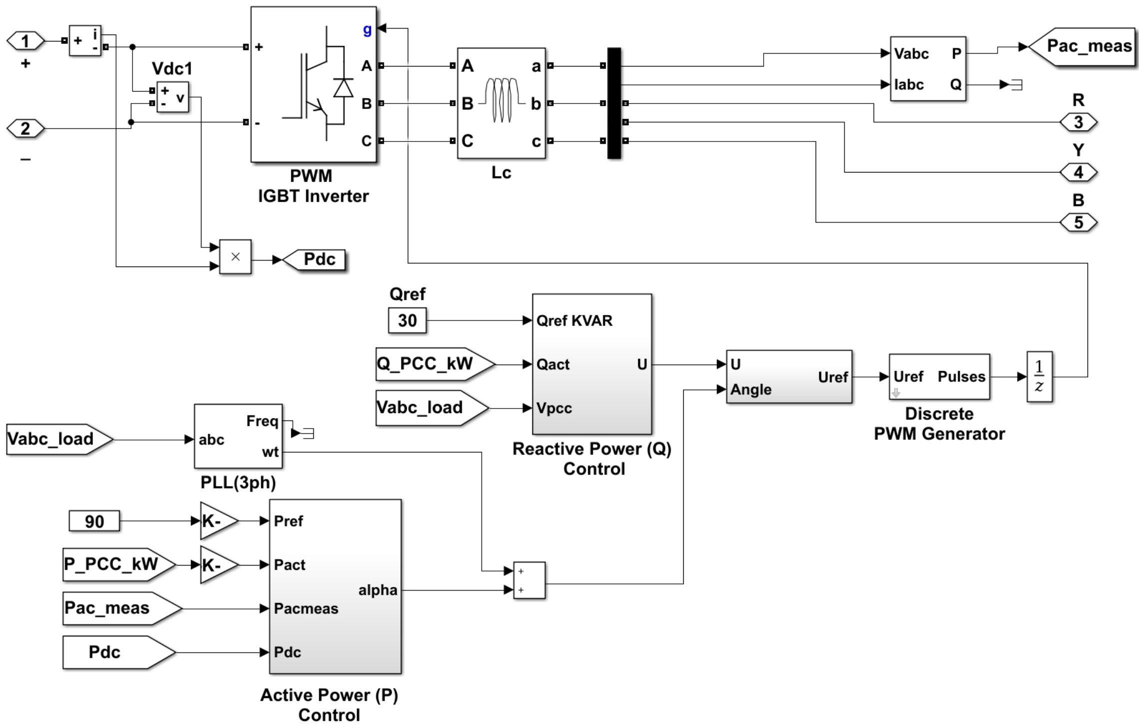

Figure 5.28: MATLAB / SIMULINK model of P-Q control

Table 5.4: Microgrid system parameters for case IV

Description	Values
Point of Common Coupling	3-phase, 440 V, 50 Hz
Solar PV System	100 kW
Battery	42 Batteries each of 300Ah capacity, Type- Lead acid
Interfacing Transformer	200kVA, 440/480 V, Y-Δ, 50 Hz
Diesel Generator Set	150 kVA, 440 V, 50 Hz
Load	3-phase, 120 kW

Here two different cases, namely case A and case B, are considered for MATLAB simulation. In real time operation load varies with time. Hence to validate P-Q control method, variation in load is considered. For both the cases solar irradiation is consider as 1000 W/m^2.

5.4.1 Case A: Solar PV Output Power is more than the Critical Load

Maximum output power available (i.e.P_{pv}) from solar PV system is 100 kW. Critical active (i.e. P_{ref}) and reactive power (i.e. Q_{ref}) of load is considered as 90 kW, 30 kVAR, respectively. i.e. $P_{pv} > P_{ref}$.

Figure 5.29 shows the active and reactive power of DG set. DG set supplies constant active power of 30 kW and reactive power of 45 kVAR throughout the simulation. Figure 5.30 shows the reference active and reactive power to the inverter. The references are chosen to demonstrate charging and discharging of battery. Figure 5.31 shows the solar PV output power, power to battery and output power of inverter. The output power of solar PV system is more than the critical load by 10 kW. This surplus power is sent to charge lead acid battery which is shown in Figure 5.31. Figure 5.32 shows the State of Charge (SOC) of battery. Here surplus power is sent to charge the battery, hence SOC of battery increases.

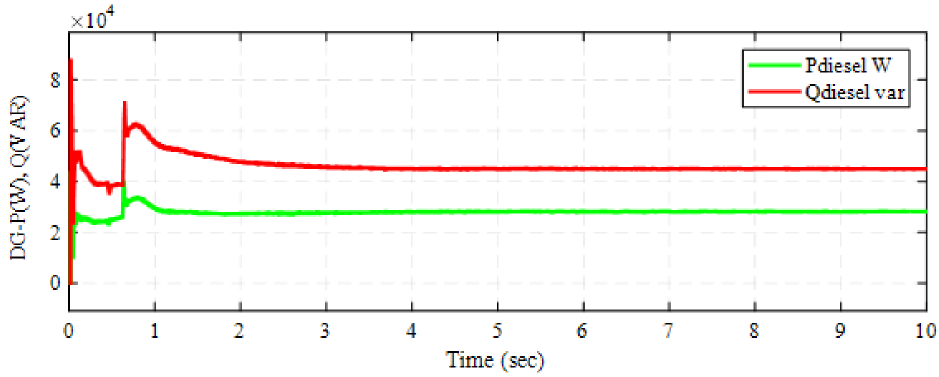

Figure 5.29: DG set active and reactive power

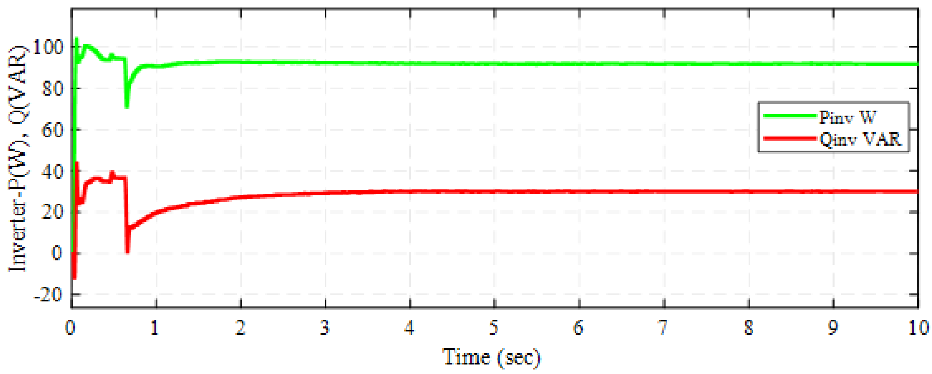

Figure 5.30: Reference active and reactive power to the inverter

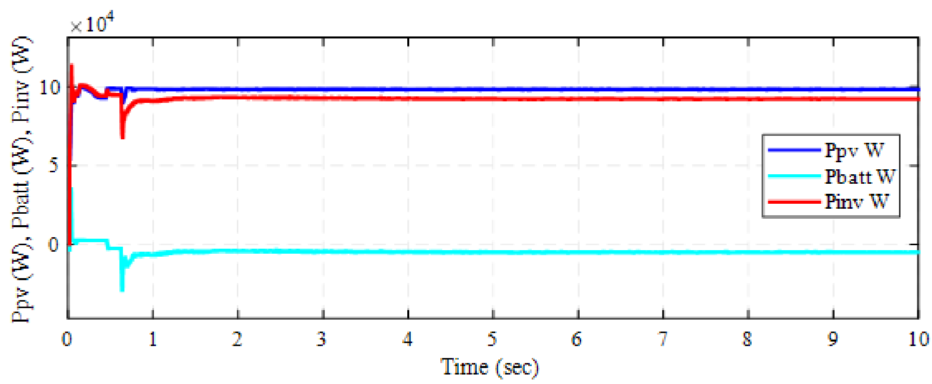

Figure 5.31: Active power of PV, battery and inverter

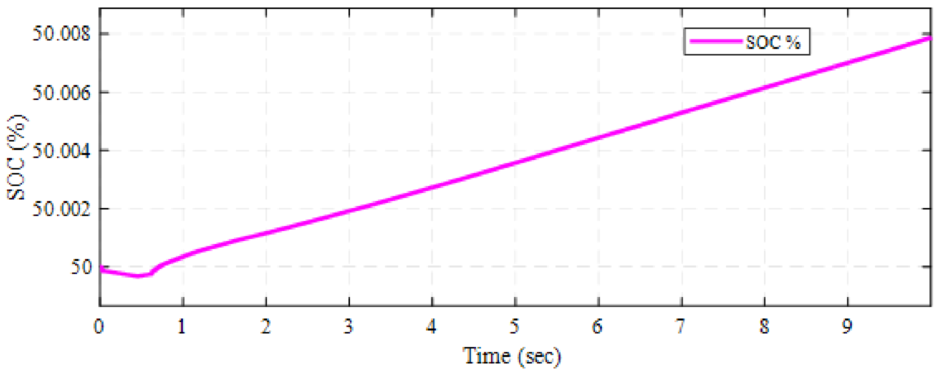

Figure 5.32: State of Charge (SOC) of battery

5.4.2 Case B: Solar PV Output Power is less than the Critical Load

Maximum output power available (i.e.P_{pv}) from solar PV system is 100 kW. Critical active (i.e. P_{ref}) and reactive power (i.e. Q_{ref}) of load is considered as 110 kW, 40 kVAR, respectively. i.e. $P_{pv} > P_{ref}$.

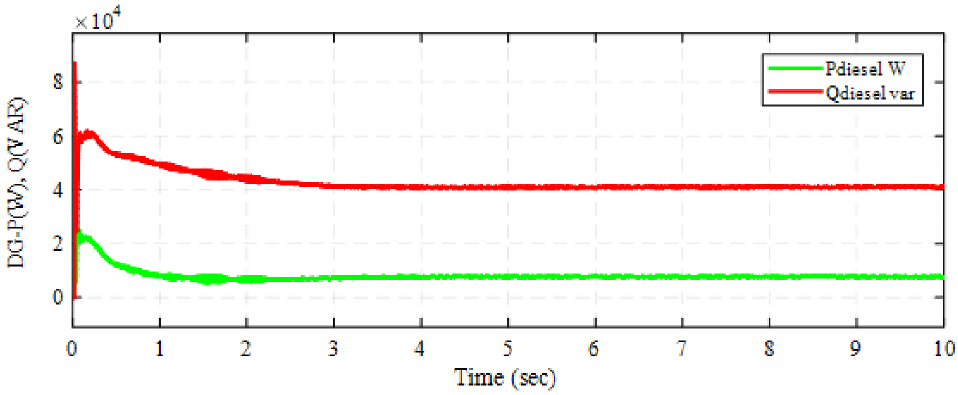

Figure 5.33: DG set active and reactive power

Figure 5.33 shows the active and reactive power of DG set. DG set supplies constant active power of 10 kW and reactive power of 35 kVAR throughout the simulation. Figure 5.34 shows the reference active and reactive power to the inverter. The references are chosen to demonstrate charging and discharging of battery. Figure 5.35 shows the solar PV output power, power to battery and output power of inverter. The output power of solar PV system is less than the critical load by 10 kW. This deficit power is given by battery which is shown in Figure 5.35. Figure 5.36 shows the State of Charge (SOC) of battery. Here battery supplies deficit power to the load, hence SOC of battery decreases.

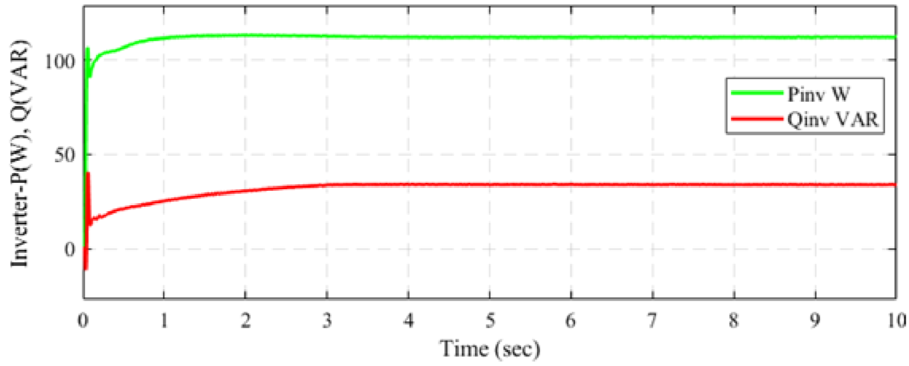

Figure 5.34: Reference active and reactive power to the inverter

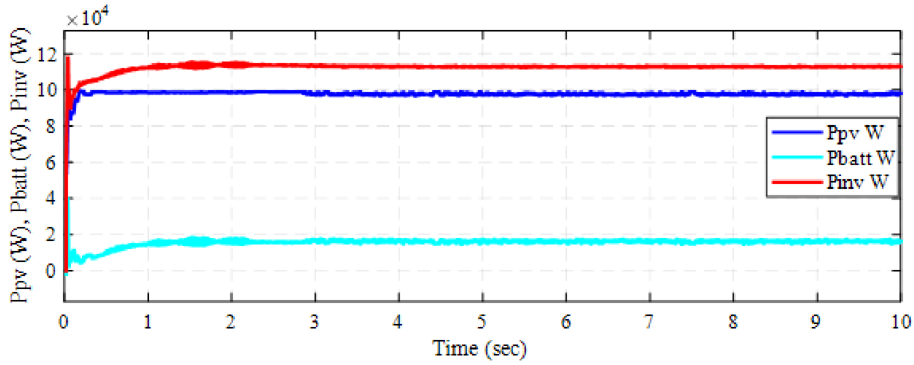

Figure 5.35: Active power of PV, battery and inverter

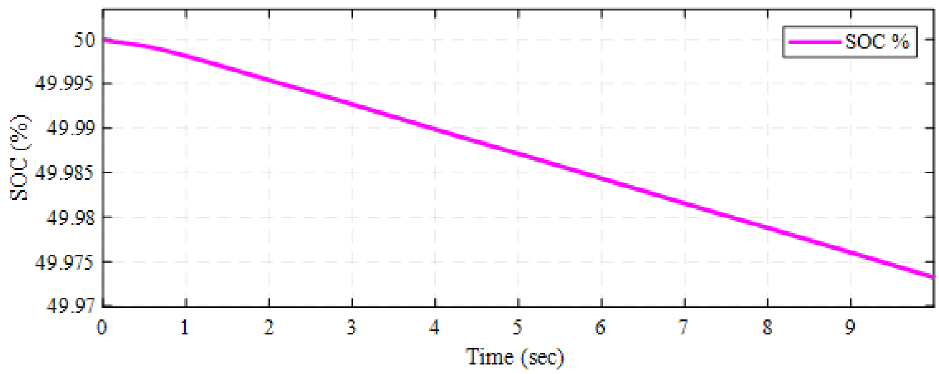

Figure 5.36: State of Charge (SOC) of battery

The effectiveness of proposed P-Q controller is verified from the presented results. This control strategy can be effectively used while supplying critical loads in microgrids.

Chapter 6

Conclusions and Future Scope

This chapter provides the conclusions of this thesis, offering a comparative study and analysis of the results obtained after various simulations. A few of the possible avenues for further study on this topic briefly discussed as well.

6.1 Conclusions

In this chapter a final conclusion is drawn based on the findings of previous discussions of this thesis. The thesis are to emphasize the role of PV based DG in microgrid application, and its operational challenges. In order to ensure the better power quality supply especially in islanded mode of microgrid, it is utmost important to take care of voltage and frequency stability. This work proposes coordinated voltage-frequency control strategy for power sharing among Distributed Energy Resources in islanded microgrid. In this control strategy MPPT is used to extract maximum power from solar PV system, and battery storage is used as a buffer in order to store or supply deficit power by using charge / discharge cycle of the battery. The results clearly shows that the performance of microgrid enhances with battery energy storage. The battery storage control strategy also handles SOC constraint of the battery to improve life cycle of battery.

An effective smooth transition of control from V-f to constant active power control at the solar PV side and from constant active power control to frequency control at the D-G side is validated. This feature helps the controller to adapt with changing irradiance and battery availability. The proposed control method shows that the voltage and frequency quickly settles down to their nominal values as compared to diesel generator control.

Uninterrupted power supply is required for critical load applications. To supply such critical load, P-Q control strategy is developed to support real and reactive power. Furthermore, this work proposes a novel adaptive control strategy to retune controller parameters with dynamically varying system conditions to maintain the voltage and frequency. A simulation result indicates that the proposed adaptive control strategy gives satisfactory performance compared to the conventional PI controller.

6.2 Future Scope

The proposed idea has been proved to work, but needed further investigation and more refinement. The future scope of work is identified as under;
A demand side management with observer based parallel islanding detection.
Different energy storage devices could be try out for economical load operation.
The effective protection coordination with centralized / distributed generator controller.

List of Publications

Publication in Journals

1 . S. S. Khule, S. W. Mohod, "Stability Enhancement of an Islanded Microgrid using Battery Storage", *The Institution of Engineers*, vol. 3, pp. 97-105, April 2019.

2 . S. S. Khule, S. W. Mohod, "Solar PV Generator with Battery Energy Storage for Critical Load", *International Journal of Innovative Technology and Exploring Engineering*, vol. 8, issue 6, April 2019.

3 . S. S. Khule, S. W. Mohod, "Soft Computing Approach for Reactive Power Compensation with Solar Photovoltaic System", *International Journal for Science and Advance Research in Technology*, vol.4, issue-3, pp-260-265, March 2018.

4 . S. S. Khule, S. W. Mohod, Mughdha Kamat, "Energy Balance in AC Is-landed Micro-grid by Frequency Bus Signaling Method", *International Research Journal of Engineering and Technology*, vol. 4, issue 7, pp. 865-870, July 2017.

Submitted in Journals

1 . S. S. Khule, S. W. Mohod, "Voltage and Frequency Control of Microgrid by Adaptive Control Technique", *Australian Journal of Electrical and Electronics Engineering.*

Published in International Conferences

1 Shridhar S. Khule, Pooja D. Ugale, Sharad W. Mohod, "Microgrid Stability Issues and PI Control Technique", *International Conference on Information, Communication, Engineering and Techology (ICICET 2018)*, November 2018.

2 S. S. Khule, S. W. Mohod, Mughdha Kamat, “Energy Balance in AC Is-landed Micro-grid by Frequency Bus Signaling Method, *International Conference on Intelligent Sustainable Systems (ICISS 2017)*, Dec.2017.

3 Shridhar S. Khule, Joydeep Sarkar, “A Study of MPPT Schemes in PMSG Based Wind Turbine System”, *International Conference on Electrical, Electronics and Optimization Techniques (ICEEOT 2016)*, November 2016.

References

[1] Magdi S. Mahmoud, Nezar M. Alyazidi, Mohamed I. Abouheaf, "Adaptive Intelligent Techniques for Microgrid Control Systems: A Survey", *Electrical Power and Energy Systems*, vol. 90, pp. 292-305, September 2017.

[2] S. W. Mohod and M. V. Aware, "A STATCOM- Control Scheme for Grid Connected Wind Energy System for Power Quality Improvement", *IEEE System Journal*, vol. 4, no. 3, pp. 346-352, June 2010.

[3] Blaabjerg F., Teodorescu R., Liserre M., Timbus A. V., "Overview of Control and Grid Synchronization for Distributed Power Generation System", *IEEE Transaction on Industrial Electronics*, vol. 53, no. 5, 1398-409, October 2006.

[4] Mahmoud M. S., Azher S. H., Abido M. A., "Modeling and Control of Micogrid: An Overview", *Journal of the Franklin Institute*, vol. 351, no. 5, pp. 2822-2859, May 2014.

[5] R. H. Lasseter, "MicroGrids", in Proceedings. *IEEE Power Engineering Society Winter Meeting*, vol. 1, pp. 305-308, August 2002.

[6] A.V. Padgavahankar, S. W. Mohod, "Solar Energy System with Digital Controller for Grid Connected System", *Journal of Electronics Science & Technology*, vol.12, no.3, pp. 277-282, September 2014.

[7] Schweer, Adolf, and Study Committee Power System Planning and Development, "Impact of Increasing Contribution of Dispersed Generation on the Power System: Final Report", *International Conference on Large High Voltage Electric Systems*, Cigr, 1999.

[8] Martins, Vinicius F., and Carmen LT, "Active Distribution Network Integrated Planning Incorporating Distributed Generation and Load Response Uncertainties", *IEEE Transactions on Power Systems*, vol. 26, no. 4, pp. 2164-2172, 2011.

[9] CIRED Working Group WG04, "Dispersed Generation", June 1999.

[10] CIGRE Working Group WG 37-23, "Impact of Increasing Contribution of Dispersed Generation on the Power System", 1997.

[11] COM (97) 559, "Communication from the European Commission: Energy for the Future, Renewable Sources of Energy", *White Paper for a Community Strategy and Action Plan*, 1997.

[12] European Commission, "Directive of the European Parliament and the Council on the Promotion of Electricity from Renewable Energy Sources in the Internal Electricity Market", 2000.

[13] Chowdhury S., and Peter C., "Microgrids and Active Distribution Networks", *The Institution of Engineering and Technology*, 2009.

[14] Joskow P. L., and Schmalensee R. "Markets for Power: An Analysis of Electric Utility Deregulation", *Massachusetts Inst. of Technology Press*, Cambridge, 1983.

[15] Zhong J., and Bhattacharya K., "Reactive power management in deregulated electricity markets-A review", *IEEE Power Engineering Society Winter Meeting*, vol. 2, pp. 1287-1292, 2002.

[16] "Future Network Design, Management and Business Environment Generation DTI/OFGEM Embedded Generation Working Group WP7", Website: www.distributedgeneration

[17] Ritwik Majumder, "Some Aspects of Stability in Microgrids", *IEEE Transaction on Power Systems*, vol. 28, no. 3, pp. 3243-3252, August 2013.

[18] P. Kammer, A. Kober, "Grid Integration of Renewable Energy Resources", *International Journal of Distributed Energy Resources*, vol. 2, no. 1, pp. 59-81, 2006.

[19] "IEEE Standard for Interconnecting Distributed Resources with Electric Power Systems", *Standard IEEE*, 1547, 2003.

[20] M. A. Elhadidy, “Performance Evaluation of Hybrid (Wind/Solar/Diesel) Power Systems”, *Renewable Energy*, vol. 26, pp. 401-413, June 2001.

[21] Sarina Adhikari, and Fangxing Li, “Coordinated V-f and P-Q Control of Solar Photovoltaic Generators With MPPT and Battery Storage in Microgrids”, *IEEE Transactions on Smart Grid*, vol. 5, no. 3, pp. 1270-1281, May 2014.

[22] Tsikalakis A. G. and Hatziargyriou N. D., “Centralized Control for Optimizing Microgrids Operation”, *IEEE power and energy society general meeting*, pp. 1-8, 2011.

[23] S. W. Mohod, S. D. Deshmukh, “DC-DC Converter for Interfacing Energy Storage”, *American International Journal of Science, Technology, Engineering & Mathematics*, vol. 5(1), pp. 76-81, Feb.2014.

[24] Najy W. K. A., Zeineldin H. H., and Wei Lee Woon, “Optimal Protection Coordination for Microgrids with Grid-Connected and Islanded Capability”, *IEEE Transactions on industrial electronics*, vol. 60, no. 4, pp. 1668-1677, 2013.

[25] Markvart T., “Photovoltaic Solar Energy Conversion”, Strasbourg European Summer University: Energy for Europe, pp. 7-14, 2002.

[26] Grubb M., “Economic Dimensions of Technological and Global Responses to the Kyoto Protocol”, *Journal of Economic Studies*, vol. 27, no. 1/2, pp. 111-125, 2000.

[27] “List of Photovoltaic Power Stations, World’s Largest Photovoltaic Power Stations”, website:https://en.wikipedia.org/wiki/ List of photovoltaic power stations.

[28] “Electricity Sector in India - Wikipedia”, pp. 1-20, 2018.

[29] India Energy Outlook - World Energy Outlook Special Report 2015, International Energy Agency, Website: www.worldenergyoutlook.org/india.

[30] A. V. Padgavahankar, S. W. Mohod, “Experimental Learning of Digital Power Controller For Photovoltaic Module Using Proteus VSM”, *Hindawi Publishing Corporation, Journal of Solar Energy*, vol. 1, 2014.

[31] Divya K. C. and Ostergaard J., “Battery Energy Storage Technology for Power Systems - an Overview”, *Electric Power Systems Research*, vol. 79, no. 4, pp. 511-520, April 2009.

[32] Nayar C. V., Ashari M. and Keerthipala W. W. L., “A Grid-Interactive Photovoltaic Uninterruptible Power Supply System using Battery Storage and a Back Up Diesel Generator”, *IEEE Transactions on Energy Conversion*, vol. 15, no. 3, pp. 348-353, September 2000.

[33] S. W. Mohod, M. V. Aware, “Battery Energy Storage to Strengthen the Wind Generator in Integrated Power System”, *Journal of Electronic Science & Technology.-JEST* vol. 9, no. 1, pp. 32-42, March 2011.

[34] A. E. Curtright and J. Apt, “The Character of Power Output from Utilityscale Photovoltaic Systems”, *IProg. Photovolt: Res. Appl.*, vol. 16, pp. 241-247, 2008.

[35] Chen, H., Cong, T. N., Yang, W., Tan, C., Li, Y., Ding, Y., “Progress in Electrical Energy Storage System: A Critical Review”, *Progress in Natural Science*, vol. 19, no. 3, pp. 291-312, March 2009.

[36] Chatzivasileiadi A., Ampatzi E., Knight I., “Characteristics of Electrical Energy Storage Technologies and their Applications in Buildings”, *Renew. Sustain. Energy Rev.*, vol. 25, pp. 814-830, 2013.

[37] Dufo-Lpez, R., Lujano-Rojas, J. M., Bernal-Agustn, J. L., “Comparison of Different Lead-Acid Battery Lifetime Prediction Models for use in Simulation of Stand-Alone Photovoltaic Systems”, *Applied Energy*, vol. 115, pp. 242-253, February 2014.

[38] N. Hamsic, A. Schmelter, A. Modh, E. Ortjohann, E. Schultze, A. Tuckey, J. Zimmermann, “Integrating Renewable Energy Penetration in Isolated Grids Using a Flywheel Energy Storage System”, *International Conference on Power Engineering, Energy and Electric Drives, Portugal*, April 2007.

[39] I. Mitra, t. Degner and M. Braun, “Distributed Generation and Microgrids for Small Island Electrification in Developing Countries: A Review”, *Solar Energy Society of India*, vol. 18, no. 1, pp. 6-20, June 2008.

[40]K. Karasavyas, “Modular Simulation of a Hybrid Power System with Diesel, Photo Voltaic inverter and Wind Turbine Generation”, *Journal of Engineering Science and Technology*, vol. 1, pp. 38-40, 2008.

[41] V. Karri, W. K. Yap, and J. Titchen, “Simulation and Configuration of Hydrogen Assisted Renewable Energy Power System”. *World Academy of Science, Engineering and Technology*, vol. 47, 2008.

[42] P. Piagi, R. H. Lasseter “Autonomous Control of Microgrid”, *IEEE PES Meeting, Montreal*, June 2006.

[43] A. Arulampalam, M. Barnes, C. Fitzer, X. Wu, N. Jenkins “Automated Control Technique to Coordinate Microgrid Sources - Grid Connected and Islanded Operation”, *International Journal of Distributed Energy Resources*, vol: 1, no: 2, pp: 133-147, 2005.

[44] G. Pepermans, J. Driesen, D. Haeseldonckx, R. Belmans, and W. D’haeseleer, 2005, “Distributed Generation: Definition, Benefits and Issues”, *Energy Policy*, 33, pp. 787-798.

[45] “IEEE 1547 Series of Standards: Interconnection Issues”, September 2003.

[46] H. L. Willis and W.G. Scott, “Distributed Power Generation: Planning and Evaluation”, *CRC Press*, 2000.

[47] R. H. Lasseter, “CERTS Microgrid”, *International Conference on System of Systems Engineering*, April 16-18, 2007.

[48] L. Mariam, M. Basu, M. Conlon, “A Review of Existing Microgrid Architectures”, *Journal of Engineering*, vol. 2013, pp. 1-8, 2013.

[49] R. S. Garcia, D. Weisser, "A Wind-Diesel System with Hydrogen Storage: Joint Optimization of Design and Dispatch", *Renewable Energy*, vol. 31, pp. 2296-2320, January 2006.

[50] J. D. Kueck, R. H. Staunton, S. D. Labinov, B. V. Kirby, "Microgrid Energy Management System", *CERTS Report*, January 2003.

[51] P. Kammer, A. Kober, "Grid Integration of Renewable Energy Resources", *International Journal of Distributed Energy Resources*, vol. 2, no. 1,pp. 59-81, 2006.

[52] A. Elmitwally, M. Rashed, "Flexible Operation Strategy for an Isolated PV-Diesel Microgrid without Energy Storage", *IEEE Transactions on Energy Conversion*, vol. 26, no. 1, pp. 235-244, March 2011.

[53]C. Guanglin, C. Rouyi, L. Yong, Z. Yongjun, "Research on Simulation and Modeling of the Isolated Wind-Solar-Diesel-Battery Hybrid Microgrid", *International Conference on Electricity Distribution*, *China*, September 2012.

[54] C. L. Smallwood "Distributed Generation in Autonomous and Non-Autonomous Micro grids", *IEEE Conference on Rural Electric Power Conference*, May 2002.

[55]D. Yamegueu, Y. Azoumah, X. Py, N. Zongo, "Experimental Study of Electricity Generation by Solar PV/Diesel Hybrid Systems without Battery Storage for Off grid Areas", *Renewable Energy*, vol. 36, pp. 1780-1787, December 2010.

[56] F. D. Kanellos, A. I. Tsouchnikas, N. D. Hatziargyriou, "Microgrid Simulation during Grid Connected and Islanded Modes of Operation", *International Conference on Power Systems Transients*, *Canada*, June 2005.

[57] G. Venkataramanan, M. S. Illindala, C. Houle and R. H. Lasseter, "Hardware Development of a Laboratory Scale Microgrid Phase: 1- Single Inverter in Island Mode Operation", *National Renewable Energy Laboratory Report*, November 2001.

[58] J. A. Pecas Lopes, C. L. Moreira, F. O. Resende, "Microgrids Black Start and Islanded Operation", *15th Power System Conference, Liege*, August 2005.

[59] T. E. Del Carpio, D. S. Ramos, R. L. Vasquez-Arnez, “Microgrid Systems”.

[60] C. Koutroulis, D. Kolokotsa, A. Potirakis, K. Kalaitzakis, “Methodology for Optimal Sizing of Stand Alone Photovoltaic/ Wind Generator Systems Using Genetic Algorithms”, *Solar Energy*, pp. 1072-1088, 2006.

[61] J. D. Rose, I. A. Hiskens, “Challenges of Integrated Large Amounts of Wind Power”, *IEEE Systems Conference, Hawaii, USA*, April 2007.

[62] M. Popov, H. Karimi, H. Nikkhajoei, V. Terzija, “Dynamic Model and Control of a Microgrid with Passive Loads”, *International Conference on Power Systems Transients in Kyoto, Japan*, June 2009.

[63] R. H. Lasseter, “Microgrids and Distributed Generation”, *Journal of Energy Engineering, American Society of Civil Engineers*, September 2007.

[64] Ali Bidram, Ali Davoudi, and Frank L. Lewis, “A Multi-objective Distributed Control Framework for Islanded AC Microgrids”, *IEEE Transactions on Industrial Informatics*, vol. 10, no. 3, pp. 1785-1798, August 2014.

[65] S. Mishra, D. Ramasubramanian, and P. C. Sekhar, “A Seamless Control Methodology for a Grid Connected and Isolated PV-Diesel Microgrid”, *IEEE Transactions on Power Systems*, vol. 28, no. 4, pp. 4393-4404, November 2013.

[66] Amin Ghazanfari, Mohsen Hamzeh, Hossein Mokhtari, “Active Power Management of Multihybrid Fuel Cell / Supercapacitor Power Conversion System in a Medium Voltage Microgrid”, *IEEE Transactions on Smart Grid*, vol. 3, no. 4, pp. 1903-1910, December 2012.

[67] Jinwei He and Yun Wei Li, “An Enhanced Microgrid Load Demand Sharing Strategy”, *IEEE Transactions on Power Electronics*, vol. 27, no. 9, pp. 3984-3995, September 2012.

[68] Alireza Kahrobaeian, and Yasser Abdey I. Mohamed, “Analysis and Mitigation of Low-Frequency Instabilities in Autonomous Medium-Voltage Converter-Based

Microgrids with Dynamic Loads", *IEEE Transactions on Industrial Electronics*, vol. 61, no. 4, pp. 1643-1658, April 2014.

[69] Mehdi Savaghebi, Alireza Jalilian, Juan C. Vasquez, and Josep M. Guerrero, "Autonomous Voltage Unbalance Compensation in an Islanded Droop-Controlled Microgrid", *IEEE Transactions on Industrial Electronics*, vol. 60, no. 4, pp. 1390-1402, April 2013.

[70] Irvin J. Balaguer, Qin Lei, Shuitao Yang, Uthane Supatti, and Fang Zheng Peng, "Control for Grid-Connected and Intentional Islanding Operations of Distributed Power Generation", *IEEE Transactions on Industrial Electronics*, vol. 58, no. 1, pp. 147-157, January 2011.

[71] Sarina Adhikari, and Fangxing Li, "Coordinated V-f and P-Q Control of Solar Photovoltaic Generators With MPPT and Battery Storage in Microgrids", *IEEE Transactions on Smart Grid*, vol. 5, no. 3, pp. 1270-1281, May 2014.

[72] Joydeep Mitra, and Mallikarjuna R. Vallem, "Determination of Storage Required to Meet Reliability Guarantees on Island-Capable Microgrids With Intermittent Sources", *IEEE Transactions on Power Systems*, vol. 27, no. 4, pp. 2360-2367, November 2012.

[73] Ritwik Majumder, Balarko Chaudhuri, Arindam Ghosh, Rajat Majumder, Gerard Ledwich, and Firuz Zare, "Improvement of Stability and Load Sharing in an Autonomous Microgrid Using Supplementary Droop Control Loop", *IEEE Transactions on Power Systems*, vol. 25, no. 2, pp. 796-803, May 2010.

[74] Milad Falahi, Karen L. Butler-Purry, and Mehrdad Ehsani, "Induction Motor Starting in Islanded Microgrids", *IEEE Transactions on Smart Grid*, vol. 4, no. 3, pp. 1323-1331, September 2013.

[75]Mohammad A. Abusara, Josep M. Guerrero, and Suleiman M. Sharkh, "Line-Interactive UPS for Microgrids", *IEEE Transactions on Industrial Electronics*, vol. 61, no. 3, pp. 1292-1300, March 2014.

[76]Koen J. P. Macken, Math H. J. Bollen, and Ronnie J. M. Belmans, "Mitigation of Voltage Dips Through Distributed Generation Systems", *IEEE Transactions on Industrial Applications*, vol. 40, no. 6, pp. 1686-1693, November 2004.

[77] Ritwik Majumder, "Some Aspects of Stability in Microgrids", *IEEE Transactions on Power Systems*, vol. 28, no. 3, pp. 3243-3252, August 2013.

[78] Pourya Shamsi, and Babak Fahimi, "Stability Assessment of a DC Distribution Network in a Hybrid Micro-Grid Application", *IEEE Transactions on Smart Grid*, vol. 5, no. 5, pp. 2527-2533, September 2014.

[79] Ajit A. Renjit, Mahesh S. Illindala and Rama K. Yedavalli, "Stability Robustness Analysis and its Improvement for an Industrial Microgrid", *Industry Application Society Annual Meeting,* PSEC-0382, pp. 1-8, December 2014.

[80] R. M. Kamel, A. Chaouachi, and K. Nagasaka, "Three Control Strategies to Improve the Microgrid Transient Dynamic Response During Isolated Mode: A comparative study", *IEEE Transactions on Industrial Electronics*, vol. 60, no. 4, pp. 1314-1322, April 2013.

[81] Qiang Fu, Adel Nasiri, Vijay Bhavaraju, Ashish Solanki, Tarek Abdallah, and David C. Yu, "Transition Management of Microgrids with High Penetration of Renewable Energy", *IEEE Transactions on Smart Grid*, vol. 5, no. 2, pp. 539-549, March 2014.

[82] C. L. Moreira, F. O. Resende, and J. A. Peas Lopes, "Using Low Voltage Micro-Grids for Service Restoration", *IEEE Transactions on Power Systems*, vol. 22, no. 1, pp. 395-403, February 2007.

[83] A. H. Kasem Alaboudy, H. H. Zeineldin, and Kirtley, Jr., "Microgrid Stability Characterization Subsequent to Fault-Triggered Islanding Incidents", *IEEE Transactions on Power Delivery*, vol. 27, no. 2, pp. 658-669, April 2012.

[84] A. K. Srivastava, A. A. Kumar, N. N. Schulz, "Impact of Distributed Generation with Energy Storage Devices on the Electricity Grid", *IEEE Systems Journal*, vol. 6, no. 1, pp. 110-117, 2012.

[85] G. Berry, "Present and Future Electricity Storage for Intermittent Renewables", *Proceeding of The 10-50 Solution Technologies and Policies for a low-carbon Future*, 2005.

[86] Sharad W. Mohod and Mohan V. Aware, "Micro Wind Power Generator with Battery Energy Storage for Critical Load", *IEEE Systems journal*, vol. 6, no. 1, pp. 118-125, March 2012.

[87]Dan Wang, Shaoyun Ge, Hongjie Jia, Chengshan Wang, Yue Zhou, Ning Lu, and Xiangyu Kong, "A Demand Response and Battery Storage Coordination Algorithm for Providing Microgrid Tie-Line Smoothing Services", *IEEE Transactions on Sustainable Energy*, vol. 5, no. 2, pp. 476-486, April 2014.

[88] Haihua Zhou, Tanmoy Bhattacharya, Duong Tran, Tuck Sing Terence Siew and Ashwin M. Khambadkone, "Composite Energy Storage System Involving Battery and Ultracapacitor With Dynamic Energy Management in Microgrid Applications", *IEEE Transactions on Power Electronics*, vol. 26, no. 3, pp. 923-930, March 2011.

[89] R. H. Lasseter, A. Akhil, C. Marnay, J. Stephens, J. Dagle, R. Guttormoson, A. Sakis, R. Yinger and J. Eto, "Integration of Distributed Energy Resources: The CERTS Microgrid Concept", *White Paper*, April 2002.

[90] Dhar S., Sridhar R., and Mathew G, "Implementation of PV Cell Based Standalone Solar Power System Employing Incremental Conductance MPPT Algorithm", *IEEE International Conference on Circuits, Power and Computing Technologies (ICCPCT)*, pp. 356-361., 2013.

[91] Khan B. H., "Non-Conventional Energy Resources", *Tata McGraw-Hill Education*, 2006.

[92] McEvoy A., Markvart T., Castaer L., Markvart T., and Castaner L. Eds., "Practical Handbook of Photovoltaic: Fundamentals and Applications", *Elsevier*, 2003.

[93] Femia N., Petrone G., Spagnuolo G., and Vitelli M., "Optimizing Sampling Rate of P& O MPPT Technique", *35th IEEE Annual Power Electronics Specialists Conference*, PESC 04, Vol. 3, pp. 1945-1949, 2004.

[94]Chin C. S., Neelakantan P., Yoong H. P., Yang S. S., and Teo K. T. K., "Maximum Power Point Tracking for PV Array Under Partially Shaded Conditions", *IEEE Third International Conference on Computational Intelligence, Communication Systems and Networks (CICSyN)*, pp. 72-77, 2011.

[95] Ishaque K., Salam Z., Amjad M., and Mekhilef S., "An Improved Particle Swarm Optimization (PSO)-Based MPPT for PV with Reduced Steady-State Oscillation", *IEEE Transactions on Power Electronics*, vol. 27, no. 8, pp. 3627-3638, 2012.

[96] Esram T., and Chapman P. L., "Comparison of Photovoltaic Array Maximum Power Point Tracking Techniques", *IEEE Transactions on Energy Conversion*, vol. 22, no. 2, pp. 439 - 449, 2007.

[97] Liu F., Duan S., Liu F., Liu B., and Kang Y., "A Variable Step Size INC MPPT Method for PV Systems", *IEEE Transactions on Industrial Electronics*, vol. 55, no. 7, pp. 2622-2628, 2008.

[98] Wu T. F., Chang C. H., and Chen Y. K., "A Fuzzy-Logic-Controlled Single-Stage Converter for PV-Powered Lighting System Applications", *IEEE Transactions on Industrial Electronics*, vol. 47, no. 2, pp. 287-296, 2000.

[99] Veerachary M., Senjyu M., and Uezato K., "Neural-Network-Based Maximum-Power point Tracking of Coupled-Inductor Interleaved-Boost-Converter-Supplied PV System using Fuzzy Controller", *IEEE Transactions on Industrial Electronics,* vol. 50, no. 4, pp. 749-758, 2003.

[100] Dhar S., and Dash P. K., "A Finite Time Fast Terminal Sliding Mode I-V Control of Grid-Connected PV Array", *Journal of Control, Automation and Electrical Systems*, vol. 26, no. 3, pp. 314-335, Springer 2015.

[101] Sarina Adhikari and Fangxing Li, "Coordinated V-f and P-Q Control of Solar Photovoltaic Generators With MPPT and Battery Storage in Microgrids", *IEEE Transactions on Smart Grid*, vol. 5, no. 3, May 2014.

[102] Sarina Adhikari, Fangxing Li and Huijuan Li, "P-Q and P-V Control of Photovoltaic Generators in Distribution Systems", *IEEE Transactions on Smart Grid*, 2015.

[103] K. J. Astrom, "Theory and Applications of Adaptive Control- A Survey", *International Federation of Automatic Control, Printed in Great Britain*, vol. 9, no. 5, pp. 471-486, 1983.

[104] Rajesh K. S., Dr. S. S. Dash, Dr. Bayinder R. Sridhar, Ragam Rajagopal, "Implementation of an Adaptive Control Strategy for Solar Photo Voltaic Generators in Microgrids with MPPT and Energy Storage",*5th International Conference on Renewable Energy Research and applications*, Birmingham, UK, November 2016.

[105] Astrom Karl Johan, Wittenmark Bjorn, Lund Institute of Technology, "Adaptive Control", Addison-Wesley Publishing company, Inc. Reading, Massachusetts Menlo Park, California New York Don Mills, Ontario Wokingham, England Amsterdam Bonn Sydney Singapore Tokyo Madrid San Juan Milan Paris, 2nd edition, 1995.